Protein Disulphide Isomerase is protective against DNA damage in Amyotrophic Lateral Sclerosis

Fabiha Farzana

Supervisor: Professor Julie Atkin

Associate Supervisor: Dr Sina Shadfar

A thesis submitted in fulfillment of the requirements for the degree of
Master of Research

Centre for Motor Neuron Disease Research

Macquarie Medical School

Faculty of Medicine, Health and Human Sciences

Macquarie University

November 2022

Declaration

I declare that the work present in this thesis titled 'Protein Disulphide Isomerase is protective against DNA damage in Amyotrophic Lateral Sclerosis' has not previously been submitted, in either whole or part, for the purposes of obtaining any other degree to any other university of institution other than Macquarie University. To the best of my knowledge this thesis does not include previously published material by another person except where due reference is made in the text. Unless otherwise acknowledged, this work was carried out by the author.

Fabiha Farzana
17th November 2022

Preface

All the work described in this thesis was performed by the author, except where hereby stated. The author acknowledges the following for assistance in performing the following experiments reported in this thesis:

Western blotting for figure 3.1 (A) was performed by Dr Sina Shadfar, Macquarie University, Sydney. PDI-CRISPR plasmids were prepared by Dr Sina Shadfar and Dr Cyril Jones Jagaraj, Macquarie University, Sydney. Western blotting for figure 3.4 was done by Ms Julie Hunter, Macquarie University, Sydney. IP experiment was conducted with the guidance of Dr Mariana Brocardo, Macquarie University, Sydney and with the help of Dr Sina Shadfar.

Acknowledgements

At first, I would like to thank my supervisors, Professor Julie Atkin and Dr Sina Shadfar. Julie, thank you so much for helping me to decide my project and supporting me throughout the year. You have been an amazing mentor and I really appreciate for what you have done for me.

Sina, I cannot thank you for enough for helping me with everything in my MRes journey. Especially when I had my injury, the way you helped me in the lab, I will never forget that. I have learned a lot from you and hope to learn more in the coming years. Thank you for helping me with my experiments and analyses.

To all other Atkin group members, Mariana, Sonam, Prachi, Julie, Cyril, Anna, Zeinab and Naima. Mariana, thank you so much for helping me with the IP experiment and all the western blotting knowledge. Sonam, thanks for helping me with the quantifications and admin work. Prachi and Julie, thanks for taking care of me and everyone in the lab. I do not know what I would do without you two. Julie, a special thanks for helping me with the CRISPR experiment. Cyril, thanks for helping me with the western blotting experiment and sharing your knowledge about lab work. Zeinab, I do not know how I would survive this year without you! You gave me constant company and I miss doing experiments together. Naima, thanks for listening to my rants and helping me to get through this year. I will cherish these memories forever.

Last but not the least, to my family, my parents, Mukti and Mithu, my husband, Tanvir, and my little brother, Shoumik, thank you for supporting and keeping me motivated always. Thank you for always believing in me and cheering me up! I am very thankful for what you do every day for me.

Abbreviations

53BP	p53 Binding Protein
5mC	5-methyl cytosine
ɣ-H2AX	Phosphorylated-H2AX
AD	Alzheimer's Disease
ALS	Amyotrophic Lateral Sclerosis
AP	Abasic or apurinic/apyrimidinic
BCA	Bicinchoninic Acid
BER	Base Excision Repair
BSA	Bovine Serum Albumin
C9ORF72	*Chromosome 9 Open Reading Frame 72*
CTCF	Corrected Total Cell Fluorescence
DDR	DNA Damage Response
DMEM	Dulbecco's Modified Eagle's Medium
DNA	Deoxyribonucleic acid
dNTP	Deoxynucleotide Triphosphate
DSB	Double-stranded Break
ER	Endoplasmic Reticulum
EV	Empty Vector
fALS	Familial ALS
FBS	Fetal Bovine Serum
FUS	*Fused in Sarcoma*
gRNA	guide RNA
H_2O_2	Hydrogen Peroxide
HD	Huntington's Disease
HR	Homologous Recombination
Hsp	Heat shock protein
ICC	Immunocytochemistry
IP	Immunoprecipitation
IPSC	Induced Pluripotent Stem Cell
IR	Ionizing Radiation
LB	Luria-Bertani
MMR	Mismatch Repair
MW	Molecular Weight
ND	Neurodegenerative Disease
NER	Nucleotide Excision Repair
NF-κB	Nuclear Factor-kappaB
NHEJ	Non-Homologous End Joining
•OH	Hydroxyl Radicals
PARP1	poly-(ADP-ribose) polymerase 1
PD	Parkinson's Disease
PDI	Protein Disulphide Isomerase
ROS	Reactive Oxygen Species
RT	Room Temperature
sALS	Sporadic ALS
siRNA	Small-interfering RNA
SOD1	*Superoxide Dismutase-1*
TARDBP	*TAR DNA-Binding Protein*

TBST	Tris Buffered Saline with Tween 20
UV	Ultraviolet
UT	Untransfected
WB	Western Blotting
WT	Wild-type
XRCC1	X-ray repair cross- complementing 1

List of tables

List of figures

Units of magnitude

C	Celsius
Da	Dalton(s)
g	gravitational acceleration at the Earth's surface
g	gram(s)
h	hour
kg	kilogram(s)
L	Litre(s)
mL	milli-Litre
min	minute(s)
M	Molar
n	nano
p	p-value
rcf	relative centrifugal force
rpm	revolution(s) per minute
s	second(s)
SD	Standard Deviation
t	t-statistics
V	Volt(s)
X	magnification
μ	micro

Abstract

Maintaining genomic integrity is essential for all organisms and for the transfer of genetic information from one generation to another. However, DNA undergoes continuous attack from many sources, which can lead to DNA damage and therefore genomic instability. The DNA damage response refers to signalling pathways that aim to detect and repair this damage. DNA damage increases significantly during ageing, which is the biggest risk factor for neurodegenerative diseases such as amyotrophic lateral sclerosis (ALS). ALS is a fatal, rapidly progressing condition in which both the upper and lower motor neurons degenerate. There are few effective treatments for ALS, and whilst DNA damage has been increasingly described in pathophysiology, there are currently no effective ways to prevent damage or enhance DNA repair. Our group has previously shown that a novel protein chaperone, protein disulphide isomerase (PDI), is protective against multiple pathologies associated with ALS. PDI is unique because unlike other chaperones it also possesses oxidoreductase activity, which modulates redox regulation. However, whilst it has been established that PDI is protective against events associated with proteostasis in ALS, it has not been shown that PDI is protective against DNA damage.

The studies from this thesis revealed that PDI is protective against DNA damage following etoposide or H_2O_2 treatment using an in vitro neuroblastoma cell line in which endogenous PDI was knocked down with siRNA. It was also shown that PDI is protective against apoptosis induced by DNA damage. Furthermore, PDI was found to translocate to the nucleus following DNA damage induced by etoposide, implying it has a direct rather than indirect role. Two ALS risk-causing mutants that display impaired redox activity, PDI-D292N and PDI-R300H, along with a PDI-Quad mutant lacking the redox active cystine sites, were also investigated. Whilst PDI-R300H displayed some residual protective activity against DNA damage, PDI-D292N and the Quad mutant were not protective. Hence these results indicate that the redox activity of PDI is protective against DNA damage, but this is perturbed in ALS. By defining these mechanisms further in future studies, these results can lead to design future therapeutics for ALS based on PDI that can prevent DNA damage.

Table of Contents

1. Introduction

1.1. Ageing and Neurodegenerative Disease

According to the World Health Organization (WHO), the ageing population will almost double in the coming decades, and the number of individuals over 60 years is predicted to increase from 12% to 22% between 2015 to 2050 (Ageing and health, 2022; Jaul & Barron, 2017). Several biological processes, including DNA repair and oxidative stress, are impaired during the normal ageing process. In addition, the risk of neurodegenerative diseases increases significantly during ageing (Niccoli et al., 2017), and limited treatments are available for these conditions. Alzheimer's disease (AD), Parkinson's disease (PD), Huntington's disease (HD), and amyotrophic lateral sclerosis (ALS) are major neurodegenerative diseases (Figure 1.1). Moreover, DNA damage is increasingly recognized to be an important mechanism associated with pathogenesis in these disorders. However, there are currently no ways to prevent DNA damage or enhance DNA repair to prevent neurodegeneration.

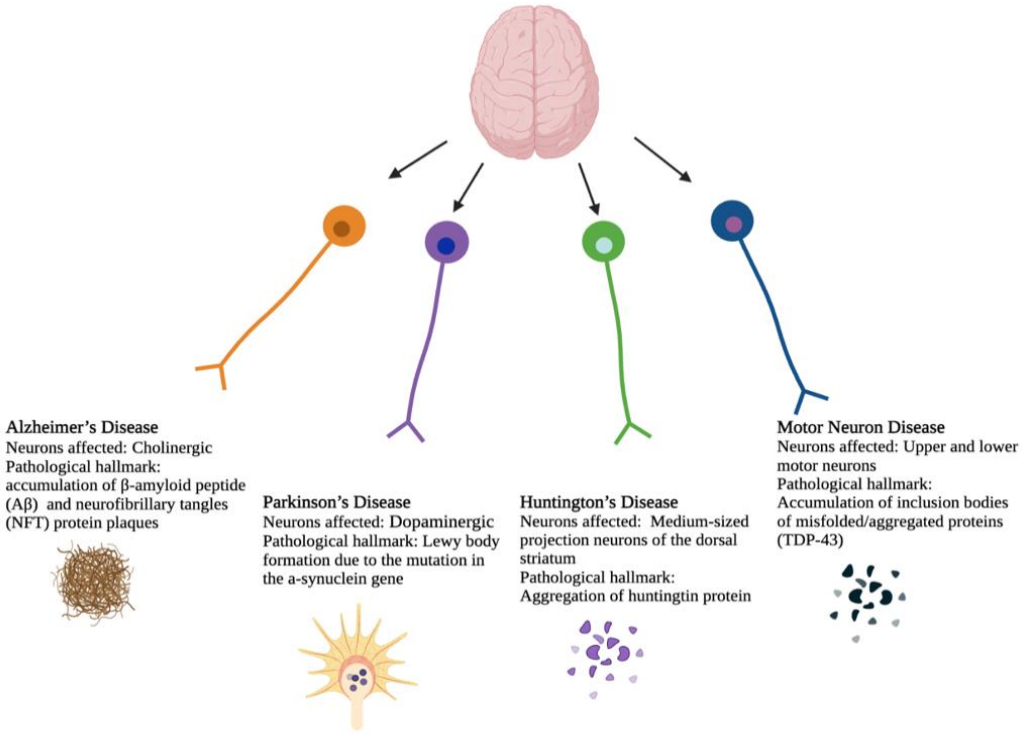

Figure 1.1: A summary of the most prevalent age-related neurodegenerative diseases.

Recently in our laboratory, the involvement of a novel redox-regulated chaperone, protein disulphide isomerase (PDI), was found to be protective against protein homeostasis (proteostasis) related mechanisms in ALS. Proteostasis refers to the integrated mechanisms that regulate proteins within the cell, from their synthesis to degradation. Hoever, receent evidence has shown that the proteostasis and genomic networks are increasingly inter-related, implying that PDI might also be protective against DNA damage. This thesis describes novel findings regarding the protective role of PDI against DNA damage, which are relevant to understanding the pathophysiology of ALS and other neurodegenerative diseases. The following sections (sections 1.2 to 1.9) provide more details about DNA damage, PDI and ALS.

1.2. Deoxyribonucleic Acid (DNA) and DNA damage

Deoxyribonucleic acid (DNA) is the carrier of genetic material in all living beings. It is known as the blueprint of the human body because it transfers genomic information from one generation to another (Fishel et al., 2007). If DNA damage is not repaired, genetic mutations,alteration of cellular functions, compromised cellular viability, and abnormal

biological activities can result (S. P. Jackson & Bartek, 2009). Hence it is very important to protect DNA from endogenous and exogenous damage. However, unlike other biological molecules, DNA cannot be simply re-synthesized (Fishel et al., 2007) and even small amounts of damage to DNA can alter its functionality (Lindahl & Barnes, 2000). In fact, almost all cells of the human body are subject to thousands of DNA lesions each day (Lindahl & Barnes, 2000). Depending on the source of the damage, different types of DNA lesions can be defined. Around 75% of these are single-stranded breaks (SSBs), whereby one DNA strand is damaged (Huang & Zhou, 2020). However, if left unrepaired, SSBs can be further converted to double-stranded breaks (DSBs), involving damage to both strands, and these are more deleterious (Tubbs & Nussenzweig, 2017).

There are several mechanisms to repair DNA that are activated specifically in response to the type of damage. DNA repair processes are known to decline with ageing (Fishel et al., 2007). As neurons are post-mitotic cells, maintaining DNA integrity is essential for normal neuronal function and viability (Fishel et al., 2007). Different types of DNA damage are described in the sections 1.3 and 1.4 below.

1.3. Endogenous DNA damage

Errors in DNA Replication and Mismatches in Basepairs

This type of DNA damage involves the incorrect incorporation of deoxynucleotide triphosphates (dNTPs) during DNA replication, defective replication fidelity due to wrong nucleotide insertion or deletion, or inaccurate base-pairing between two DNA strands (Chatterjee & Walker, 2017; S. P. Jackson & Bartek, 2009; Mertz et al., 2017).

Deamination of DNA Bases

This process involves the lack of exocyclic amination of adenine (A), guanine (G), 5-methyl cytosine (5mC), cytosine (C) to hypoxanthine, xanthine, thymine (T), and uracil (U), where C and 5mC deaminate most frequently (Chatterjee & Walker, 2017; Lindahl, 1979; Waters & Swann, 1998; Wiebauer & Jiricny, 1990). It is more common in single-stranded DNA (Chatterjee & Walker, 2017). Several environmental factors, such as UV light and intercalatingreagents, can also trigger the deamination of DNA bases (Chatterjee & Walker, 2017). Consequently, mutations are formed due to consecutive cycles of DNA replication, and the transition of GC to AT, which accounts for a large portion (1/3) of single-site

mutations (Lindahl, 1979; Waters & Swann, 1998; Wiebauer & Jiricny, 1990; Chatterjee & Walker, 2017).

Methylation of DNA

Every day DNA methylation results in the spontaneous production of 4,000 N7-methylguanine, 600 N3-methyladenine and 10-30 O^6-methylguanine residues by S-adenosylmethionine (SAM), a reactive methyl group donor (Chatterjee & Walker, 2017; De Bont, 2004; Holliday & Ho, 1998; O'Driscoll et al., 1999; Rydberg & Lindahl, 1982; Zhao et al., 1999). Endogenous alkylating agents, choline and betaine, can also be responsible for DNA methylation (Chatterjee & Walker, 2017). These originate from endogenous cellular mechanisms, however, they can be also formed from exogenous sources such as smoke, pollution or even diet (Zhaoet al., 1999 ; Chatterjee & Walker, 2017). DNA methylation causes the transition of G:C to A:T and T:A to C:G in mammalian cells because O^6-methylguanine, O^4-methylthymine and O^4- ethylthymine are highly mutagenic (Rydberg & Lindahl, 1982; Holliday & Ho, 1998; De Bont,2004; O'Driscoll et al., 1999; Zhao et al., 1999; Chatterjee & Walker, 2017). N3-methyladenine can also inhibit DNA synthesis (De Bont, 2004; Chatterjee & Walker, 2017).

Reactive Oxygen Species (ROS) and DNA damage

The formation of reactive oxygen species (ROS) such as hydrogen peroxide (H_2O_2), superoxide ($\bullet O2^-$), singlet oxygen ($^1O2$), and hydroxyl radicals ($\bullet OH$) during cellular metabolism and respiration processes can also induce DNA damage (De Bont, 2004; Chatterjee & Walker, 2017). Low levels of ROS facilitate redox signalling reactions and cellular defense mechanisms to protect cells, however, excessive ROS can oxidise DNA bases (De Bont, 2004; Chatterjee& Walker, 2017). Among ROS, $\bullet OH$ is the most dangerous and abundant species that damages DNA by its addition to hydrogen bonds, thus depleting hydrogen atoms from their methyl groups, and disrupting the sugar backbone of DNA (Chatterjee & Walker, 2017; Cooke et al., 2003; De Bont, 2004; Friedberg, 2005; Segal, 2005). Excess ROS causes the formation of SSBs and DSBs and inhibits transcription processes (De Bont, 2004; Chatterjee & Walker, 2017). The oxidation of DNA also causes transversion of GC to TA after DNA replication (Cooke et al., 2003; De Bont, 2004; Segal, 2005; Friedberg, 2005; Chatterjee & Walker, 2017). Lipid peroxidation, a process whereby free radicals attack caron-carbon double bonds containing lipids, also causes DNA damage (Ayala et al., 2014).

Formation of Abasic Sites

Abasic or apurinic/apyrimidinic (AP) sites are formed by the loss of nucleobases in DNA (Burton E. Tropp, 2011; Chan et al., 2013; Chatterjee & Walker, 2017; Lindahl, 1993). This is produced by spontaneous hydrolyzation of the N-glycosyl bond between the nitrogenous ring and the sugar-phosphate backbone (Lindahl, 1993; Tropp BE. 2011; Chan et al., 2013; Chatterjee &Walker, 2017). The N-glycosyl bond can also become cleaved by DNA glycosylase (Chan et al., 2013; Chatterjee & Walker, 2017). Every day, around 10,000 abasic sites are created in mammalian cells by alterations in pH and/or temperature (Chatterjee & Walker, 2017). These abasic sites form SSBs by β-elimination reactions targeting the 3' phosphodiester bond, which triggers the base excision repair (BER) pathway (Chan et al., 2013; Chatterjee & Walker, 2017).

1.4. Exogenous DNA damage

Exposure to Ultraviolet (UV) and Ionizing Radiation

There are three types of UV radiation, UV-A, UV-B and UV-C based on wavelength (Chatterjee & Walker, 2017; Davies RJ, 1995; Kiefer, 2007; Rastogi et al., 2010) and mammalian cellsbecome exposed to UV-C the most frequently (Davies RJ. 1995; Kiefer, 2007; Rastogi et al., 2010; Chatterjee & Walker, 2017). UV-C radiation damages DNA by forming covalent bonds between two neighbouring pyrimidines (Rastogi et al., 2010; Chatterjee & Walker, 2017). These covalent linkages form two main photoproducts - cyclobutene pyrimidine dimers (CPDs) and pyrimidine (6–4) pyrimidine photoproducts (Davies RJ. 1995; Kiefer, 2007; Rastogi et al., 2010; Chatterjee & Walker, 2017). This results in distortion of the helix by the formation of bulky photoproducts in DNA, the formation of DNA protein crosslinks, photooxidation and the breakage of DNA strands (Davies RJ. 1995; Kiefer, 2007; Rastogi et al., 2010; Chatterjee & Walker, 2017).

Along with UV, ionizing radiation (IR) consisting of X-rays, α,β, or γ-rays also cause DNA damage (Chatterjee & Walker, 2017; Mavragani et al., 2019). IR is present in many environmental factors such as soil, rock, water, and various medical devices used in disease treatment (Mavragani et al., 2019). IR damages DNA by interacting with biological materials from cells and tissues, forming highly reactive hydroxyl radicals (Chatterjee & Walker, 2017; Mavragani et al., 2019). IR also forms SSBs with 3′ phosphate or 3′-phosphoglycolate ends, and DSBs (Chatterjee & Walker, 2017; Mavragani et al., 2019).

Chemical Reagents

Many chemical reagents cause DNA damage, including aromatic amines from tobacco smoke, coal, car fuels, and dyes from industries, alkylating agents from cigarette smoke, chemotherapeutic agents, laboratories, biofuels, and industries, polycyclic aromatic hydrocarbons (PAH) from vehicle exhausts, and fossil fuels (Loechler, 1994; Luch, 2009; Wyatt & Pittman, 2006). Many toxins and electrophiles are also present in the environment, which damage DNA regularly (Wyatt & Pittman, 2006; Loechler, 1994; Luch, 2009). Benzo(*a*)pyrene, a prominent PAH, generates the carcinogen (+)-anti-BPDE, and the intermediates of (±)-anti-BPDE (Wyatt & Pittman, 2006; Loechler, 1994; Luch, 2009). These toxic chemical agents form AP sites and induce G:C to A:T mutations, and weaken glycosylic bonds (Wyatt & Pittman, 2006; Loechler, 1994; Luch, 2009).

1.5. DNA Damage Response (DDR)

The DNA damage response (DDR) refers to the complex signalling pathways by which a cell maintains the integrity of its genome after DNA damage. During the DDR, DNA damage is first sensed by various sensor proteins, and the signal is then amplified by transducer and effector proteins (Chatterjee & Walker, 2017). SSBs and DSBs are sensed by phosphorylated H2A histone family member X (ɣ-H2AX) (Paull et al., 2000), poly (ADP-ribose) polymerase 1 (PARP1) (Schreiber et al., 2002), p53 binding protein (53-bp1) (Schultz et al., 2000), X-ray repair cross-complementing 1 (XRCC1) (Brem, 2005), Ku70/80 (Fell & Schild-Poulter, 2012), and the MRN complex consisting of MRE11, RAD50, and NBS1 (J. R. Walker et al., 2001). Once DNA damage signalling is activated, specific DNA repair pathways are initiated (S. P. Jackson & Bartek, 2009). In proliferating cells, if errors or DNA damage are detected, cell division is stalled at cell cycle checkpoints during the DNA replication step (G1/S checkpoints) or before the division of cells (G2/M checkpoints) (Pellegata et al., 1996). However, neurons are post-mitotic cells, so they do not go through a normal cell cycle (Pan et al., 2014).

Activated ataxia-telangiectasia mutated (ATM) mediates the formation of the phosphorylated form of H2AX (ɣ-H2AX) by the phosphorylation of Seine-139 residue in H2AX, which then activates the repair of DSBs (Burma et al., 2001; S. P. Jackson & Bartek, 2009; Paull et al., 2000). ɣ-H2AX is directly recruited to DSB sites of DNA damage, where it binds as small and round distinct ‘foci’ structures that can be visualized using microscopy (Löbrich et al., 2010).

Hence the formation of ɣ-H2AX foci are widely used as an early DSB marker (Podhorecka et al., 2010). 53-bp1 also plays an important role in sensing DNA damage and activating DSB repair via the ATM pathway (Dahl & Aird, 2017). The Ku70/80 and MRN complex senses DSBs. Ku70/80 mediates DNA repair by forming a ring structure near the DNA damage site, which allows the binding of DNA-dependent serine/threonine protein kinase (DNA-PKcs) to activate downstream DNA repair nucleases (Gottlieb & Jackson, 1993; J. R. Walker et al., 2001). The MRN complex senses two ends of DSBs and mediate DNA repair by the ATM and DNA-PKcs pathways (Moreno-Herrero et al., 2005). In contrast, PARP1 senses SSBs and the accumulation of PARP1 activates SSB DDR pathways (Eustermann et al., 2015) . XRCC1 protein is directly recruited to SSB sites and it accelerates DNA repair by acting as a scaffold protein, which is involved in DNA ligation and DNA end-processing (L. M. Polo et al., 2019). The DDR is linked functionally to multiple other signalling mechanisms, as illustrated in Figure 1.2.

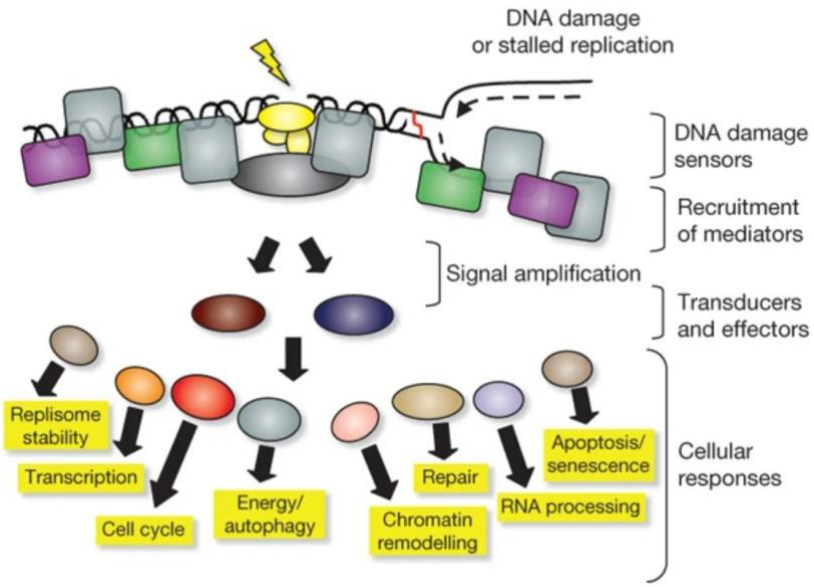

Figure 1.2: A schematic diagram showing the processes involved in DNA damage recognition, signal amplification and initiation of multiple cellular responses. This figure is adapted from (S. P. Jackson & Bartek, 2009).

There are five main DDR pathways to repair SSBs and DSBs: base excision repair (BER), nucleotide excision repair (NER) or mismatch repair (MMR) to repair SSBs, and homologous recombination (HR) or non-homologous end joining (NHEJ) to repair DSBs. However, in neurons, whilst SSBs are repaired by MMR, NER, or BER, DSBs are thought to be repaired only by NHEJ because they lack HR, which requires an active cell cycle

(Boesch et al., 2011; Chang et al., 2017; Dip et al., 2004; Krokan & Bjoras, 2013; Li & Heyer, 2008; Mason & Lightowlers, 2003). Table 1.1 summarises each DNA repair process. For a more detailed understanding, the reader is directed to several excellent detailed reviews on this subject (Chatterjee & Walker, 2017; S. E. Polo & Jackson, 2011).

Table 1.1: The Major DNA Repair Mechanisms.

SSB/DSB	DNA Damage Repair Pathways and Mechanisms	Relevant Organelles	References
SSB	Base Excision Repair (BER): BER works by correcting small base lesions which are caused by methylation, oxidation, and deamination. These base lesions do not cause much damage to the DNA helix.	Nucleus, Mitochondria	(Krokan & Bjoras, 2013); (Boesch et al., 2011);
SSB	Nucleotide Excision Repair (NER): The NER pathway removes and re-synthesizes damaged short DNA strand fragments. The damaged region is recognized by specific endonucleases that remove and restore the sequence.	Nucleus	(Dip et al., 2004); (Boesch et al., 2011).
SSB	Mismatch Repair (MMR): MMR is involved in recognizing and cleaving G:T and G:G mismatches in the DNA helix. MMR mainly repairs nucleotide mismatches However, it is also thought that MMR repairs short loops of DNA damage as well as mismatches.	Nucleus, Mitochondria	(Mason & Lightowlers, 2003); (Boesch et al., 2011).
DSB	Homologous Recombination (HR): HR process has a vital role in repairing DNA DSBs. However, HR is only limited to the S and G2 phases of the cell cycle because HR uses sister chromatid templates to repair DSBs. Hence it is not thought to be a major mechanism in neurons. HR is also involved in DNA replication mechanisms by restoring defective replication forks.	Nucleus, Mitochondria	(Li & Heyer, 2008); (Boesch et al., 2011).
DSB	Non-homologous End Joining (NHEJ): NHEJ is the most common pathway that repairs DNA DSBs in neurons. NHEJ is more error-prone but can occur in any part of the cell cycle. NHEJ pathway is mediated by proteins that first identify the DSB and then facilitate the ligation process for DSBs flexibly. 53-bp1 is specific to NHEJ.	Nucleus, Mitochondria	(Chang et al., 2017); (Boesch et al., 2011); (Gupta et al., 2014)

1.6. Amyotrophic Lateral Sclerosis (ALS)

ALS was first described in the 19th century by a French neurologist, Jean-Martin Charcot (Turner & Swash, 2015), as a disease characterised by the degeneration of motor neurons (Turner & Swash, 2015). ALS involves degeneration of both the upper and lower motor neurons of the brain, brainstem, and spinal cord (Turner & Swash, 2015). In the less common 'primary lateral sclerosis', only upper motor neurons are involved (Gordon et al., 2006) whereas lower motor neurons are targeted in progressive muscular atrophy (Gordon et al., 2006).

The progressive loss of motor neurons leads to wasting of voluntary muscles in ALS patients, leading to increasing paralysis (Turner & Swash, 2015) and impairment of breathing, walking, eating, and speaking (Kiernan et al., 2011). Around 70% of ALS patients have limb-onset disease and 25% of patients have the bulbar-onset form of disease (Kiernan et al., 2011). ALS patients with limb-onset forms display muscle weakness, fasciculations, muscle wasting, and muscle contraction (Duffy et al., 2007; Ferguson & Elman, 2007). However, patients with bulbar-onset ALS face distorted speech, weakness in facial expressions, and weakness in the tongue, resulting in difficulties in swallowing (Kiernan et al., 2011). On average, ALS patients survive for 2 to 4 years after the initial diagnosis and death usually is due to respiratory failure (Chiò, Logroscino, et al., 2009). However, 3-5% of ALS patients suffer from the rarer respiratory form of ALS and die within 1.4 years (Swinnen & Robberecht, 2014). Among ALS cases, 5-10% are characterized as familial (fALS), which are caused by specific genetic mutations. In contrast, 90-95% of ALS cases are sporadic (sALS) with no known hereditary cause (Renton et al., 2014). The mean disease onset age for ALS patients is ~ 63 years (Chio et al., 2002), with 2.5 times more cases in men than in women (Manjaly et al., 2010). Along with motor neurons, non-neuronal cells such as astrocytes and microglia are also involved in neurodegeneration in ALS (Perkins et al., 2021; Zhao et al., 2020).

Only three drugs are approved by the Food and Drug Administration (FDA) for ALS; riluzole (Bensimon et al., 1994), edaravone (Abe et al., 2017), and relyvrio (Paganoni et al., 2020). However, they are not effective in the prevention of neurodegeneration in patients, and only riluzole is available in Australia (Bensimon et al., 1994; Lacomblez et al., 1996;

Miller et al., 2012; Mora, 2017). Hence there is an urgent need to develop new therapeutics. Understanding the molecular processes underlying the degeneration of motor neurons is essential in identifying better therapeutic approaches (Kiernan et al., 2011).

There are more than 50 genetic mutations associated with ALS (Mejzini et al., 2019). Among these mutations, the most frequent cases in Europe/North America are caused by hexanucleotide repeat expansions (HRE) in *chromosome 9 open reading frame 72 (C9ORF72)*, followed by *superoxide dismutase-1 (SOD1)*, *fused in sarcoma (FUS)*, and *TAR DNA-Binding Protein (TARDBP)* genes (Corcia et al., 2017). Mutations in *sequestosome 1 (SQSTM1)*, *ubiquitin 2 (UBQLN2)*, *TANK-binding kinase1 (TBK1)*, *valosin-containing protein (VCP)*, *CCNF* and *optineurin(OPTN)* genes amongst others are also present in the rarer cases of fALS (Renton et al., 2014). ALS-linked mutations have also been detected in *prolyl-4-hydroxylase subunit beta (P4HB)*, the gene encoding PDI (Gonzalez-Perez et al., 2015). Two missense variants were described, p.D292N (PDI-D292N) and p.R300H (PDI-R300H), (Gonzalez-Perez et al., 2015), although these are implicated as risk factors for ALS rather than fALS causing mutations (Gonzalez-Perez et al., 2015). The etiology of sALS cases remain unclear, however, many environmental risk factors and genetic mutations are thought to contribute (Oskarsson et al., 2015). Like other neurodegenerative diseases, ALS is a protein misfolding disorder whereby the key pathological hallmark is the formation of misfolded proteins inclusions in affected tissues (Neumann et al., 2006). In almost 97% of ALS patients, these inclusions contain pathological forms of TDP-43, the protein encoded by *TARDBP* (Prasad et al., 2019).

ALS-related mutations in *SOD1* were first discovered in 1993 (Rosen et al., 1993), and since then SOD1-ALS disease models have been widely studied. *SOD1* encodes an important cytoplasmic antioxidant enzyme, Cu/Zn superoxide dismutase (Rosen etal., 1993), which prevents oxidative stress by the detoxification of superoxide radicals, ($O2^-$) (Valentine et al., 2005). ALS-associated *SOD1* mutations induce oxidative and endoplasmic reticulum (ER) stress, neuronal toxicity, ER-Golgi network dysfunction, neuroinflammation, and hyperexcitability of ALS neurons (Bunton-Stasyshyn et al., 2015; Zhang et al., 2007). The formation of SOD1 protein aggregates (either mutant or wildtype) in neurons is detected in both fALS and sALS (Benkler et al., 2018; Kato et al., 2001; Tak et al., 2020; Watanabe et al., 2001).

In 2008, the link between mutations in the *TARDBP* gene and ALS was first established (Sreedharan et al., 2008). TDP-43 is a DNA/RNA binding protein that is ubiquitously expressed but predominantly present in the nucleus of healthy cells (Y.-F. Xu et al., 2011). In fALS, mislocalization of mutant TDP-43 from the nucleus to cytoplasm occurs whereas in sALS mislocalization of wildtype TDP-43 is present, and cytoplasmic aggregates form in both cases (Neumann et al., 2006; Suk & Rousseaux, 2020). Mislocalized cytosolic TDP-43 loses its normal function in the nucleus, and gains toxic mechanisms in the cytoplasm, and both processes are implicated the progressive degeneration of ALS neurons (Suk & Rousseaux, 2020). The pathological forms of TDP-43 are also truncated and hyper-phosphorylated (Y.-F. Xu et al., 2011). TDP-43 is normally involved in RNA processing (Y.-F. Xu et al., 2011) and recent studies from our group and others have also established that TDP-43 functions in the repair of DNA damage (Guerrero et al., 2019; Konopka et al., 2020; Mitra et al., 2019).

Like TDP-43, FUS is also a DNA and RNA binding protein (Kwiatkowski et al., 2009) that plays a pivotal role in RNA metabolism including transcription and post-transcriptional processes such as mRNA splicing, trafficking and transport (Ratti & Buratti, 2016). Moreover, similar to TDP-43, it also facilitates DNA repair (H. Wang et al., 2018). ALS-causing mutations in FUS are also thought to lead to both loss and gain of toxic functions in pathogenesis (Dormann & Haass, 2013). Similar to TDP-43, FUS mainly exists in the nucleus, however, it also mislocalises to the cytoplasm in ALS (Vance et al., 2009). Aggregates of FUS are also found in both fALS and sALS patient neurons, implying that FUS inclusions are present in the most common forms of ALS, similar to TDP-43 (Kwiatkowski et al., 2009). Whilst this was previously controversial, two recent studies confirmed the presence of FUS inclusions in sALS patients (Ikenaka et al., 2020; Tyzack et al., 2019).

The identification of the *C9ORF72* mutation in ALS was first demonstrated in 2011 (Renton et al., 2011). The GGGGCC expansion within the first intron of the *C9ORF72* gene contain less than 11 repeats in the normal population (Chio et al., 2012). However, in ALS patients these repeat expansions can range from hundreds to thousands (Rutherford et al., 2012). Almost 40% of fALS and 7% of sALS cases are caused by the *C9ORF72* mutation,

respectively (Iacoangeli et al., 2019). The mechanisms by which *C9ORF72* mutations impair biological processes in ALS are not fully known (Sellier et al., 2016), but three hypotheses are implicated. Firstly, loss of function of the C9ORF72 protein, causing haploinsufficiency, secondly, a gain of toxic mechanism due to production of the repeat RNA and lastly, production of dipeptide repeat proteins as a result of repeat associated non-ATG translation (RAN) (Balendra & Isaacs, 2018; Smeyers et al., 2021).

1.7. Molecular mechanisms contributing to neurodegeneration in ALS

It is important to understand the molecular pathways that are involved in inducing neurodegeneration in ALS. It is well established that proteostasis, or protein homeostasis, is disrupted in ALS (Webster et al., 2017). Other molecular pathways involve disruptionin RNA metabolism and mitochondria, interruption in the autophagy process, hyperexcitability, excitoxicity, defects in nucleocytoplasmic transport, DNA damage, neuroinflammation, accumulation of aggregated neurofilaments, and dysfunctional axonal transport (Chen et al., 2022; Goutman et al., 2022). As a multifactorial disease, various environmental factors are thought to contribute to the development of sALS (Armon, 2009; Fang et al., 2010; Michaelson et al., 2017; Spencer et al., 2019; Sutedja et al., 2009), including cyanotoxicity (Michaelson et al., 2017), exposure to chemical reagents and heavy metals (Spencer et al., 2019; Sutedja et al., 2009), pesticides (Spencer et al., 2019), previous brain trauma (Pupillo et al., 2012), physical activities (Abel, 2007; Chiò, Calvo, et al., 2009), tobacco smoking (Armon, 2009; Fang et al., 2010), and viral infections (Verma & Berger, 2006). Interestingly, some of these factors are also implicated in causing DNA damage (H. Wang et al., 2021). Figure 1.3 illustrates the major molecular mechanisms thought to contribute to neurodegeneration in ALS.

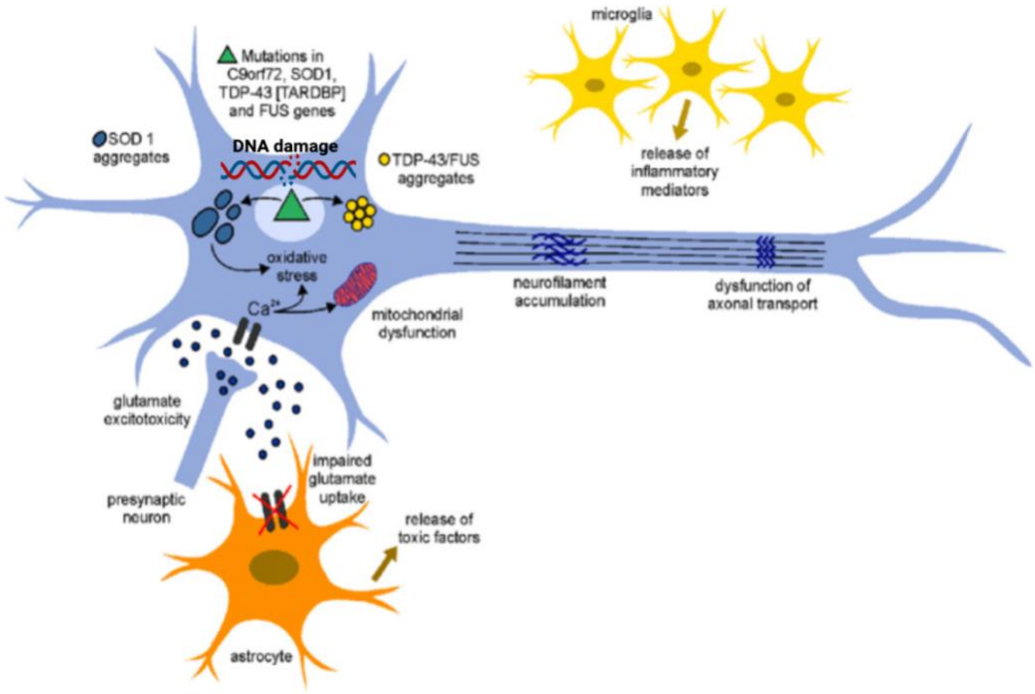

Figure 1.3: A schematic diagram presenting the molecular processes contributing to neurodegeneration in ALS. This figure is adapted from (Bonafede & Mariotti, 2017).

As mentioned earlier, damage to neuronal DNA is increasingly implicated in ALS (Kim et al., 2020). The following section will describe in detail our current understanding of the role of DNA damage in ALS.

1.8. DNA Damage and Repair in ALS

Several studies have identified DNA damage as one of the contributing factors to neuronal death in ALS (Kim et al., 2020; Kok et al., 2021; Sun et al., 2020). A study using induced pluripotent stem cell (iPSC)-derived motor neurons from fALS *SOD1*^{G93A} and *SOD1*^{A4V} patients as well as human post-mortem tissue (Kim et al.,2020) revealed significant DNA damage, including the presence of abasic sites, SSBs, and 8-hydroxy-deoxyguanosine (OHdG, indicative of oxidative stress). This was also present in motor neurons of human post-mortem tissues compared to controls (Kim et al., 2020) along with upregulation of DDR sensor proteins, such as activated c-Abl (a tyrosine kinase), ATM, and breast cancer gene 1

(BRCA1) (Kim et al., 2020). Whilst post-mortem tissues represent disease end-stage, the iPSC findings imply DNA damage is involved earlier in disease (Kim et al., 2020), (Kim et al., 2020). This study therefore showed that DNA damage and activation of the DDR is present in SOD1-associated ALS (Kim et al., 2020).

Another study investigated the consequences of loss of function of *FUS* in ALS (H. Wang et al., 2018) using human neuroblastoma and kidney cell lines, human post-mortem sporadic tissueswith FUS pathology, and iPSC-derived motor neurons with fALS R521H and P525L mutations (Wang et al., 2018). FUS knockdown cells failed to repair endogenous DNA damage compared to the control cell lines (Wang et al., 2018) and FUS was associated with SSB DNA damage sensor proteins PARP1, XRCC1 and LigIII using a co-immunoprecipitation assay (co-IP). These findings indicate that FUS is recruited to DNA damage sites in ALS neurons where it repairs DNA damage (Wang et al., 2018). Furthermore, a 2-fold increase in DNA strand breaks was observed in *FUS* ALS human tissues compared to the control tissues, revealing that DNA damage is present in *FUS*-ALS patients. This study also showed that correction of the R521H and P525L mutations using CRISPR/Cas9 methods also retrieved the functionality of FUS protein in the iPSC-derived motor neurons (Wang et al., 2018). Hence, this study suggests that there FUS functions in the DDR, but this process is perturbed in ALS.

A role for TDP-43 in the DDR has been established in a recent study from our laboratory (Konopka et al., 2020) using NSC-34 motor neuron-like cells and primary cortical neurons expressing familial *TDP-43*^{A315T} and sporadic *TDP-43*^{Q331K} ALS mutations (Konopka et al., 2020). Wildtype (WT) TDP-43 was found to facilitate NHEJ during DSB repair. However, TDP-43 A315T or Q331K mutations lacked the protective nature of WT, causing DNA damage in both cell lines and primary cortical neurons, (Konopka et al., 2020). Furthermore, in tissues from a TDP-43 mouse model, DNA damage was present before disease onset, indicating DNA damage is actively involved in ALS progression. Similarly, two more studies also reported similar findings, showing the involvement of WT TDP-43 in NHEJ and the loss of function by ALS-mutant TDP-43 (Guerrero et al., 2019; Mitra et al., 2019). TDP-43 was found to co-localize with DSB sensor protein Ku70 by co-IP in cell lines (Mitra et al., 2019), and Ku70 was identified as part of the XRCC4-DNA ligase 4 complex involved in NHEJ in iPSC-derived motor neurons (Mitra et al., 2019). Subsequently, sALS

spinal-cord tissues showed the accumulation of TDP-43 aggregates and upregulation of DNA damage markers ɣ-H2AX and phospho-53BP1 compared to controls (Mitra et al., 2019). Enhanced mislocalization of TDP-43 in the cytoplasm activated DDR factors ATM, ɣ-H2AX and phospho-53BP1, and more neuronal death in fALS *TDP-43*^{Q331K} expressing cells compared to controls cells (Guerrero et al., 2019). Similar to FUS, together these studies show that TDP-43 is an essential protein that mediates NHEJ in neurons and thus maintains genomic integrity.

Induction of DNA damage has also been associated with the *C9ORF72* mutation (Konopka & Atkin, 2018). Abnormal secondary DNA structures such as G-quadruplex, hairpins, DNA- RNA hybrids R-loops can induce DNA damage (Mirkin, 2008). The G-rich GGGGCC repeat favours the formation of R-loops and thus the formation of these abnormal DNA structures. The presence of R-loops and DSBs was detected in human cell lines, rat neurons and human ALS spinal cord tissues with *C9ORF72* mutations compared to controls (C. Walker et al., 2017). This was accompanied by impairment of H2A ubiquitylation and hence, defective ATM signalling due to the accumulation of DNA damage (C. Walker et al., 2017). Similarly, another study from our laboratory demonstrated upregulation of DDR markers ɣ-H2AX, phospho-53BP1, activated ATM and PARP1, in motor neurons of human ALS spinal cord tissues compared to controls (Farg et al., 2017), as well as upregulation of ɣ-H2AX and phospho-ATM due to expression of dipeptide repeat proteins (DRPs) (poly(GR)$_{100}$ and poly(PR)$_{100}$) in neuronal cells compared to controls (Farg et al., 2017). Another study showed the link between oxidative stress and the *C9ORF72* mutation (Lopez-Gonzalez et al., 2016). *C9ORF72* motor neurons derived from iPSCs of ALS-patients showed more oxidative stress and DNA damage compared to control motor neurons. Moreover, pharmacological or genetic reduction of oxidative stress improved DNA damage in iPSC-derived *C9ORF72* motor neurons (Lopez-Gonzalez et al., 2016). Hence, these findings reveal that the *C9ORF72* mutation induces DNA damage by the formation of abnormal DNA structures, which can inhibit DNA replication and transcription (Konopka & Atkin, 2018).

In several previous studies, the involvement of oxidative DNA damage in ALS was shown in post-mortem tissues (Calingasan et al., 2005; Shaw et al., 1995), and in cerebrospinal fluid (CSF) (Simpson et al., 2004; Tohgi et al., 1999). A recent study showed that ROS

mechanisms are involved in DNA damage in wobbler mice (Junghans et al., 2022). This mouse model contains a point mutation in the *Vps54* gene leading to progressive degeneration of upper and lower motor neurons (Moser et al., 2013) . The phenotype of the wobbler mouse is similar to ALS as the mouse develops progressive degeneration of upper and lower motor neurons, hence it is used as a disease model (Moser et al., 2013). However, the *Vps54* mutation has not been detected in ALS patients (Meisler et al., 2008). DNA damage associated markers ɣ-H2AX and 53BP1 were significantly upregulated in the spinal motor neurons of wobbler mice compared to controls due to an elevated level of ROS, implying that impedance of redox homeostasis could play a key role in DNA damage in ALS (Junghans et al., 2022). Another study showed that during oxidative stress, phosphorylation of SOD1 by checkpoint kinase 2 (Chk2) leads its translocation to nucleus to protect DNA from oxidative damage in ALS (Bordoni et al., 2019). Figure 1.4 illustrates the processes linking DNA damage to neurodegeneration in ALS.

The involvement of key proteins associated with ALS, particularly FUS and TDP-43, in the DDR is an important finding because it implies that DNA damage is a central mechanism in ALS. Hence novel therapeutics for ALS based on enhancing DNA repair or preventing DNA damage could be designed in future studies. However, there are currently no effective mechanisms to do this in ALS or other neurodegenerative diseases. Our laboratory has previously identified PDI as a possible new therapeutic target for ALS. However, it has not been previously established whether PDI is protective against DNA damage in ALS. The next section will provide more information about the structure of PDI and its roles.

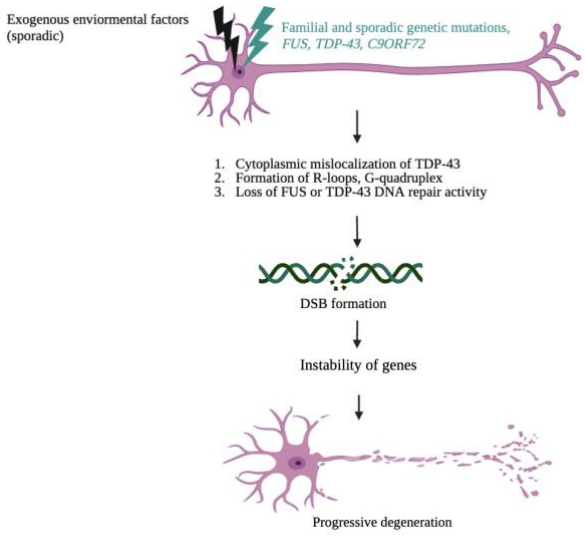

Figure 1.4: The processes by DNA damage is implicated in the progressive death of motor neurons in ALS.

PDI is a chaperone first identified as a folding catalyst from rat liver, that is primarily located in the ER (Goldberger et al., 1963). PDI accounts for almost 0.8% of the total cellular protein, so it is highly abundant (Freedman et al., 1994). As a general chaperone, it aids in the folding of other proteins to form their native confirmations (Freedman et al., 1994; Parakh & Atkin, 2015). However, it also has an oxidoreductase (redox) function whereby it mediates disulphide bond formation in proteins and rearranges incorrect disulphide bonds (Laboissière et al., 1995). PDI is encoded by the *P4HB* gene which encodes a 55-kDa sized protein with 508 amino acids (Kemmink et al., 1997). It has two redox active domains, *a* and *a'*, which contain the cysteine-glycine- histidine-cysteine (CGHC) motif responsible for disulphide bond formation and hence redox regulation (Parakh et al., 2013; Tian et al., 2006). PDI also has two more domains, *b* and *b'*, responsible for substrate binding and protein folding (Parakh et al., 2013; Tian et al., 2006). The x and c domains of PDI facilitate either the flexibility between other domains or the chaperone activity, respectively (Parakh et al., 2013; Tian et al., 2006). The domain structure of PDI is illustrated schematically in Figure 1.5.

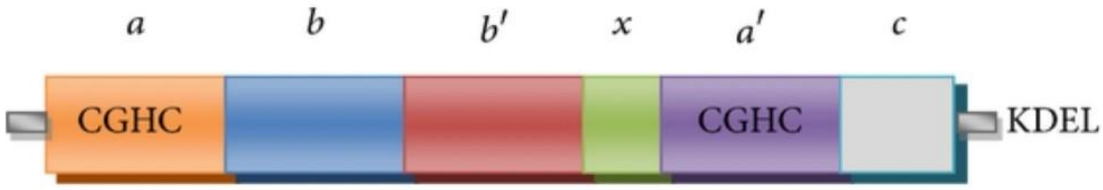

Figure 1.5: Schematic diagram illustrating the domains of PDI. The *a* and *a'* domains are involved in disulphide bond formation and the *b* and *b'* domains mediate the chaperone activity. The *x* domain is associated with mediating flexibility among the domains and the *c* domain also facilitates the chaperone activity. The CGHC motifs of the *a* and *a'* domains mediate disulphide formation and the KDEL at the C-terminus is the ER retrieval signal. This figure is adapted from Parakh et al., 2013.

PDI is upregulated by ER stress in cells (Wilkinson & Gilbert, 2004) and it mitigates this stress by the chaperone activity and by translocating misfolded proteins from the ER to cytoplasm for degradation (Parakh et al., 2013). Although PDI is an ER dominant protein,

it is also found in other locations such as the cytoplasm and nucleus (Lambert & Freedman, 1985; VanderWaal et al., 2002). PDI is the prototype of the PDI family (containing 21 members) and Erp57 is its closest homologue (Appenzeller-Herzog & Ellgaard, 2008). Similar to PDI, ERp57 is found in non-ER locations, including the nucleus where it is observed in the nuclear matrix (Turano et al., 2002). An active role for PDI is implicated in multiple diseases, including cancer (S. Xu et al., 2014), cardiovascular diseases (Ali Khan & Mutus, 2014), infectious disease (Benham, 2012), diabetes (Grek & Townsend, 2014), and neurodegenerative diseases (Andreu et al., 2012).

1.10. The protective role of PDI in ALS

This thesis focusses on the relationship between PDI and DNA damage, and its relevance to ALS. Previously our group showed that PDI is protective against the formation of misfolded mutant SOD1 inclusions and toxicity in neuronal cells (A. K. Walker et al., 2010). Honjo and colleagues subsequently found that PDI was associated and co-localised with SOD1 and TDP-43 inclusions in ALS post-mortem tissues (Honjo et al., 2011), also implying that PDI prevents the formation of misfolded protein aggregates in ALS (Honjo et al., 2011). Our group also showed that PDI co-localises with FUS in human tissues (Farg et al., 2012) and that ERp57 also has a protective role against the formation of misfolded SOD1 inclusions in neuronal cells and primary neurons, (Parakh et al., 2018). Furthermore, TDP-43 and ERp57 partially co-localised in sALS patient tissues indicating a role for ERp57 in sALS (Parakh et al., 2018). Hence, these studies demonstrated that there is a connection between PDI and Erp57 to ALS (Honjo et al., 2011; Parakh et al., 2018).

The mechanism by which PDI performs its protective role was not initially clear. However, a more recent study by our group showed that the oxidoreductase activity, rather than the chaperone activity, of PDI was protective against many cellular pathologies linked to proteostasis that were induced by SOD1, TDP-43 and FUS mutations in ALS (Parakh et al., 2020, 2021). These include mutant SOD1, FUS or TDP-43 misfolding, mislocalization of TDP-43 to cytoplasm, disrupted ER-Golgi and nucleocytoplasmic transport, ER stress, and apoptotic cell death in neuronal cells expressing mutant forms of SOD1, TDP-43, or FUS (Parakh et al., 2020, 2021). PDI and ERp57 were also protective against motor impairment in zebrafish expressing mutant SOD1 and neuromuscular junction (NMJ) connectivity in SOD1 mice,

respectively (Parakh et al., 2020; Rozas et al., 2021). However, a PDI mutant, PDI-Quad (Figure 1.6), lacking the two active site cystine residues that mediate oxidoreductase activity, showed no protectiveness against ALS phenotypes, unlike PDI-WT (Parakh et al., 2020). This mutant was previously shown to retain the chaperone function of PDI but lack all redox activity (Hashimoto et al., 2008; LaMantia & Lennarz, 1993; Whiteley et al., 1997). Furthermore, the previously described PDI mutants detected in ALS patients, PDI-D292N and PDI-R300H (Gonzalez-Perez et al., 2015), were found to lack this redox activity and failed to protect ALS pathologies related to *SOD1* and *TDP-43* mutations (Parakh et al., 2020). Hence these findings reveal that the redox activity of PDI is protective in ALS. They also imply that PDI has potential as a novel therapeutic target in ALS, including against SOD1, TDP-43 and FUS associated fALS cases.

Figure 1.6: Schematic diagram illustrating the mutations present in PDI-Quad. In the PDI-Quad mutant, all four active cystine sites are replaced by serine (SGHS instead of CGHC). This mutant only contains *b* and *b'* domains, which mediate the chaperone activity.

However, PDI can become aberrantly modified by S-nitrosylation, involving the attachment of nitrogen monoxide (NO) to the thiol side chain of its active site cysteine residues, which inhibits its normal oxidoreductase enzymatic activity (Hess et al., 2005). Our group also showed that despite of the upregulation of PDI, it was inactivated by S- nitrosylation in $SOD1^{G93A}$ ALS mice and sALS tissues (A. K. Walker et al., 2010). Another study showed that *S*-nitrosylation of PDI, which is redox dependent, inhibited both the chaperone and redox activities of PDI in mutant SOD1 expressing cell lines, ALS patients and rat primary neurons, compared to controls (Jeon et al., 2014). Hence together these studies show that *S*-nitrosylation of PDI can inhibit its normally protective activities in ALS.

Figure 1.7 summarizes the protective roles of PDI in ALS.

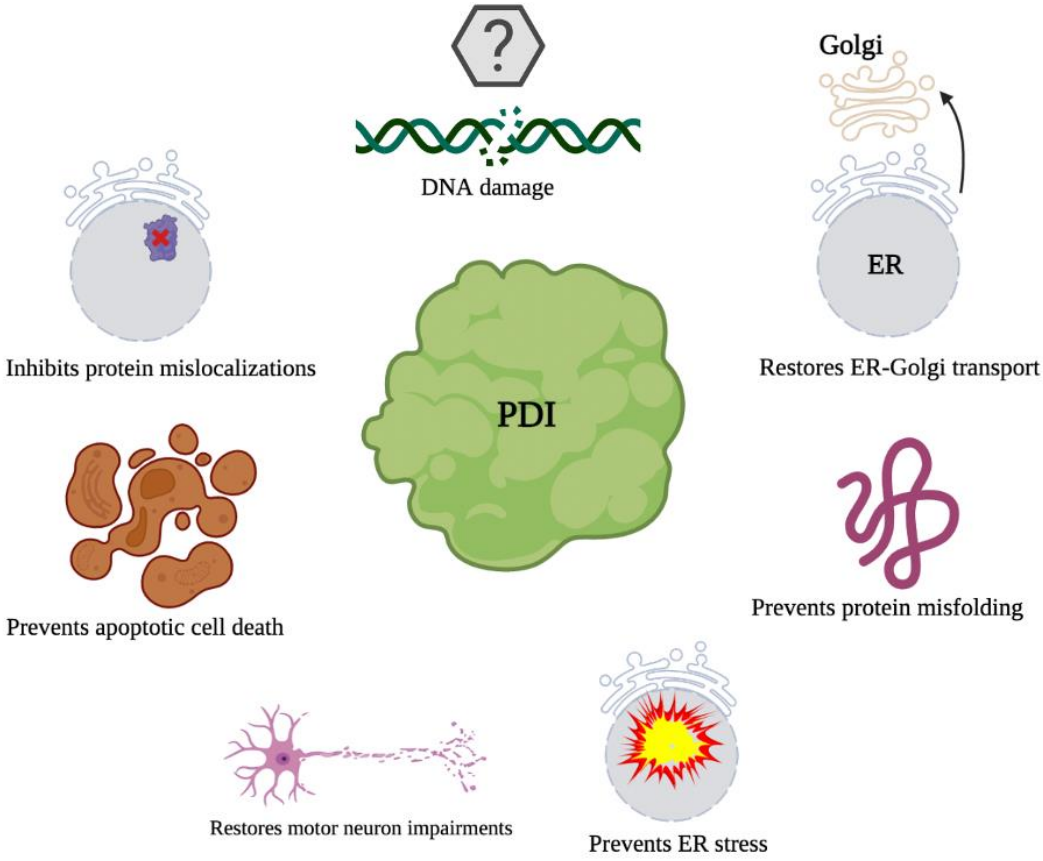

Figure 1.7: A summary diagram showing the protective effect of PDI against ALS phenotypes. The cellular phenotypes involve mechanisms associated with proteostasis. It has not been previously established whether PDI is protective against DNA damage.

Whilst these previous studies show that PDI is protective against proteostasis mechanisms, it remains unclear whether PDI is protective against DNA damage in ALS,which is increasingly implicated as an important pathogenic mechanism. However, there are several lines of indirect evidence that PDI may function in DNA damage. Several previous studies have shown that inhibition or knockdown of PDI proteins downregulates many DNA repair genes (Liu et al., 2019; S. Xu et al., 2019). Similarly, Erp57 binds to DNA (Chichiarelli et al., 2007) and PDI/Erp57 immunoprecipitate with DNA repair proteins, including apurinic/apyrimidinic endonuclease 1 (APE1), an important redox-regulated DNA repair enzyme that mediates BER (Grillo et al., 2006). However, preliminary studies from our group have indicated that overexpression of PDI may inhibit DNA damage induced by etoposide or hydrogen peroxide, as assessed by the formation of ɣ-H2AX foci.

1.11. Aims of this thesis

In summary, PDI has shown to be protective against many cellular pathologies present in ALS. Whilst our preliminary studies indicated that overexpression of PDI may inhibit DNA damage, this has not been previously examined in the absence of artificial protein overexpression. Furthermore, it remains unclear whether PDI acts directly, at sites of DNA repair, or indirectly by modulating redox conditions in the nucleus. Furthermore, it remains unclear whether the ALS-associated PDI mutations are also protective against DNA damage.

Hypothesis

In this thesis it was hypothesized that (i) PDI has a direct protective function against DNA damage, and (ii) that the ALS-associated PDI mutants lack this protective activity, resulting in DNA damage.

Aims

To address this hypothesis, the studies described in this thesis aimed to:

1. Investigate the protective role of endogenous PDI in DNA damage by knocking down PDI with siRNA.
2. Investigate whether PDI has a direct function in the DDR by examining its cellular location following DNA damage and whether it interacts with ɣ-H2AX.
3. Investigate whether the redox activity of PDI is protective against DNA damage using redox-inactive ALS-associated, PDI-D292N, PDI-R300H and Quad mutants.

2. Methods and Materials

2.1. Molecular biology techniques

2.1.1. Preparation of Luria-Bertani (LB) medium

Firstly, 20 g of LB broth was dissolved in 1 L of milli-Q water and autoclaved. This liquid mixture was used as a culture media for *Escherichia coli* (*E. coli*). Then a final concentration of 50 μg/ml of the antibiotic ampicillin was added to nuclease-free H_2O (Milli-Q) water, from a stock concentration of 100 mg/ml.

2.1.2. Isolation of small and large-scale plasmids

From previously prepared glycerol stocks stored at -80ºC, 1 μl of bacterial strain previously transformed with the desired plasmid was inoculated into ~ 30 ml LB medium to prepare a culture for midipreparations of plasmid. Then 50 μg/ml ampicillin was added and incubated at 37ºC for 16-18 h at ~ 250 rpm. After centrifuging (Heraeus X3R Centrifuge) at 4500 rpm (4528 g) at 4ºC for 25 min, following the manufacturer's protocol, plasmid DNA (Table 1) was then isolated using QIAGEN PLASMID PLUS midi kits (Qiagen, Hilden, Germany). Plasmid DNA was eluted with 80 μl nuclease-free H_2O (Milli-Q) and stored at -20°C.

2.1.3. Preparation of glycerol stocks

Glycerol stocks were prepared for long-term storage of plasmids using sterile (autoclaved) 80% glycerol (Sigma-Aldrich, Australia). Bacterial culture was mixed with 80% glycerol in a 1:1 (v/v) ratio in nuclease free water and the stocks were stored at -80°C.

2.1.4. DNA quantification

For quantifying DNA concentrations, a nanodrop 2000 spectrophotometer (ThermoScientific) using a conversion of 1.0 optical density (O.D.) at 260 nm for double-stranded DNA = 50 ng/μL was used. This is based on the principle that nucleic acids absorb ultraviolet (UV) light at precise wavelengths, and for pure DNA, the maximum absorbance is approximately 260 nm. The A260/A280 ratio was used to examine the purity of DNA, where A260 < 1.75/A280 < 1.85 was considered satisfactory. The DNA concentration was analysed using Nanodrop-2000

software (ThermoScientific).

2.1.5. Constructs

The constructs used in this project are described in Table 2.1 below. A map of backbone vector pcDNA3.1(+) is attached in Appendix 1.

Table 2.1: **Plasmids used in this study.**

Plasmid	Vector	Tag	Antibiotics	Source
Empty vector	pcDNA3.1(+)	NA	Ampicillin	Professor Casanova, Rockefeller University, New York
PDI-WT	pcDNA3.1(+)	V5	Ampicillin	Professor Neil Bulleid, University of Glasgow, UK
PDI-Quad	pcDNA3.1(+)	V5	Ampicillin	Generated by former master's student
PDI-D292N	pcDNA3.1(+)	V5	Ampicillin	Professor Claudio Hetz, University of Chile, Chile
PDI-R300H	pcDNA3.1(+)	V5	Ampicillin	Professor Claudio Hetz, University of Chile, Chile

2.2. Cell culture techniques

2.2.1. Fetal bovine serum (FBS)

FBS (Bovogen Biologicals, Victoria, Australia) was stored at -20°C until required. It was firstly thawed to room temperature (RT) and then heated in water bath at 60°C for 30 min by repeated inversion to heat inactivate the complement system, antibodies, and enzymes present in the serum. Finally, the heat-inactivated FBS was distributed into 50 ml aliquots and kept frozen at -20°C for future usage.

2.2.2. Maintenance of mammalian cell culture

The mouse neuroblastoma cell line, Neuro2a, purchased from Cellbank Australia (cat. 89121404), was used throughout this study. Cells were cultured in a T75 flask (Corning, NY, USA) and maintained in Dulbecco's Modified Eagle's Medium-high in glucose (DMEM) (cat.

11995, Gibco, Waltham, MA, USA) containing 10% (v/v) heat-inactivated FBS. Mammalian cells were kept in a CO_2 incubator at 37°C (Heracell 150i CO_2 Incubator, ThermoFisher Scientific, Waltham, MA, USA). Cell growth was monitored daily using a brightfield microscope (Olympus CKX41). Fresh DMEM containing FBS was applied to the cell culture every 2-3 days depending on cell growth.

When the Neuro2a cells were ~ 80-90% confluent, they were passaged. Firstly, cells were washed with phosphate-buffered saline (PBS, 3.2 mM Na_2HPO_4, 0.5 mM KH_2PO_4, 1.3 mM KCl, 135 mM NaCl, pH 7.4) (cat. 20012, Gibco, Waltham, MA, USA) and then treated with 1x Trypsin-EDTA (Gibco, Waltham, MA, USA) to detach cells from the flask. They were then incubated in a CO_2 incubator for ~ 2 min at 37°C, and the dissociated cells were washed with 1x DMEM containing 10% FBS and collected in a 15 ml falcon. Subsequently, cells were centrifuged at 1000 g for 5 min at room temperature. The cell pellet was then resuspended in 1x DMEM with 10% FBS. The total number of cells present was counted using a Countess II Automated Cell Counter (cat. AMQAX1000, ThermoFisher Scientific, Waltham, MA, USA). Using the calculated seeding density, cells were then plated into 6-well (cat. 3516, Corning, NY, USA) or 24-well (cat. 3524, Corning, NY, USA) plates, or T25 flasks (cat. 353014, Corning, NY, USA) when required for specific experiments. For maintaining the cell line, they were sub-cultured into T75 flasks (Corning, NY, USA) using a 1:10 dilution factor.

2.2.3. Transfection

At ~ 75% confluency, Neuro2a cells were transiently transfected with the appropriate plasmids using the manufacturer's protocol with lipofectamine 2000 (1 mg/ml) (Invitrogen, Waltham, MA, USA) and 1x Opti-MEM medium (cat. 31985, Gibco, Waltham, MA, USA). For 24-well and 6-well plates, cells were plated at densities of 2.5 x 10^4 and 25 x 10^4, respectively. Firstly, the appropriate DNA or siRNA was added to opti-MEM in one Eppendorf 1.5 ml tube and lipofectamine 2000 was mixed with opti-MEM in another tube. After 5 min incubation at room temperature, the appropriate volume of lipofectamine 2000 and opti-MEM mix was transferred to the other tube with DNA or siRNA mixture in opti-MEM to produce a transfection master mix. This was incubated for 20 min at room temperature before adding to cells. Transfected cells were stored for 5 h in an incubator at 37°C (Heracell VIOS 160i CO_2 Incubator, ThermoFisher Scientific, Waltham, MA, USA). The media containing DNA was replaced with fresh DMEM with 10% FBS, and cells were placed back in the incubator with 5% CO_2 for 72

hours.

For siRNA experiments, using the manufacturer's protocol, PDI targeting siRNA (cat. DHA-L-HUMAN-XX-0010, Dharmacon, Lafayette, CO, USA), and scrambled siRNA (cat. DHA-D-001810-10-05, cat. DHA-D-001810-10-05) were resuspended in 1x siRNA buffer. The siRNA buffer was prepared from 5x siRNA buffer (Dharmacon, Lafayette, CO, USA) by performing a 1:5 (v/v) dilution in RNase-free water (Dharmacon, Lafayette, CO, USA). Several different concentrations of PDI siRNA (0 nM, 20 nM, 40 nM, 60 nM, 80 nM, 100 nM, and 120 nM) were examined in Neuro2a cells to detect the most effective concentration to silence PDI protein. The optimum concentration for PDI was determined to be 100 nM (see section 3.1) was used in all subsequent experiments. For plasmid transfection, 1 μg of plasmid DNA was used in all experiments.

2.2.4. Treatment with DNA damage inducers

After 72 h transfection, cells were treated with pharmacological agents to induce DNA damage, either etoposide (Sigma-Aldrich, Burlington, MA, USA) or H_2O_2 (cat. AJA260, Ajax Finechem, NSW, Australia). Cells were treated with 100 μM H_2O_2 for 1 h in the dark. Alternatively, cells were treated with 13.5 μM Etoposide for 30 min. During both treatments, cells were incubated at an incubator at 37ºC (Heracell VIOS 160i CO_2 Incubator, ThermoFisher Scientific, Waltham, MA, USA).

2.3. Protein chemistry methods

2.3.1. Preparation of cell lysates for western blotting (WB) and immunoprecipitation (IP)

Cell lysates were prepared for western blotting following transfection or DNA damage treatment. Firstly, ~ 30 x 10^4 cells were washed with ice-cold PBS (Gibco) and then incubated with ice-cold radio-immunoprecipitation assay (RIPA) buffer (50 mM Tris pH 7.5,150 mM NaCl, 1% NP-40, 5 mM EDTA, 0.5% sodium deoxycholate, 0.1% SDS, 1mM PMSF) with protease inhibitor cocktail (cat. 04693159001, 'cOmplete' tablets mini, Roche, Basel, Switzerland) and 1% (w/v) phosphatase inhibitor (cat. 04906837001, PhosStop, Roche, Basel, Switzerland). After 15 min, cells were scraped and collected in 1.5 ml Eppendorf tubes. The cell lysates were kept on ice and vortexed every 5 min for 30 min before centrifugation at 4ºC

for 25 min at 13,000 rpm (12,298 g).

For immunoprecipitation, Neuro2a cells were seeded at a density of $4x10^6$ on T150 flasks (Corning, NY, USA). The following day, cells were trypsinized and collected in a 15 ml falcon and centrifuged for 5 min at 1000 rpm (~ 200 g). After discarding the supernatant, cell pellet was resuspended in 1 ml PBS (Gibco). After counting the cells, the volume of non-denaturing NP-40 lysis buffer, pH 7.4 (20 mM Tris-HCL pH 7.4, 150 mM NaCl, 2 mM EDTA, 1% (v/v) NP-40) with PP (protease inhibitor cocktail (Roche) and 1% (w/v) phosphatase inhibitor (Roche) was calculated. Cells were centrifuged one more time at 1000 rpm (~ 200 g) at 5 min and resuspended in lysis buffer. After incubating for 30 min on ice, the cell lysates were centrifuged at 4°C for 20 min at 13,000 rpm (~12,298 g). Finally, the supernatants were gently collected in new 1.5 ml Eppendorf tubes. Then total protein concentration was determined performing a Bicinchoninic acid (BCA) assay by following the manufacturer's guide.

2.3.2. Bicinchoninic acid (BCA) protein assay

A BCA assay was used to determine the protein concentration of cell lysates, where 0-2 mg/ml of bovine serum albumin (BSA) (Thermo Scientific) were used as protein concentration reference standards to determine the concentration of protein in each lysate. Both the BSA standards and the experimental samples were added to a 96-well plate (cat. 3599, Corning, NY, USA) in duplicates to a volume of 10 µl and 200 µl BCA reagent was added to each well, followed by incubation for 30 min at 37°C. The absorbance of each well was then measured with a PHERstar FS microplate reader at a wavelength of 562 nm. Protein concentrations were determined for western blotting experiments by comparison to the reference standards.

2.3.3. Immunoprecipitation

Immunoprecipitation of 1 mg/ml (w/v) of specifically prepared cell lysates was performed using either an anti-PDI or an isotype control antibody. For immunoprecipitations, 1 µg of PDI (cat. ab2792, Abcam, Cambridge, UK) or IgG (cat. sc-2025, Santa Cruz Biotechnology, Dallas, Texas, USA) antibodies were added to either untreated or etoposide-treated cell lysates and incubated on a rotating wheel for overnight at 4°C. Normal mouse IgG was used as an isotype control for this study. The next day, samples were then collected incubated on ice until required. Protein A/G PLUS-Agarose beads (cat. sc-2003, Santa Cruz Biotechnology, Dallas, Texas, USA), containing both protein A and protein G conjugated to agarose beads, were used

to pull down the antibodies. The beads were first centrifuged for 1 min at 2000 rpm (~ 420 g) and resuspended in 1% (v/v) NP-40 lysis buffer before being added to each lysate (30 µl). Following a 2 h incubation at 4ºC on a rotating wheel, the samples were centrifuged for 1 min at 2000 rpm (~ 420 g) at 4ºC to pellet the beads. The supernatant was discarded, and pellets were resuspended in 0.1% NP-40 lysis buffer, followed by another 2 min incubation at 4ºC on a rotating wheel, and then centrifuged for 1 min at 2000 rpm (~ 420 g) at 4ºC. This washing step was then repeated three times. After that IP samples were run immediately on a gel following the steps mentioned below.

2.3.4. SDS polyacrylamide gel electrophoresis (PAGE) and western blotting

Equal amount (20 µg) of protein samples was prepared using SDS loading buffer from 4x Laemmli sample buffer (cat. 1610747, Bio-Rad, Hercules, California, USA) and 10X NuPAGE Sample Reducing Agent (cat. NP009, Invitrogen, Waltham, MA, USA). The proteins were denatured by boiling in a heat block for 6 min at 95ºC and analysed using 4-15% gradient SDS-PAGE gels (Bio-Rad). To estimate the molecular weights (MW) of proteins resolved by SDS-PAGE, 6 µl of Precision Plus Protein Dual Colour Standards (Bio-Rad) were also loaded onto the gel. Electrophoresis was performed at 80 V to 110 V for 1 h at RT with 1x running buffer (25 mM Tris, 192 mM Glycine and 0.1% (w/v) SDS, pH 8.3). Proteins were then transferred to 0.45 mm nitrocellulose membranes (cat. 162-0115, Bio-Rad) using a Trans-Blot Turbo semi-dry Transfer System (Bio-Rad) for 30 min using 1x semi-dry transfer buffer (48 mM Tris, 39 mM Glycine, 0.037% (w/v) SDS, 20% Methanol, pH 8.5) for low to medium MW proteins (low MW: < 30 kDa and medium MW: 37-74 kDa). Alternatively, the wet transfer method was performed for higher molecular weight proteins (high MW : > 74 kDa) (Kuna et al., 2018), using 1x neutral wet transfer buffer (3 g Tris, 14.8 g Glycine, 20% Methanol). For performing wet transfer, a wet electroblotting system from Bio-Rad was used for 2 h in the 4ºC cold room.

After transferring, the membrane was washed three times with milli-Q water. The membrane was then incubated with 0.1% (w/v) Ponceau S solution in 5% acetic acid (cat. SLCF9006, Sigma-Aldrich) to stain all protein on the blot, followed by three more washes with milli-Q water. Subsequently, the membrane was blocked for 1.5 h with 5% (w/v) BSA (cat. A7906-500G, Sigma-Aldrich, Burlington, MA, USA) or 5 % (w/v) skim milk in 1x Tris Buffered Saline with Tween 20 (TBST) (20 mM tris-HCl, pH 7.4, 0.5 M NaCl, 0.1% Tween 20) at room temperature. Meanwhile the gel was incubated with Coomassie stain (cat. 1610786, Bio-Rad) to identify any remaining bands on gel and thus determine if the transfer had been successful.

Once the blocking step was complete, the membrane was washed three times with 1x TBST and incubated overnight at 4ºC with the appropriate primary antibodies (Table 2), which were diluted in the appropriate blocking buffer (5% (w/v) BSA or skim milk). Then the membrane was washed 3x with TBST and incubated with specific secondary antibodies (Table 2) for 1 h at room temperature with shaking. The membrane was then washed in TBST three times and proteins were detected by adding 800 µl of ECL chemiluminescent reagents from Bio-Rad: Clarity Western ECL Substrates, Luminol/enhancer solution, and Peroxide solution. Subsequently, imaging was performed using a ChemiDoc MP imaging system from Bio-Rad. Western blotting images were then used to quantify the protein bands using densitometry with ImageJ software (v. 1.53) (National Institutes of Health (NIH).

Table 2.2: Antibodies used in Western blotting experiments.

Serial No.	Name	Host Species	Class	Antibody Type	Company	Catalogue Number	Dilution
1	PH4B/PDI	Mouse	Monoclonal	Primary	Abcam	ab2792	1:1000
2	GAPDH	Rabbit	Polyclonal	Primary	Sigma-Aldrich	G954	1:1000
3	ɣ-H2AX	Rabbit	Polyclonal	Primary	Novus Biologicals	NB-100-384	1:2000
4	Goat anti-mouse IgG/IgM HRP	Mouse	Polyclonal	Secondary	Merck Millipore	AP130P	1:3000
5	Goat Anti-Rabbit IgG HRP, Peroxidase Conjugated	Rabbit	Polyclonal	Secondary	Merck Millipore	AP132P	1:3000

2.4. Microscopy

2.4.1. Immunocytochemistry (ICC)

After Neuro2a cells were transfected with siRNA or plasmids and treated etoposide or H_2O_2, DMEM was removed from the 24-well plate and cells were washed with PBS for two times. Then Neuro2a cells were fixed with 4% paraformaldehyde (PFA) for 20 min at room temperature in the dark. After that, cells were permeabilized with 0.1% (v/v) Triton-X in PBS (Gibco) for 15 min at room temperature, followed by blocking with 3% (w/v) BSA in PBS (Gibco) for 1.5 h at room temperature. Cells were then incubated with the appropriate primary antibodies diluted in 1% BSA (Table 3) overnight at 4^{o}C. The subsequent day, cells were washed with PBS (Gibco) and then incubated with the appropriate secondary antibodies (Table 3) for 1 h at room temperature. These steps were performed in darkness to avoid photobleaching. The cells were then washed with PBS (Gibco) and the nuclei were stained with Hoechst (cat. no. 33342, Sigma-Aldrich) at a 1:3000 dilution for 7 min at room temperature. Cells were washed again with PBS (Gibco) and mounted on slides (cat. no. SF41296SP, ThermoFisher Scientific), facing down in 3 µl Dako mounting medium (cat. no. S3023, Dako).

Table 2.3: Antibodies used in ICC experiments.

Serial No.	Name	Host Species	Class	Antibody Type	Company	Catalogue Number	Dilution
1	ɣ-H2AX	Rabbit	Polyclonal	Primary	Novus Biologicals	NB-100-384	1:500
2	PH4B/PDI	Mouse	Monoclonal	Primary	Abcam	ab2792	1:500
3	Anti-V5	Mouse	Monoclonal	Primary	Invitrogen	P/N 46-0705	1:500
4	Goat anti-Rabbit IgG (H+L) Cross-Adsorbed, Alexa Fluor 488	Rabbit	Polyclonal	Secondary	Invitrogen	A11008	1:500
5	Donkey anti-Mouse IgG (H+L) Highly Cross-Adsorbed, Alexa Fluor 594	Mouse	Polyclonal	Secondary	Invitrogen	A21203	1:500

2.4.2. Image Acquisition

Fluorescently labelled Neuro2a cells were captured using a Zeiss LSM 880 confocal microscope or a Zeiss Axioimager epifluorescence microscope. 40X and 63X magnifications were used to capture images. For channels, DAPI, Alexa Fluor 488 and Alexa Fluor 568 were chosen to visualize cells for nuclei (blue), ɣ-H2AX (green) and PDI (red), respectively. All images were taken with epifluorescence microscope unless stated otherwise.

2.4.3. Analysis of ɣ-H2AX foci

DNA damage was identified by the presence of ɣ-H2AX foci in Neuro2a cells. The number of foci per cell (Mah et al., 2010) was calculated using Zen blue software (edition 3.4) (Oberkochen, Germany). A total of 50 cells per replicate were examined.

2.4.4. Analysis of apoptotic nuclei

Abnormal cellular morphology with condensed (≤ 5 μm in diameter) or fragmented nuclei (numerous condensed Hoechst-positive formations in a single cell) were counted as cells undergoing apoptosis (Elmore, 2007). Using ImageJ software (v. 1.53) (NIH), the percentage of apoptotic nuclei were counted. Apoptotic nuclei were quantified as a percentage of non-apoptotic cells, from at least 100 cells expressing the desired plasmid.

2.4.5. Analysis of PDI intensity inside nucleus relative to whole cell

Using ImageJ, the ‘corrected total cell fluorescence (CTCF)’ was measured to determine the endogenous fluorescence of PDI inside nucleus relative to whole cell (Parakh et al., 2018). Briefly, 50 cells were selected using the freeform selection tool from ImageJ, and then from ‘Analyze’ menu, ‘Set measurements’ was selected by ticking ‘Area’, ‘Integrated Density’ and ‘Mean Gray Value’. Subsequently, cell fluorescence was measured inside nucleus and a region next to each cell without fluorescence was selected as background. Then cell fluorescence was measured for the whole cell. The formula used for CTCF was: CTCF = Integrated Density – (Area of Selected Cell x Mean Fluorescence of Background Readings). Once CTCF was calculated, the CTCF for PDI inside nucleus was divided by the CTCF for PDI in whole cell to achieve this data.

2.5. Preparation of the figures

All the figures in this thesis were prepared with biorender.com unless states otherwise.

2.6. Generation of PDI CRISPR-Cas9 cell lines

This experiment was performed with the assistance of another member of the laboratory (Ms Julie Hunter). Neuro2a cells were transfected with 3 μg of PDI-CRISPR plasmid when there was ~ 70% cell confluency in a 6-well plate using lipofectamine following the method above (section 2.2.3). PDI-CRISPR plasmid was designed using CRISPR/Cas9 method, which does not have the PDI gene by Dr Sina Shadfar and Dr Cyril Jones Jagaraj. The guide RNA (gRNA) was designed with GeneArt CRISPR Nuclease Vector with OFP Reporter Kit by ThermoFisher. Vector plasmid is attached in Appendix 2. Following 48 h transfection, cells were transferred into 96-well plates by serial limiting dilution so that only one cell per well was present. After one week incubation at 37ºC in 5% CO_2 incubator, wells were examined every 2 days and wells with only single cell colonies were identified. Two-three weeks later, single cell colonies from the 96-well plate were transferred into a 24-well plate until confluent, before being transferred to a 12-well plate. Once the 12-well plate was confluent, cells were transferred to a 6-well plate and T25 flasks. Cell lysates were prepared from 6-well plates and western blotting was performed on cell lysates to detect a PDI knock-out clone. Membrane was imaged using ChemiDoc from Bio-Rad.

2.7. Statistical Analysis

All data were statistically analyzed using GraphPad Prism (v. 9.3.1) (San Diego, CA, USA). One-way ANOVA followed by *post-hoc* Tukey test or t-test with Welch's correction was used to analyze all data. Welch's correction is used when it is assumed that two samples do not have same standard deviation. All data are represented as mean $\pm$ standard deviation (SD). P-values of 0.05 or less were considered significant for all data, * $p < 0.05$, ** $p < 0.01$, *** $p < 0.001$, **** $p < 0.0001$. Total 150 cells were counted for each experiment from n = 3 biological replicates unless stated otherwise.

3. Results

Given previous preliminary studies from our had established that overexpression of PDI inhibited DNA damage, we first aimed to examine the role of endogenous PDI, representing a different paradigm and arguably more physiological conditions. For this purpose, we aimed to both knockdown PDI using siRNA and knockout PDI using CRISPR/Cas9 methods.

3.1. Optimization of the PDI siRNA concentration to knockdown endogenous PDI in Neuro2A cells

siRNA targeted against PDI was previously designed and used successfully to knockdown its expression in another neuronal cell line (NSC-34) by our group (A. K. Walker et al., 2010). Hence the same siRNA was used here, with a control scrambled (non-targeting) siRNA as a negative control. Scrambled siRNAs have the same nucleotide composition, but not the same sequence, as the target siRNA. Hence they should not target the gene of interest, and they provide a baseline to evaluate the specificity of targeted siRNA-treated samples (Buehler et al., 2012). In this study, the mouse neuroblastoma cell line, Neuro2a, was used because it displays neuronal morphology and was originally isolated from brain tissue (Ferrari et al., 2018).

First, to determine the siRNA concentration required for the most efficient knockdown of PDI, Neuro2a cells were transfected with 0 nM, 20 nM, 40 nM, 60 nM, 80 nM, 100 nM and 120 nM of PDI siRNA or 80 nM control scrambled (non-targeting) siRNA or untransfected cells. At 72 h post-transfection, cell lysates were collected to perform western blotting using a PDI antibody and GAPDH as a loading control (Figure 3.1 (A)). Quantification of the band intensity using densitometry revealed that using the lowest (0-20 nM) or highest (120 nM) concentrations of PDI siRNA there was little effective knockdown for PDI because the PDI band was still present. However, using 100 nM PDI siRNA reduced levels of PDI effectively: 17-fold decrease compared to control (untransfected or UT, without lipofectamine) group and 18.4-fold increase compared to scrambled or non-targeting siRNA (Figure 3.1 (B)). To further confirm this result, this experiment was then repeated using four separate cell lysates prepared with 100 nM PDI siRNA along with two other controls, scrambled siRNA and UT. Western blotting was performed using a PDI antibody and GAPDH as a loading control (Figure 3.1 (C), *Top panel*). Quantification revealed that there was a significant 4.6-fold decrease in PDI expression compared to scrambled siRNA (* $p < 0.05$) and a significant 4.5-fold decrease compared to the UT group (Figure 3.1 (C), *Bottom panel*), confirming the knockdown of PDI

using this siRNA.

Given that the experiments investigating DNA damage need to be performed in the presence of the pharmacological agent, etoposide, the knockdown of PDI was then investigated further in etoposide treated cells. We also decided to confirm knockdown using another technique, immunocytochemistry (ICC), to validate the western blotting results. UT cells, scrambled siRNA and PDI siRNA transfected cells were treated with previously optimized 13.5 μM etoposide to induce DNA damage for 30 mins. The concentration and duration of etoposide treatment to induce DNA damage without cell death induction in Neuro2a cells was previously optimized in our laboratory (Konopka et al., 2020). The cells were then fixed and immunocytochemistry using an anti-PDI (red) antibody was performed (Figure 3.1 (D), *Top panel*). After fluorescence imaging, PDI expression in individual cells was then measured with ImageJ. It was observed that there was a significant decrease in PDI expression in PDI siRNA transfected cells compared to scrambled siRNA (**** $p < 0.0001$) and UT (**** $p < 0.0001$) cells following etoposide treatment (Figure 3.1 (D), *Bottom panel*). Hence this result shows that in the presence of etoposide, there is a significant knockdown of PDI using the specific siRNA. We aimed to then confirm this result using western blotting with lysates from cells treated with etoposide. Cell lysates were prepared from cells transfected with either PDI siRNA or controls, scrambled siRNA and UT, and western blotting performed using antibodies against PDI antibody and GAPDH as a loading control (Figure 3.1 (E), *Top panel*). A decreasing trend for reduced PDI expression was detected in PDI siRNA transfected lysates compared to scrambled siRNA and UT samples (Figure 3.1 (E), *Bottom panel*). However, due to time constraints, it was only possible to perform two replicates for this experiment and the result did not reach statistical significance. Hence, in the future, this experiment needs to be repeated.

Hence overall these results indicate that 100 nM is an effective concentration to knockdown endogenous PDI in Neuro2a cells via siRNA transfection, both in the absence and the presence of etoposide.

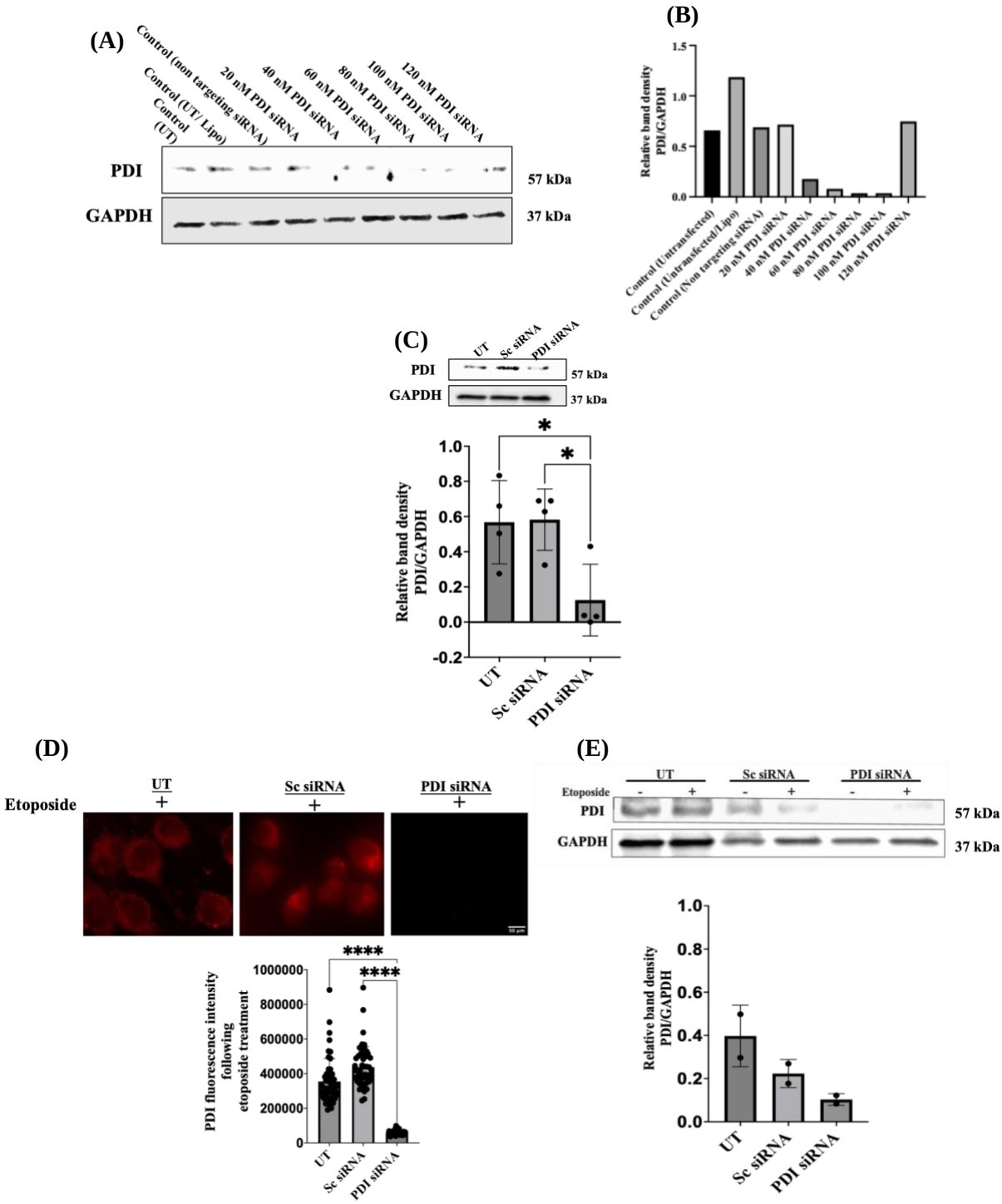

Figure 3.1: Determination of siRNA concentrations required to knockdown PDI. (A) Western blotting for endogenous PDI and GAPDH as a loading control in Neuro2a cells, transfected with 80 nM non-targeting (scrambled) siRNA, and 0 nM, 20 nM, 40 nM, 60 nM, 80 nM, 100 nM and 120 nM PDI siRNA, lipofectamine only (UT+Lipo) or untransfected cells (UT), n = 1. (B) Densitometry quantification of endogenous PDI levels in the blot in (A). PDI expression was reduced in 100 nM PDI siRNA transfected cells, compared to untransfected (UT) and scrambled siRNA transfected cells. (C) *Top panel:* Western blotting for PDI and GAPDH as a loading control in Neuro2a cells, transfected with 80 nM non-targeting (scrambled) siRNA, 100nM PDI siRNA or UT cells; *bottom panel:* Densitometry quantification of PDI levels in the blots in the top panel. PDI expression was significantly reduced in PDI siRNA transfected cells, compared to untransfected (UT) (* $p < 0.05$) and

scrambled siRNA transfecetd cells (* $p < 0.05$). One-way ANOVA followed by Tukey's multiple comparison *post-hoc* test, * $p < 0.05$. Values are presented as mean ± SD from n = 4 experiments. (D) *Top panel:* Neuro2a cells were either untransfected (UT) or transfected with either 80 nM scrambled siRNA, or 100 nM PDI siRNA. At 72 h post-transfection, cells were treated with 13.5 μM etoposide for 30 min. After fixing the cells with 4% PFA, ICC was performed with anti-PDI (red) antibody. Scale bar represents 50 μm. *Bottom panel:* PDI expression quantification by ICC revealed that following transfection, PDI level significantly decreased in 100 nM PDI siRNA transfected cells compared to scrambled siRNA and UT cells following etoposide treatment (13.5 μM for 30 min). One-way ANOVA followed by Tukey's multiple comparison *post-hoc* test, **** $p < 0.0001$. 50 cells were counted from each group for n = 3 biological replicates. Values are presented as mean ± SD. (E) *Top panel:* Western blotting for PDI and GAPDH as a loading control in Neuro2a cells, transfected with 80 nM non-targeting (scrambled) siRNA, PDI siRNA or UT cells, which were either untreated or etoposide-treated (13.5 μM for 30 min); *bottom panel:* Densitometry quantification of PDI levels in the blots in the top panel. A trend for reduced PDI expression in 100 nM PDI siRNA transfected cells, compared to untransfected (UT) and scrambled siRNA transfected cells was observed. One-way ANOVA followed by Tukey's multiple comparison *post-hoc* test was performed. Values are presented as mean ± SD from n = 2 experiments.

3.2. PDI knockdown increases the formation of ɣ-H2AX DNA damage foci following etoposide treatment in Neuro2a cells

To investigate the role of endogenous PDI against DNA damage, Neuro2a cells were then transfected with the optimised concentration of PDI siRNA (100 nM) to knockdown its expression with the same batch of cells. As controls, untransfected (UT) cells and cells were transfected with 80 nM scrambled siRNA were used. At 72 h post-transfection, cells were treated with 13.5 μM etoposide to induce DNA damage for 30 min. Cells were then fixed, and immunocytochemistry was performed using ɣ-H2AX (green) and anti-PDI (red) antibodies (Figure 3.2 (A)). An antibody specific for phosphorylated, rather than total, H2AX was used, because phosphorylation of Seine-139 residue in H2AX is recognised to be an early event in the DDR (Farg et al., 2017; Mah et al., 2010). The formation of distinct nuclear ɣ-H2AX foci, a widely used marker for DSBs, was therefore examined and quantified using fluorescence microscopy to detect DSBs and hence DNA damage (Mah et al., 2010).

The number of ɣ-H2AX foci was significantly increased in etoposide treated cells in each group (untransfected, scrambled siRNA transfected and PDI siRNA transfected cells) compared to their respective control groups, indicating that damage was successfully induced by this treatment (Tukey's multiple comparison *post-hoc* test, **** $p < 0.0001$) (Figure 3.2 (B)). Interestingly, significantly more ɣ-H2AX foci were detected in etoposide treated cells with endogenous PDI knockdown, compared to both untransfected and scrambled siRNA transfected groups (Tukey's multiple comparison *post-hoc* test, **** $p < 0.0001$) (Figure 3.2

(B)). Hence, this data implies that knockdown of endogenous PDI increases DNA damage followed by etoposide treatment in Neuro2a cells.

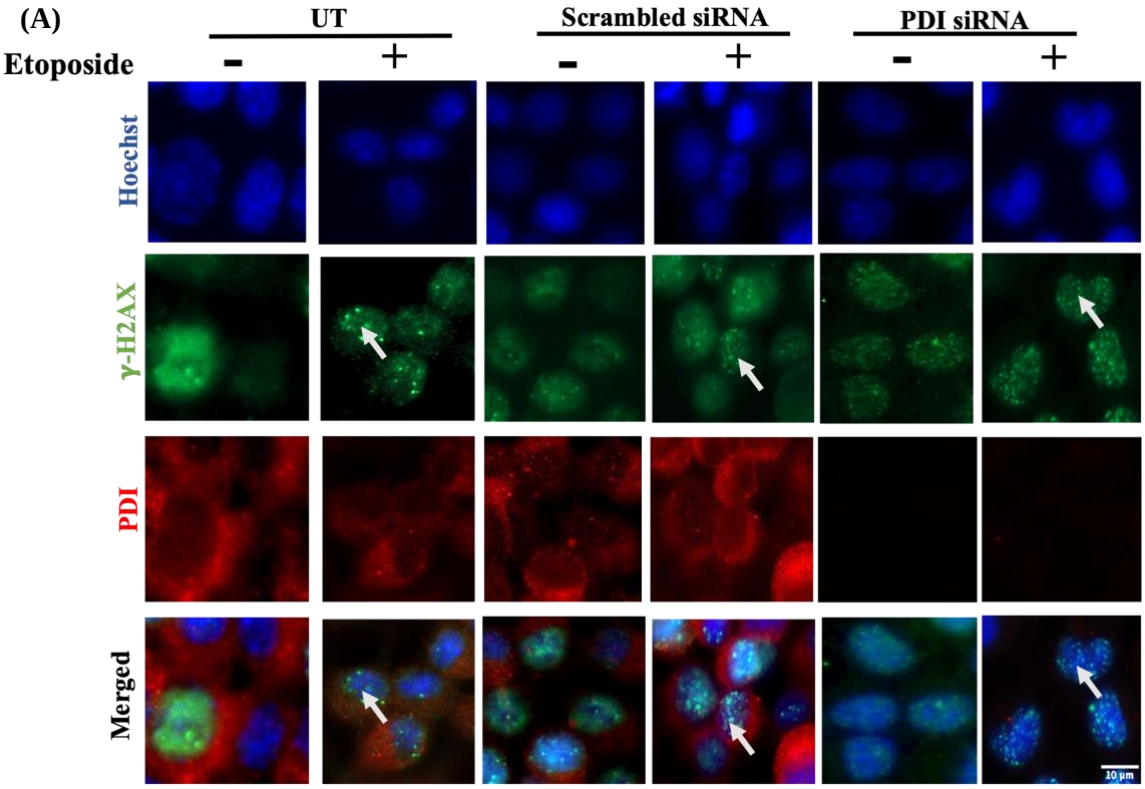

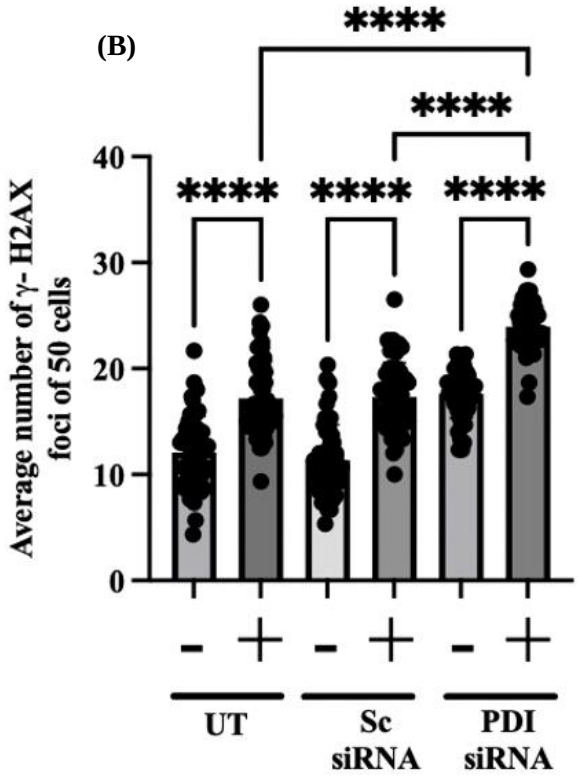

Figure 3.2: PDI knockdown increases DNA damage induced by etoposide, indicated by the formation of ɣ-H2AX foci. (A) Neuro2a cells were either untransfected (UT, first two columns) or transfected with either scrambled siRNA (second two columns), or PDI siRNA (third two columns). At 72 h post-transfection, cells were treated with 13.5 μM etoposide for 30 min. After fixing the cells with 4% PFA, ICC was performed with ɣ-H2AX (green) and anti-PDI (red) antibodies and nuclei were stained with Hoechst (blue). Scale bar represents 50 μm. Arrows indicate ɣ-H2AX foci. (B) Quantification of the average number of ɣ-H2AX foci, indicating DNA damage, per 50 cells. Significantly more ɣ-H2AX foci were detected in Neuro2a cells transfected with PDI siRNA, compared to UT (**** $p < 0.0001$), and scrambled siRNA transfected cells (**** $p < 0.0001$). Induction of DNA damage in cells treated with 13.5 μM etoposide treatment, compared to untreated cells for all groups, was also confirmed by the presence of significantly more ɣ-H2AX foci (**** $p < 0.0001$). One-way ANOVA followed by Tukey's multiple comparison *post-hoc* test, **** $p < 0.0001$ was performed. 50 cells were counted from each group for n = 3 replicates. Values are presented as mean ± SD.

3.3. PDI knockdown increases the formation of ɣ-H2AX DNA damage foci following H_2O_2 treatment in Neuro2a cells

As PDI knockdown increased DNA damage induced by etoposide, further experiments were performed with another DNA damage inducing agent. Hydrogen peroxide (H_2O_2) induces oxidative DNA damage in Neuro2a cell lines and oxidative stress and oxidative DNA damage are implicated in the pathophysiology of ALS (Bordoni et al., 2019). The concentration and duration of H_2O_2 treatment required to induce DNA damage in Neuro2A cells was previously optimized in our laboratory (Konopka et al., 2020), so the same conditions were used here. Neuro2a cells were transfected with PDI siRNA or scrambled siRNA and after 72 h, cells were treated with 100 μM H_2O_2 for 1 h. Then cells were fixed, and ICC was performed with phosphorylated H2AX specific (green) and anti-PDI (red) antibodies (Figure 3.3 (A)). Fluorescence microscopy and quantification of the number of ɣ-H2AX foci revealed a significant increase following H_2O_2 treatment for all groups compared to the equivalent untreated group, confirming induction of DNA damage (Tukey's multiple comparison *post-hoc* test, **** $p < 0.0001$) (Figure 3.3 (B)). Moreover, similar to the etoposide results, significantly more ɣ-H2AX foci were detected in H_2O_2 treated cells with PDI knockdown, compared to both untransfected and scrambled siRNA transfected cells (Tukey's multiple comparison *post-hoc* test, **** $p < 0.0001$) (Figure 3.3 (B)). Thus, these results indicate that knockdown of endogenous PDI leads to more oxidative DNA damage induced by H_2O_2 in Neuro2a cells, providing further evidence that PDI is protective against DNA damage.

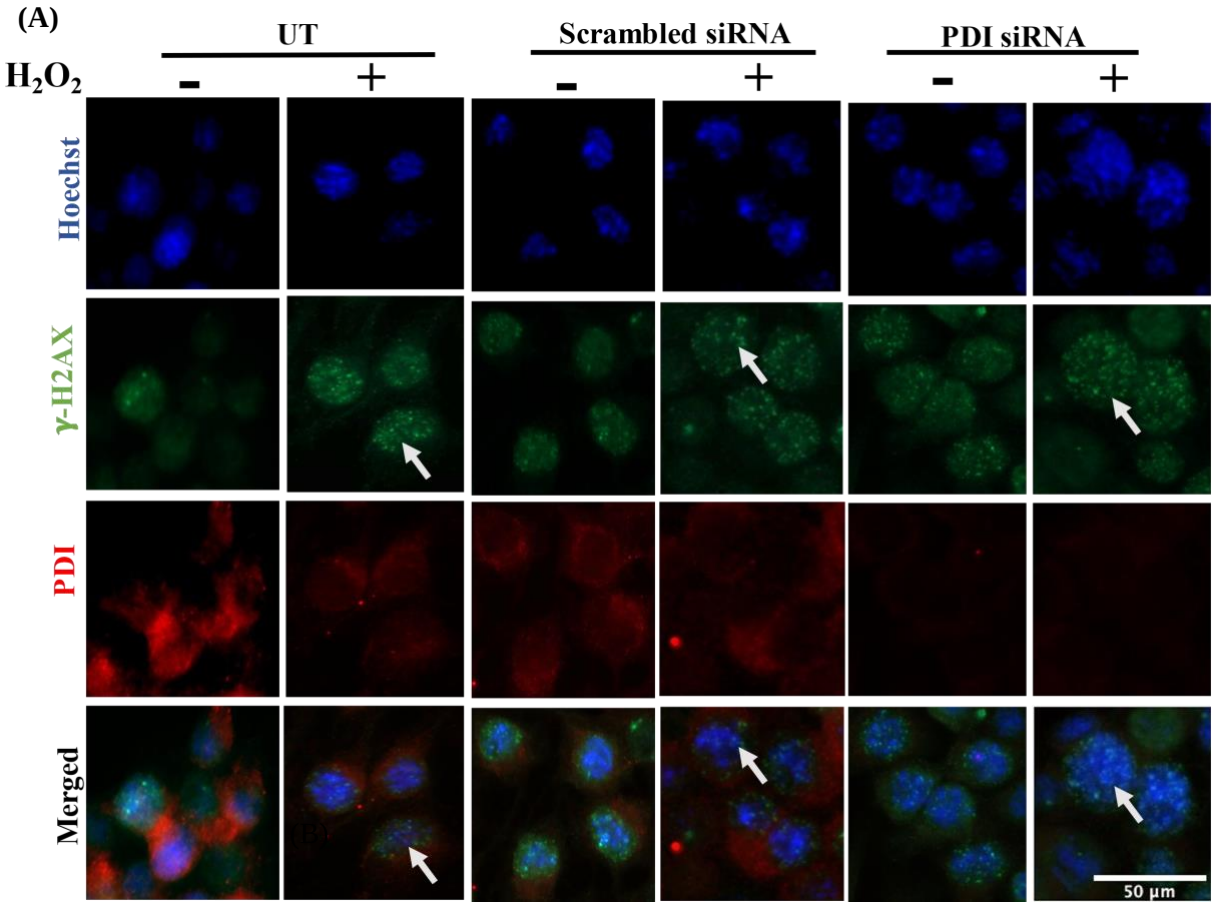
(A)
UT
Scrambled siRNA
PDI siRNA
H_2O_2
-
+
-
+
-
+
Hoechst
γ-H2AX
PDI
Merged
50 µm

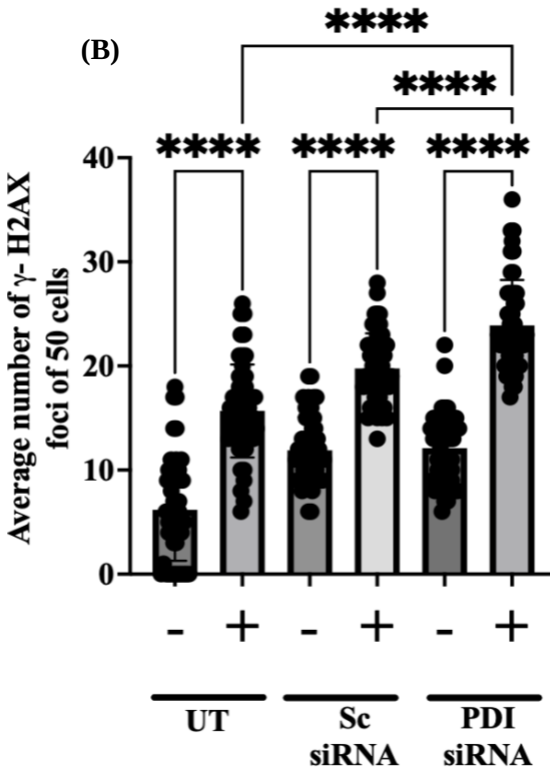
(B)
****
****
****
****
****
Average number of γ- H2AX foci of 50 cells
0
10
20
30
40
-
+
-
+
-
+
UT
Sc siRNA
PDI siRNA

Figure 3.3: PDI knockdown increases DNA damage induced by H_2O_2, indicated by the formation of ɣ-H2AX foci. (A) Neuro2a cells were transfected with either PDI siRNA (second two columns), or scrambled siRNA (third two columns). At 72 h post-transfection, these cells and untransfected (first two columns) controls were treated with 100 μM H_2O_2 for 1 h. Immunocytochemistry was performed with ɣ-H2AX (green) and anti-PDI (red) antibodies and the nuclei were stained with Hoechst (blue). Scale bar represents 50 μm. Arrows indicate ɣ-H2AX foci. (B) Quantification of the average number of ɣ-H2AX foci per 50 cells. A significant increase in ɣ-H2AX foci was detected in Neuro2a cells transfected with PDI siRNA (**** $p < 0.0001$), compared to untransfected and scrambled siRNA transfected control cells. Significantly more ɣ-H2AX foci were also detected in cells treated with 100 μM H_2O_2, compared to untreated groups (**** $p < 0.0001$), confirming induction of DNA damage with One-way ANOVA followed by Tukey's multiple comparison *post-hoc* test, **** $p < 0.0001$. 50 cells were counted from each group for $n = 3$ replicates. Values are presented as mean ± SD.

3.4. Generation of PDI knockout cell lines

To confirm the results obtained by knocking down PDI using siRNA, the next aim was to generate a PDI knockout cell line using CRISPR-Cas9 methods and then examine DNA damage in this line. A sgRNA sequence (GGCGTCGGCGCGCACCAGGGCGG) targeting PDI was previously designed in our laboratory and cloned into the plasmid GeneArt CRISPR Nuclease Vector. Neuro2a cells were then transfected with the PDI-CRISPR plasmid in a 6-well plate. At 48 h post-transfection, cells were plated into four 96-well plates and left to expand in medium. From the 96-well plate, cells were cloned by limiting dilution and left to grow for at least 2 weeks. Possible positive clones were identified by the presence of orange fluorescence using fluorescence microscopy because the CRISPR/Cas9 vector contains an orange fluorescent protein (OFP) reporter (See Appendix, Figure 7.2). Wells with single cells were identified and expanded following the growth of the single cell colony. A total of 30 single cell colonies were screened from four 96-well plates. These colonies were then expanded into 6-well plates, lysates were collected, and western blotting was performed using a PDI antibody. However, unfortunately, all clones examined were found to express PDI (Figure 3.4). A total of 30 clones were examined by western blotting. Due to time constraints, it was not possible to examine any further clones, and thus it was not possible to examine whether more DNA damage was present in CRISPR/Cas9 PDI knockout cells.

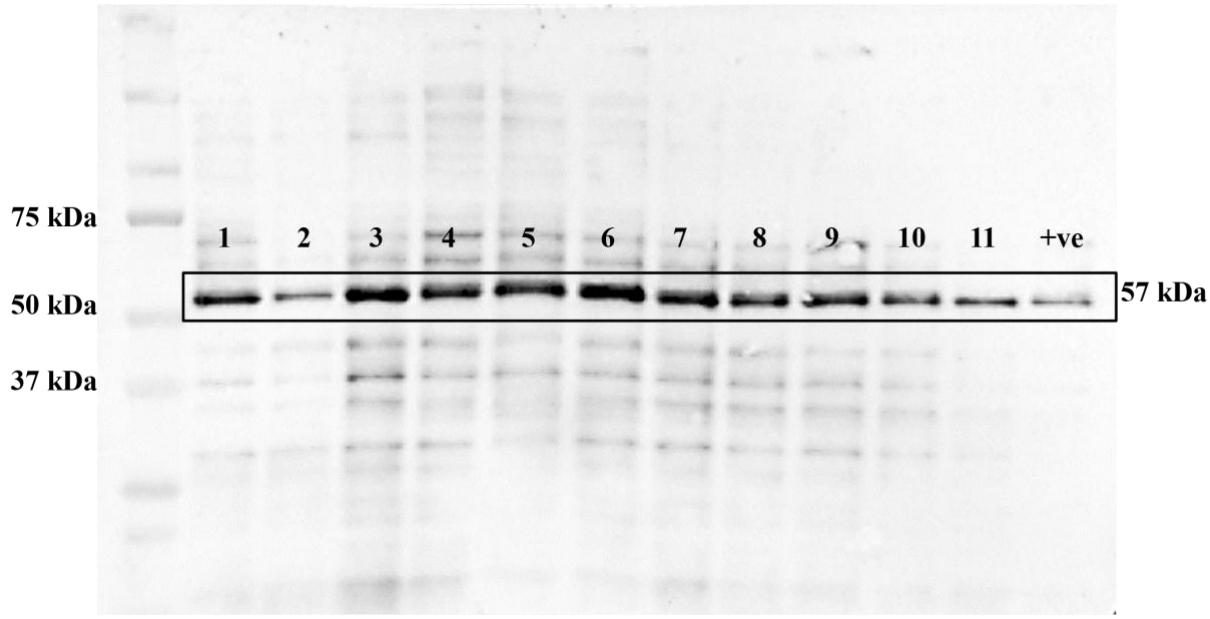

Figure 3.4: All CRISPR/Cas9 clones examined displayed expression of PDI. The black box represents the PDI bands for 11 PDI-CRISPR clones. From left, first lane indicates protein MW ladder, and the last lane indicates a untransfected Neuro2a cell lysate (positive control).

3.5. PDI knockdown enhances DNA damage induced apoptosis following etoposide treatment

DNA fragmentation is one of the last stages of apoptosis, which can be visualized by the presence of condensed or fragmented nuclei following Hoechst staining (Elmore, 2007). Next it was examined whether PDI knockdown enhances DNA damage induced apoptosis. Neuro2a cells were firstly transfected with PDI siRNA and scrambled siRNA. At 72 h post-transfection, these cells and untransfected cells were treated with 13.5 μM etoposide for 30 min. The cells were then fixed, and immunocytochemistry was performed using ɣ-H2AX (green) and anti-PDI (red) antibodies (Figure 3.5 (A)). Using fluorescence microscopy, the proportion of cells undergoing apoptosis was investigated by quantifying the presence of apoptotic nuclei, identified by Hoechst staining.

Few (5.4%) untreated untransfected cells displayed fragmented nuclei, and following etoposide treatment, whilst there was no significant increase in the proportion of cells undergoing apoptosis (Figure 3.5 (B)). Hence, this shows untransfected cells did not go through significant apoptosis following etoposide treatment. Similarly, 9% scrambled siRNA transfected cells displayed fragmented nuclei whereas this proportion increased to 12.8% when treated with etoposide (Figure 3.5 (B)), although this was not statistically significant. Hence, cells transfected with scrambled siRNA did not go through significant apoptosis after etoposide

treatment. In contrast, 11% PDI siRNA transfected cells showed fragmented nuclei but significantly more (2.3-fold, **** $p < 0.0001$) were detected following etoposide treatment (Figure 3.5 (B)). There was also a significant increase in apoptotic nuclei in untreated PDI siRNA cells compared to untreated untransfected cells (2.1-fold, * $p < 0.05$) (Figure 3.5 (B)). Hence, knockdown of endogenous PDI induces apoptosis in both etoposide treated and untreated cells. Thus, this suggests that other pathways lead to apoptosis in the absence of DNA damage when PDI is knocked down. Moreover, a significant increase in the percentage of fragmented nuclei, and hence apoptosis, was detected in etoposide treated PDI siRNA transfected cells compared to both untransfected and scrambled siRNA transfected cells (**** $p < 0.0001$) (Figure 3.5 (B)). These data reveal that endogenous PDI protects Neuro2a cells from apoptosis following etoposide treatment.

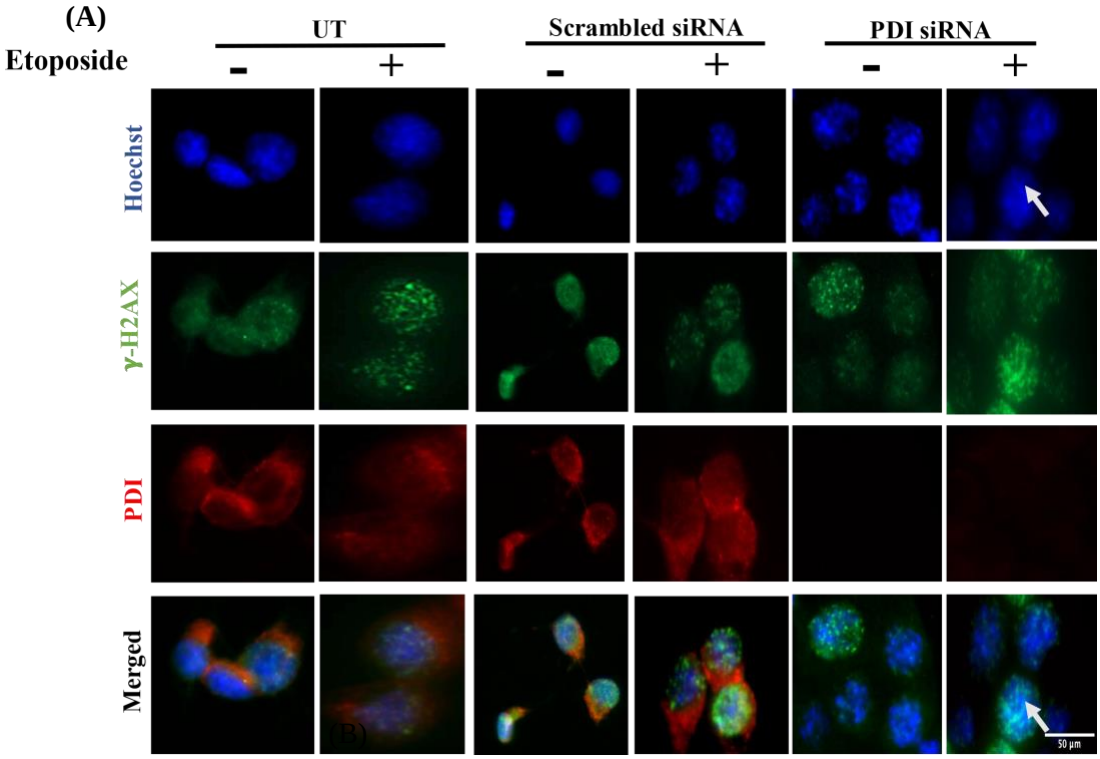

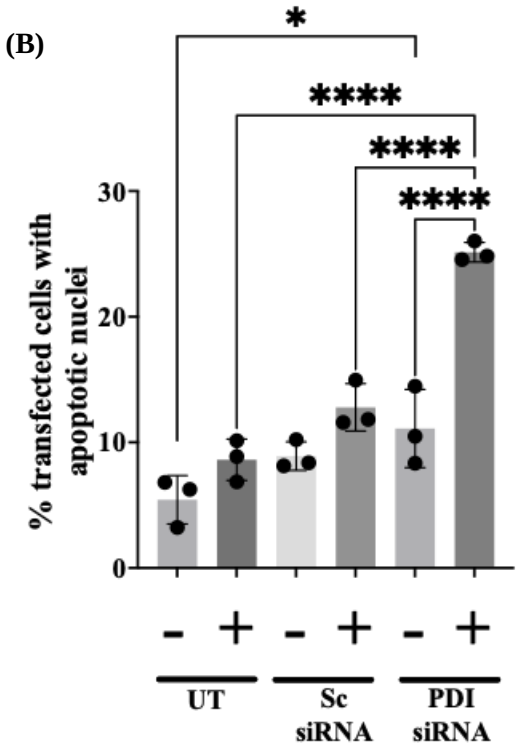

Figure 3.5: Knockdown of PDI enhances apoptosis following DNA damage by etoposide in Neuro2a cells. (A) Neuro2a cells transfected with either scrambled siRNA (second two columns) or PDI siRNA (third two columns), or untransfected (first two columns) cells were treated with 13.5 μM etoposide for 30 min after 72 h transfection. Immunocytochemistry was performed with ɣ-H2AX (green) and anti-PDI (red) antibodies and the nuclei were stained with Hoechst (blue). Scale bar represents 50 μm. Arrows indicate Hoechst-stained fragmented nuclei. (B) Quantification of Neuro2a cells in (A) bearing apoptotic nuclei, either untreated or treated with 13.5 μM etoposide. There was a significant increase in the percentage of apoptotic nuclei in PDI siRNA transfected cells following etoposide treatment compared to the equivalent untreated group, confirming induction of apoptosis by DNA damage (**** $p < 0.0001$). Also, significantly more apoptotic nuclei in PDI siRNA transfected cells compared to untransfected and scrambled siRNA transfected cells were detected, confirming that PDI plays a role in apoptosis following DNA damage (**** $p < 0.0001$). There was significant difference in apoptotic nuclei between untreated PDI siRNA cells and the untreated UT group (* $p < 0.05$) showing that independent of DNA damage, other mechanisms might lead to apoptosis following knockdown of endogenous PDI. One-way ANOVA was performed followed by Tukey's multiple comparison *post-hoc* test, **** $p < 0.0001$, * $p < 0.05$. Apoptotic nuclei were quantified as a percentage of non-apoptotic cells from 100 cells from each group for n = 3 replicates. Values are presented as mean ± SD.

3.6. PDI knockdown enhances DNA damage induced apoptosis following H_2O_2 treatment

Apoptosis induced by DNA damage was further examined by using another pharmacological treatment, H_2O_2, in Neuro2a cells. Following 72 h transfection with PDI and scrambled siRNA, these cells and untransfected cells were treated with 100 μM H_2O_2 for 1 h. The cells were then fixed, and immunocytochemistry was performed using ɣ-H2AX (green) and anti-PDI (red)

antibodies (Figure 3.6 (A)). Using fluorescence microscopy, the proportion of cells undergoing apoptosis was investigated by quantifying the presence of apoptotic nuclei, identified by Hoechst staining.

Few (2.5%) untreated untransfected cells displayed fragmented nuclei, and following H_2O_2 treatment, whilst there was no significant increase in the proportion of cells undergoing apoptosis (Figure 3.6 (B)). Hence, this shows untransfected cells did not go through significant apoptosis following H_2O_2 treatment. Similarly, 2.5% scrambled siRNA transfected cells displayed fragmented nuclei whereas this proportion increased to 2.1-fold when treated with H_2O_2, (Figure 3.6 (B)), although this was not statistically significant. Hence, cells transfected with scrambled siRNA did not go through significant apoptosis after H_2O_2 treatment. In contrast, 6.1% PDI siRNA untreated transfected cells showed fragmented nuclei but significantly more (1.7-fold, * $p < 0.05$) were detected following H_2O_2 treatment (Figure 3.6 (B)). Hence, depletion of endogenous PDI induces apoptosis in both H_2O_2 treated or untreated cells, also implying that other mechanisms besides DNA damage induce apoptosis in PDI siRNA cells. Moreover, a significant increase in the percentage of fragmented nuclei, and hence apoptosis, was detected in H_2O_2 treated PDI siRNA transfected cells compared to both untransfected (* $p < 0.05$) and scrambled siRNA transfected cells (** $p < 0.01$) (Figure 3.6 (B)). These data reveal that endogenous PDI protects Neuro2a cells from apoptosis following H_2O_2 treatment.

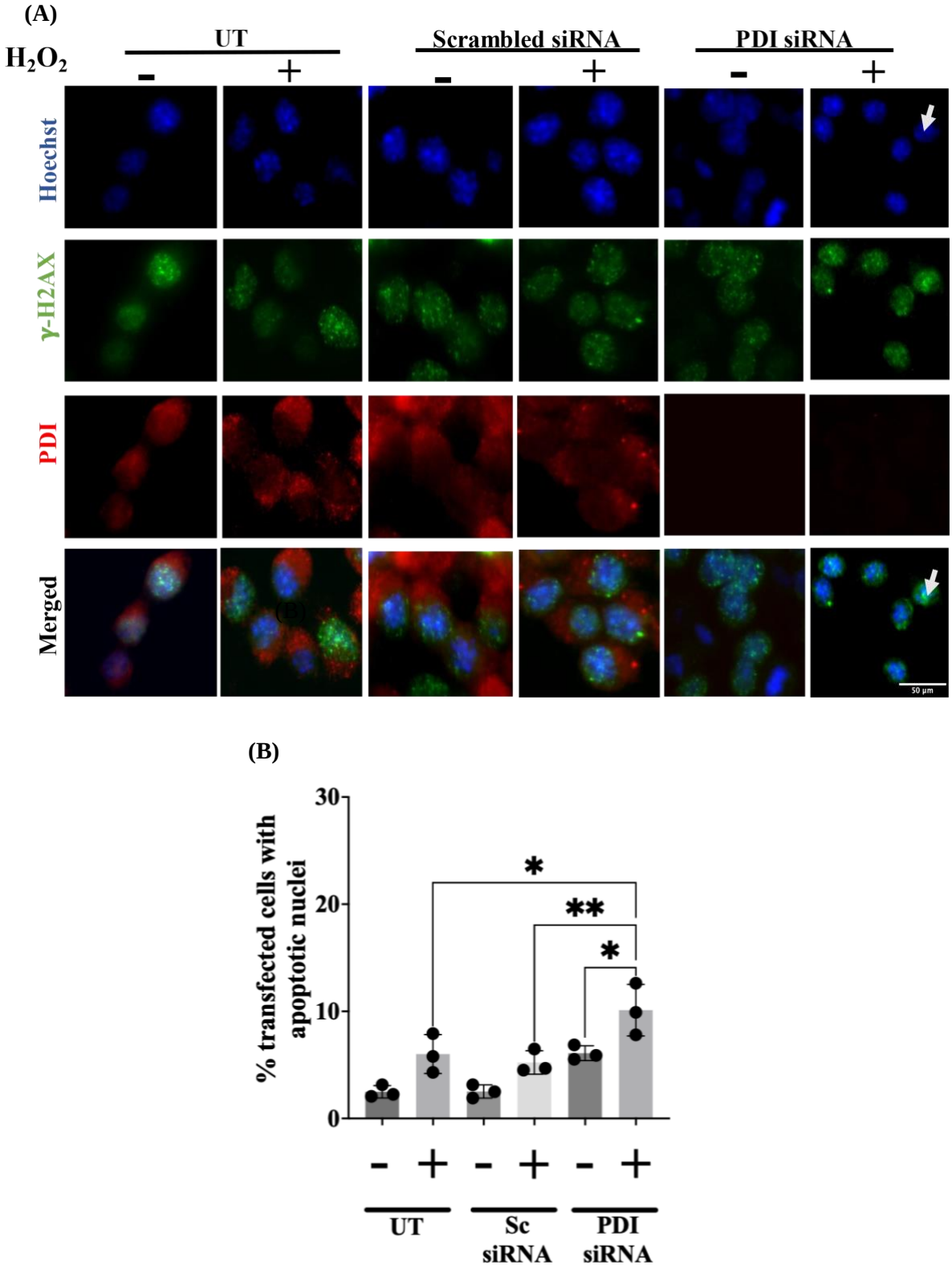

Figure 3.6: Knockdown of PDI increases apoptosis following DNA damage by H_2O_2 in Neuro2a cells. (A) Neuro2a cells transfected with either scrambled siRNA (second two columns), or PDI siRNA (third two columns) or untransfected (first two columns) cells were treated with 100 µM H_2O_2 for 1 h after 72 h. Immunocytochemistry was performed with ɣ-H2AX (green) and anti-PDI (red) antibodies and the nuclei were stained with Hoechst (blue).

Scale bar represents 50 μm. Arrows indicate Hoechst-stained fragmented nuclei. (B) Quantification of apoptotic nuclei cells in Neuro2a cells in (A) bearing apoptotic nuclei, either untreated or treated with 100 μM H_2O_2. There was a significant increase in the percentage of apoptotic nuclei in PDI siRNA transfected cells following H_2O_2 treatment compared to the equivalent untreated group (* $p < 0.05$). Also, significantly more apoptotic nuclei in PDI siRNA transfected cells compared to untransfected (* $p < 0.05$) and scrambled siRNA transfected cells (** $p < 0.01$) were detected, confirming that PDI plays a role in apoptosis following DNA damage by H_2O_2. One-way ANOVA was performed followed by Tukey's multiple comparison *post-hoc* test, ** $p < 0.01$, * $p < 0.05$. Apoptotic nuclei were measured as a percentage of non-apoptotic cells from 100 cells from each group for n = 3 replicates. Values are presented as mean ± SD.

3.7. Overexpression of PDI prevents DNA damage induced apoptosis in Neuro2a cells following etoposide treatment

Whilst previous studies in the laboratory had shown that overexpression of PDI inhibits DNA damage in Neuro2a cells, it had not been previously established that overexpression of PDI prevents apoptosis induced by DNA damage. Given that knockdown of endogenous PDI using siRNA enhanced the formation of apoptotic nuclei, next it was examined whether overexpression of PDI could inhibit apoptosis, to further validate the siRNA results. Overexpression of PDI was performed by another member of the laboratory: Neuro2a cells were transfected with pcDNA3.1 empty vector (EV, expressing V5 tag only), and V5-tagged PDI-WT plasmids. EV and PDI-WT transfected cells, and untransfected cells were used as controls. At 24 h post-transfection, DNA damage was induced using 13.5 μM etoposide for 30 min. Then cells were fixed, and immunocytochemistry was performed using γ-H2AX (green) and anti-V5 (red) antibodies (Figure 3.7 (A)). Images were taken using fluorescence microscopy.

Quantification of these images revealed that the percentage of cells bearing apoptotic nuclei was higher in etoposide treated groups compared to control groups for EV and PDI-WT transfected cells, confirming the induction of DNA damage; EV (2.3-fold increase, ** $p < 0.01$); PDI-WT (5.7-fold, * $p < 0.05$) (Figure 3.7 (B)). Significantly more EV transfected cells treated with etoposide displayed apoptotic nuclei compared to PDI-WT, and untransfected cells, both treated with etoposide (* $p < 0.05$) (Figure 3.7 (B)). Interestingly, only 1.1% PDI-WT cells showed apoptotic nuclei, which was the lowest percentage amongst all other groups for this experiment (Figure 3.7 (B)). These results therefore suggest that overexpression of PDI protects cells from apoptosis induced by DNA damage.

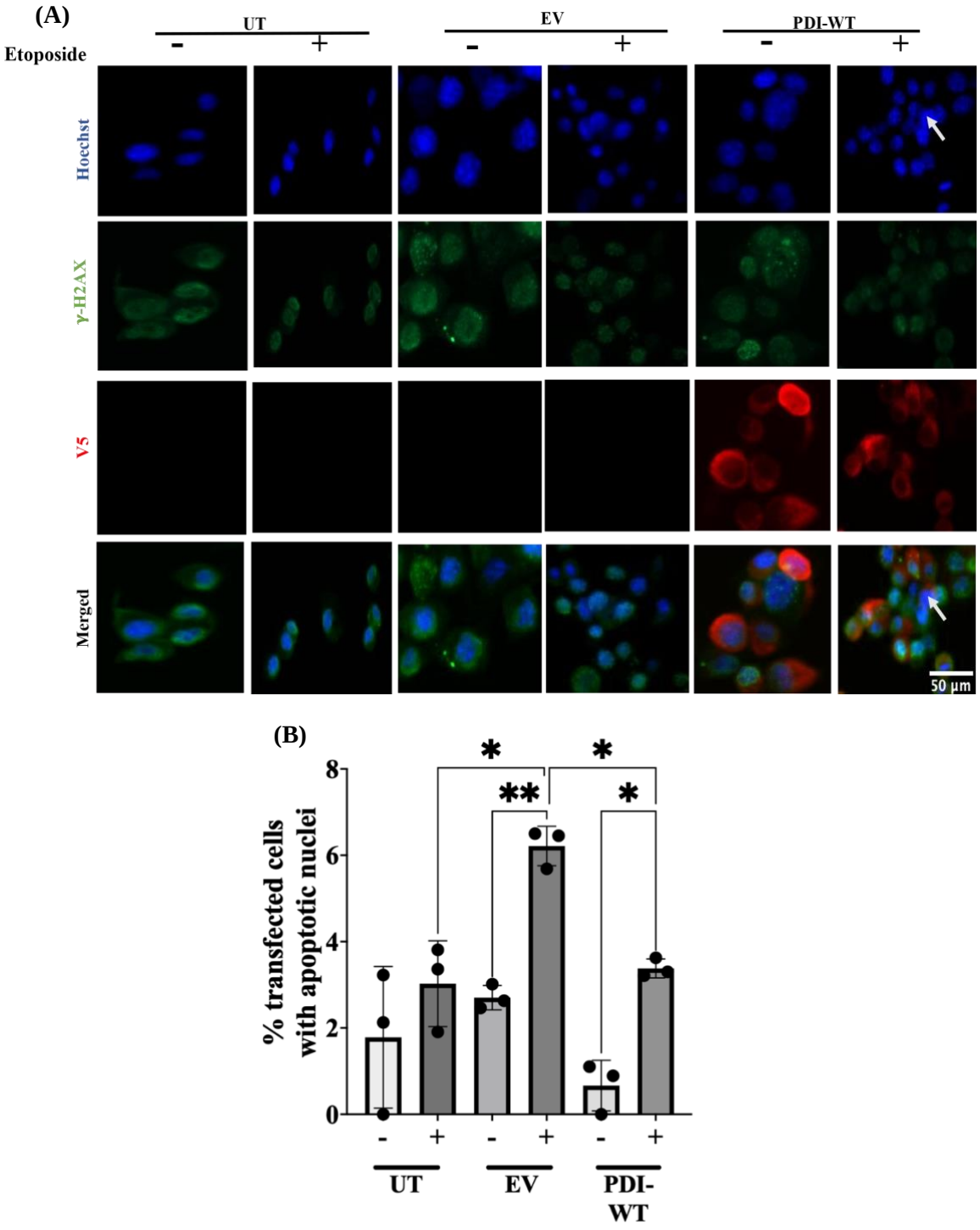

Figure 3.7: Expression of PDI-WT is protective against apoptosis in Neuro2a cells following etoposide treatment. (A) Neuro2a cells transfected with pcDNA3.1 empty vector (EV) (second two columns), V5-tagged PDI-WT (third two columns), or untransfected cells (first two columns) were treated with 13.5 µM etoposide for 30 min at 24 h post-transfection. Immunocytochemistry was performed with ɣ-H2AX (green) and anti-v5 (red) antibodies and the nuclei were stained with Hoechst (blue). Scale bar represents 50 µm. Arrows indicate Hoechst-stained fragmented nuclei. (B) Quantification of apoptotic nuclei cells in Neuro2a cells in (A). A significant increase in the percentage of cells with apoptotic nuclei in EV expressing cells treated with etoposide compared to its untreated group (** $p < 0.01$) was detected, confirming that apoptosis is increased following etoposide treatment in EV

transfected cells. A significant increase in apoptotic nuclei was observed between PDI-WT expressing cells treated with etoposide compared to its untreated group (* $p < 0.05$). Also, significantly more apoptotic nuclei in EV transfected cells compared to untransfected (* $p < 0.05$) and PDI-WT transfected cells (* $p < 0.05$) were detected, revealing that overexpression of PDI is protective against DNA damage induced apoptosis. One-way ANOVA was performed followed by Tukey's multiple comparison *post-hoc* test, ** $p < 0.01$, * $p < 0.05$. Apoptotic nuclei were measured as a percentage of non-apoptotic cells from 100 cells from each group for $n = 3$ replicates. Values are presented as mean ± SD.

3.8. Examining whether PDI has a direct or indirect role in DNA damage

Whilst the results described above reveal that endogenous PDI is protective against DNA damage, it remains unclear how this is mediated. It is possible that PDI has a direct function in the DDR at sites of DNA damage. Alternatively, PDI may have a more indirect role, such as by modulating the cellular redox environment. Finally, it is possible that PDI performs both direct and indirect roles in the DDR.

3.8.1. Etoposide treatment of Neuro2a cells leads to recruitment of endogenous PDI into the nucleus

PDI is predominantly present in the ER, although it is known to translocate from the ER to both the cell surface and cytoplasm in some circumstances (Terada et al., 1995). If PDI has a direct role in the DDR, we hypothesised that following DNA damage it would relocate from the ER into the nucleus. Hence, we next examined the localisation of endogenous PDI before and after DNA damage treatment using immunocytochemistry. Neuro2a cells were plated on coverslips and 24 h later, they were treated with 13.5 μM etoposide for 30 min. Immunocytochemistry was then performed using ɣ-H2AX (green) and anti-PDI (red) antibodies, followed by confocal microscopy (Figure 3.8.1 (A)). The intensity of PDI expression in the nucleus relative to the whole cell was then quantified using Image J. These analyses revealed that there was a significant increase in the ratio of endogenous PDI expression inside nucleus relative to the total cellular PDI in etoposide treated cells compared to control cells (*** $p < 0.001$) (Figure 3.8.1 (B)). This finding suggests that following DNA damage, endogenous PDI translocates into the nucleus, implying that it has a direct role in the DDR. However further experiments are required to confirm this.

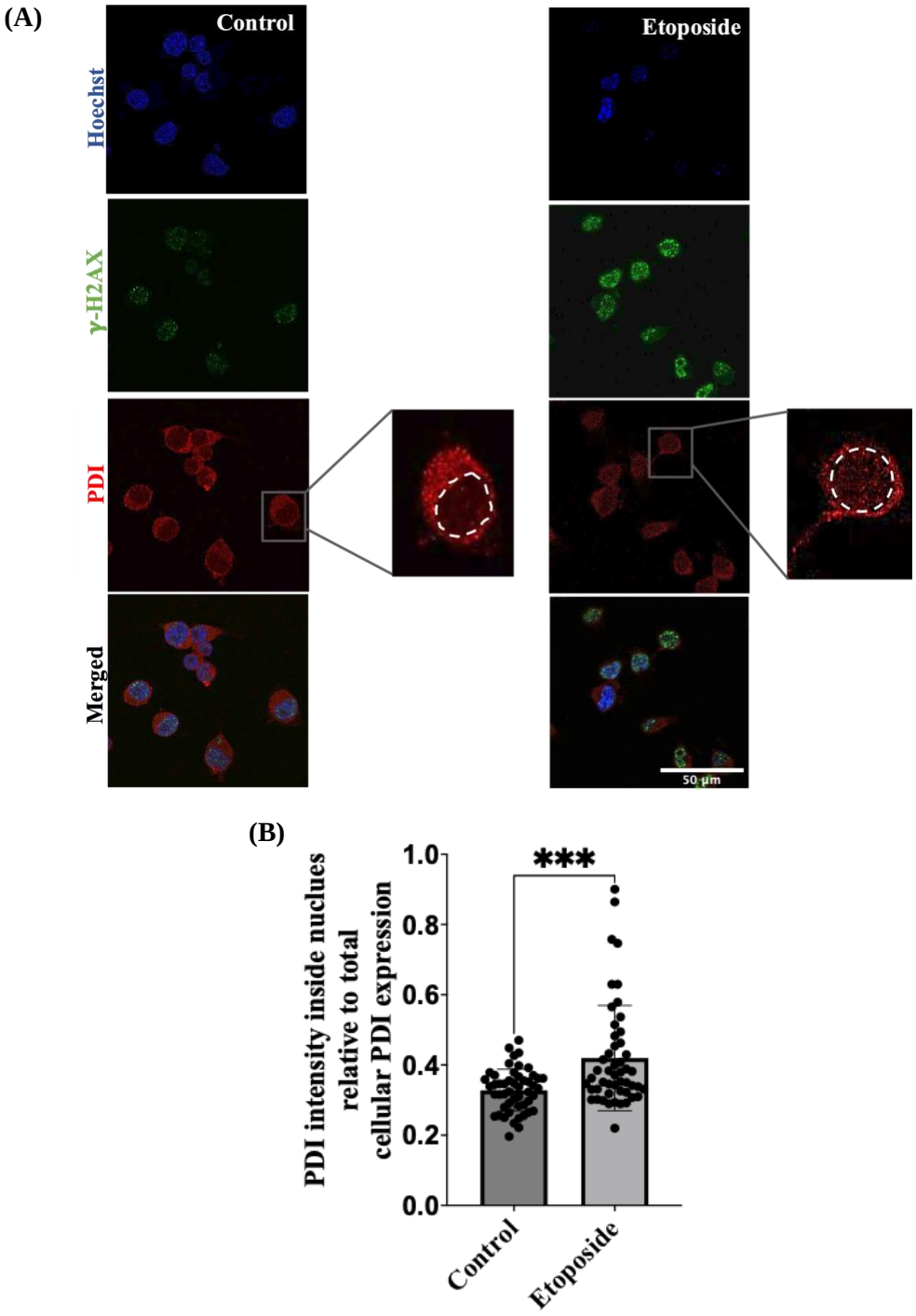

Figure 3.8.1: PDI is recruited to the nucleus following etoposide treatment. (A) Untransfected Neuro2a cells were either untreated (first column) or treated with 13.5 µM etoposide for 30 mins (second column). Immunocytochemistry was performed with γ-H2AX (green) and anti-PDI (red) antibodies and the nuclei were stained with Hoechst (blue). Scale bar represents 50 µm. Insert shows 3.5 times enlarged image of endogenous PDI intensity inside nucleus. Dashes indicate PDI intensity inside nucleus. (B) Quantification of mean fluorescence of endogenous PDI inside the nucleus (relative to total cellular PDI expression) before and after etoposide treatment. A significant increase was observed in endogenous PDI intensity inside the nucleus following etoposide treatment (*** $p < 0.001$), compared to the untreated group with unpaired t-test with Welch's correction. Mean fluorescence of PDI

intensity inside nucleus compared to total cellular PDI for each group from n = 3 replicates. Values are presented as mean ± SD.

3.8.2. Immunoprecipitation (IP) to examine whether there is an association between PDI and ɣ-H2AX following DNA damage treatment with etoposide

To further examine whether PDI has a direct role in the DDR, we next examined whether there is an association between PDI and ɣ-H2AX. We hypothesised that this would imply that PDI has a direct role in the DDR as ɣ-H2AX is recruited directly to DNA damage sites (Mah et al., 2010). Immunoprecipitation was performed using a PDI antibody, of untreated and etoposide-treated cell lysates, to determine whether an association exists between PDI and ɣ-H2AX following DNA damage induction with 13.5 μM etoposide for 30 min. To detect this association, western blotting using an ɣ-H2AX antibody was used. Input samples were loaded as positive controls for PDI and ɣ-H2AX protein bands on the membrane. A mouse IgG isotype control antibody was also used to IP the same lysates as a negative control to examine whether any signals detected are specific for PDI. Hence, using the isotype control in an IP, there should be no band present for either PDI or ɣ-H2AX. However, it can be observed from the result that there were positive bands for both PDI and ɣ-H2AX using both the isotype control and the PDI antibodies (Figure 3.8.2). Hence, this experiment could not provide any specific conclusion because non-specific bands were obtained for the isotype control antibody. Hence, the result is not conclusive, and these experiments need further optimization. However, due to time limitations in this study, this was not possible.

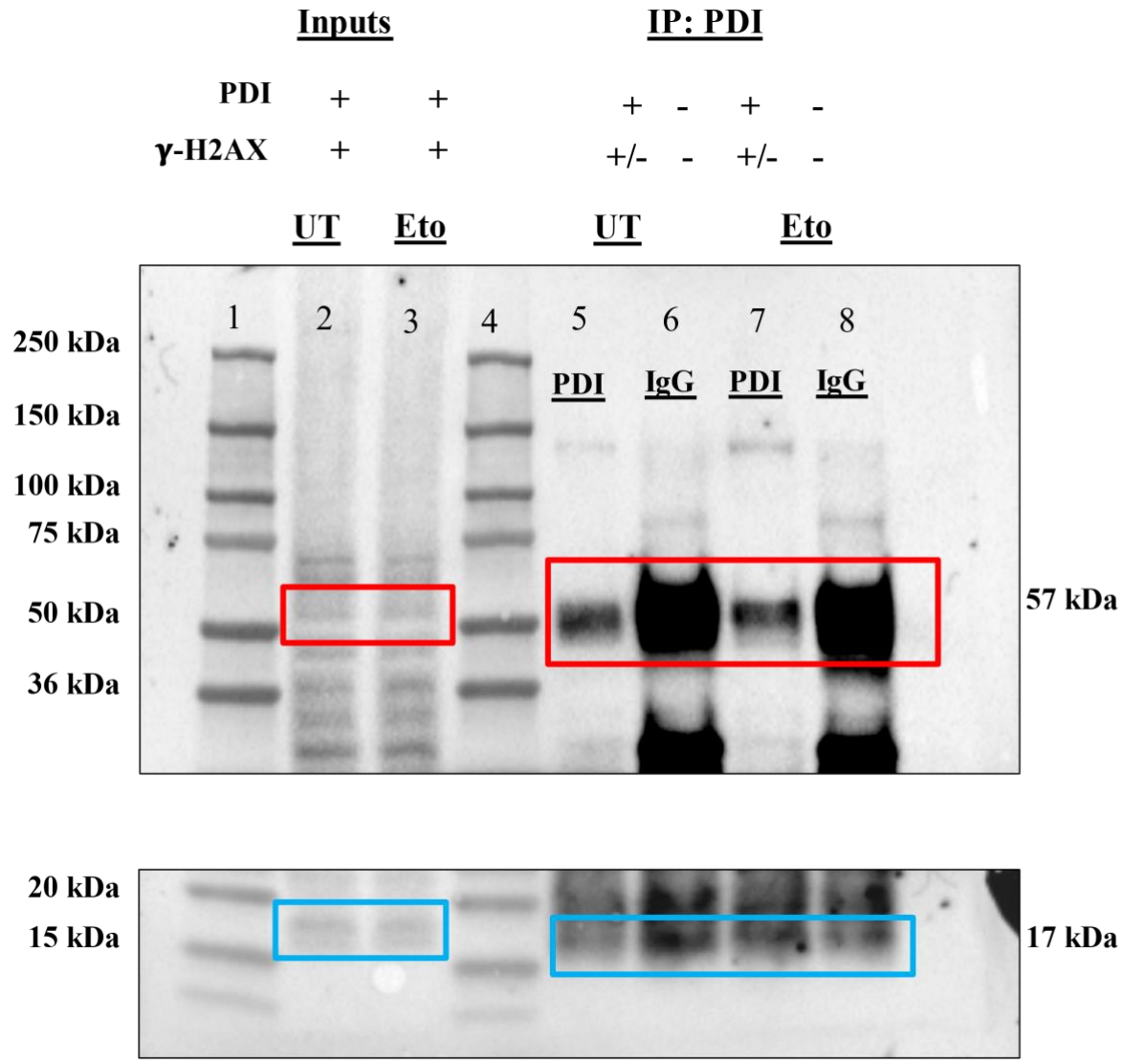

Figure 3.8.2: Immunoprecipitation of Neuro2A cell lysates to examine whether there is an association between PDI and ɣ-H2AX following DNA damage. Western blotting image of IP using ɣ-H2AX and IgG isotype control antibodies. *Top panel:* blot was probed for PDI to detect whether the IP of PDI was successful, and *bottom panel:* blot was probed for ɣ-H2AX antibody to detect any association between PDI and ɣ-H2AX following DNA damage. Red boxes (top panel) and sky blue boxes (bottom panel) indicate PDI and ɣ-H2AX bands, respectively. MW markers (lanes 1 and 4), input samples (lanes 2 and 3), untreated lysates precipitated with PDI or IgG antibodies (lanes 5 and 6 respectively), lysates from etoposide treated cells precipitated using with PDI or IgG antibodies (lanes 7 and 8 respectively). If there is an association between PDI and ɣ-H2AX, a signal should appear with PDI and ɣ-H2AX antibodies for samples precipitated with the PDI antibody. As the IgG isotype antibody was used as a negative control, there should not be any protein band present using PDI and ɣ-H2AX antibodies on the blot. Hence, due to the positive bands in the IgG lanes with both PDI and ɣ-H2AX antibodies, this result is inconclusive.

3.9. Etoposide treated Neuro2a cells increase DNA damage foci in ALS-associated PDI mutants

Given the increasingly described role of DNA damage in the pathogenesis of ALS, we next examined whether the mutations in PDI identified in ALS patients, PDI-D292N and PDI-R300H, were protective or not against DNA damage. For this purpose, previously generated constructs encoding V5-tagged PDI-D292N and PDI-R300H were used to overexpress PDI. The PDI-Quad mutant was also examined used in this study, which possesses only chaperone activity (Figure 1.6) so that it can be ascertained whether the redox or chaperone activity is protective against DNA damage. Neuro2A cells were transfected with pcDNA3.1 empty vector (EV), or V5-tagged PDI-WT, PDI-Quad, PDI-D292N or PDI-R300H plasmids. Untransfected cells were also included as a control group. At 72 h post-transfection, DNA damage was induced using 13.5 µM etoposide for 30 min. Immunocytochemistry was then performed using ɣ-H2AX (green) and anti-V5 (red) antibodies (Figure 3.9 (A)).

Fluorescence microscopy and quantification revealed a significant increase in the number of ɣ-H2AX foci following etoposide treatment for all groups compared to their untreated controls (**** $p < 0.0001$), confirming induction of DNA damage (Figure 3.9 (B)). In addition, a significant difference in ɣ-H2AX foci was detected between PDI-WT and EV transfected cells following etoposide treatment (**** $p < 0.0001$) (Figure 3.9 (C)), confirming the previously observed finding that PDI is protective against DNA damage. PDI-Quad transfected cells displayed significantly higher ɣ-H2AX foci compared to untransfected cells (**** $p < 0.0001$), but not EV cells, following etoposide treatment (Figure 3.9 (C)), implying that the redox activity of PDI is required for its protective activity. Moreover, a significant decrease in ɣ-H2AX foci was observed in etoposide treated PDI-WT cells compared to PDI-Quad (**** $p < 0.0001$), PDI-D292N (**** $p < 0.0001$) and PDI-R300H (*** $p < 0.001$) transfected cells (Figure 3.9 (C)). Hence these results suggest that the ALS-associated mutants and Quad-mutant lack the normal protective activity of PDI against DNA damage. Also, a significant difference was observed in the number of ɣ-H2AX foci between untransfected cells and EV transfected cells following etoposide treatment (**** $p< 0.0001$), implying that transfection with the empty vector induces a low level of DNA damage (Figure 3.9 (C)). Furthermore, a significant difference was detected between PDI-Quad, and both PDI-D292N and PDI-R300H cells (*** $p < 0.001$) following etoposide treatment (Figure 3.9 (C)), implying that PDI-D292N and PDI-R300H have more protective activity than the PDI-Quad mutant. There was also a significant increase in ɣ-H2AX foci in etoposide treated PDI-R300H cells compared to the etoposide

treated EV group (* $p < 0.05$) (Figure 3.9 (C)), indicating that the PDI-R300H retains some of the protective activity of PDI against DNA damage, although this was significantly reduced compared to WT PDI. However, no statistically significant difference was detected between ɣ-H2AX foci in either the PDI-D292N or PDI-Quad cells and EV cells following etoposide treatment (Figure 3.9 (C)), indicating that the PDI-D292N and PDI-Quad mutants display little protective activity against etoposide induced DNA damage. However, the significant difference between PDI-Quad and PDI-D292N implies that the Quad mutant lacks the most protective activity.

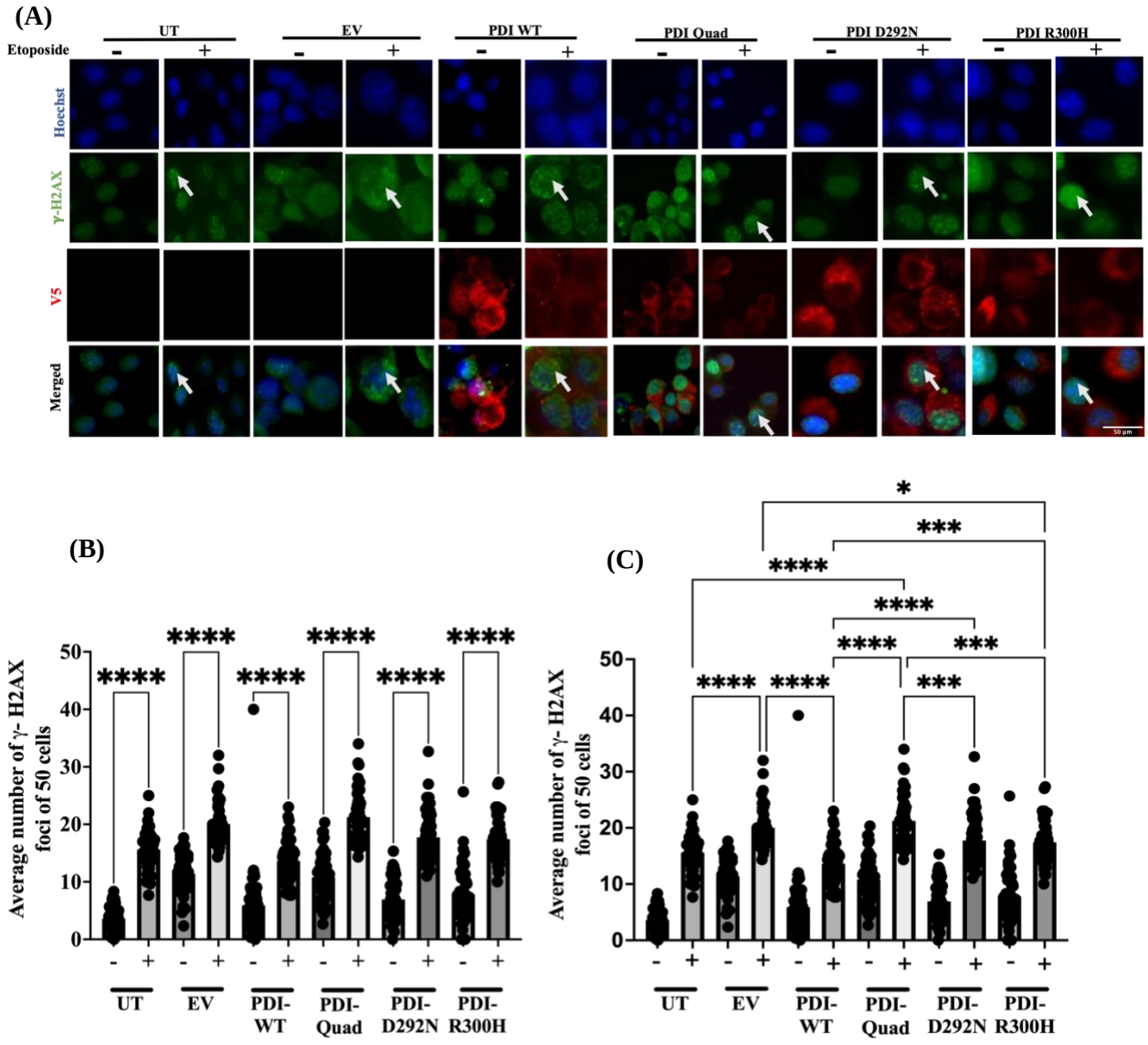

Figure 3.9: ALS-associated PDI mutants and Quad mutant display reduced protective activity against DNA damage compared to WT PDI. (A) Neuro2a cells were either untransfected (UT, first two columns) or transfected with pcDNA3.1 empty vector (EV) (second two columns), V5-tagged PDI-WT (third two columns), V5-tagged PDI-Quad

plasmids (fourth two columns), V5-tagged PDI-D292N plasmids (fifth two columns) and V5-tagged PDI-R300H (sixth two columns). At 72 h post-transfection, cells were treated with 13.5 μM etoposide for 30 min. Immunocytochemistry was performed with ɣ-H2AX (green) and anti-V5 (red) antibodies and the nuclei were stained with Hoechst (blue). Scale bar represents 50 μm. Arrows indicate ɣ-H2AX foci. Data presented in (B) and (C) are from same graph, but the statistical comparisons are shown on two separate graphs for better visualization. Both show quantification of the average number of ɣ-H2AX foci, indicating DNA damage, per 50 cells, in (A). (B) Induction of DNA damage in cells treated with 13.5 μM etoposide treatment, compared to untreated cells for all groups, was confirmed by the presence of significantly more ɣ-H2AX foci (**** $p < 0.0001$). (C) Significantly less ɣ-H2AX foci were present in PDI-WT cells compared to PDI-Quad (**** $p < 0.0001$), PDI-D292N (**** $p < 0.0001$) and PDI-R300H (*** $p < 0.001$) populations following etoposide treatment. Interestingly, both ALS-linked PDI mutants, PDI-D292N (*** $p < 0.001$) and PDI-R300H (*** $p < 0.001$) showed a significant difference in DNA damage foci compared to the PDI-Quad group following 13.5 μM etoposide treatment, indicating that these mutants are more protective against DNA damage than the Quad mutant. A significant (* $p < 0.05$) difference was also present between PDI-R300H and EV groups following etoposide treatment, indicating PDI-R300H has some residual protective activity. Also, significantly more ɣ-H2AX foci were present in the PDI-Quad group compared to untransfected cells (**** $p < 0.0001$) following etoposide treatment. One-way ANOVA was performed followed by Tukey's multiple comparison *post-hoc* test, **** $p < 0.0001$, *** $p < 0.0002$, ** $p < 0.0021$, * $p < 0.0332$. 50 cells were counted from each group for $n = 3$ replicates. Values are presented as mean ± SD.

4. Discussion

This study provides evidence that PDI functions in the DDR, and that this is relevant to ALS. Endogenous PDI was successfully knocked down using siRNA and following etoposide or H_2O_2 treatment, more DNA damage was detected in neuroblastoma cell lines, implying that PDI is protective against DNA damage. These results are consistent with previous studies in the laboratory showing that overexpression of PDI prevented DNA damage. Antibodies used for this study were previously examined as negative staining controls to determine immuno-staining specificity (data now shown). To confirm the siRNA results, we aimed to generate a PDI knockout cell line using CRISPR-Cas9 methods. However, in the restricted timeframe of this study, the generation of this cell line was not successful. It was unclear why no PDI-KO was found. One of the confounding factors could be cell division. As PDI is hard to knockout, cells could be viable. It will be interesting to follow this up in future studies. This study also identified a new relationship between PDI and induction of apoptosis by DNA damage. Significantly more cells with apoptotic nuclei were detected in PDI-targeting siRNA transfected populations compared to controls, implying that endogenous PDI prevents DNA damage induced apoptosis. Consistent with these findings, significantly less apoptotic nuclei were present when PDI was overexpressed compared to controls following DNA damage. This study also showed that after treating cells with etoposide, PDI translocates into the nucleus, implying a direct role for PDI at DNA damage sites. An IP was performed to investigate whether PDI interacts with ɣ-H2AX, which would provide further evidence for this possibility. However, nothing conclusive could be drawn from the IP result. Thus, the question remains open whether PDI and ɣ-H2AX directly interact following DNA damage treatment. Finally, to investigate whether these results are applicable to ALS, two ALS-linked redox-inactive PDI mutants and the Quad mutant were also examined to determine if they are protective against DNA damage. After treating with etoposide, these mutants were significantly less protective against DNA damage compared to WT PDI. Hence the redox activity of PDI is necessary for its protective activity against DNA damage.

The involvement of DNA damage in ALS is increasingly recognised (Kim et al., 2020; Wang et al., 2018; Konopka et al., 2020; Mitra et al., 2019; C. Walker et al., 2017; Farg et al., 2017) and has been detected in *in vitro* iPSC-models, neuronal cell lines, and human tissues (Junghans et al., 2022; Kim et al., 2020; Konopka et al., 2020; Mitra et al., 2019; C. Walker et al., 2017;

Wang et al., 2018). Previous studies using cell models based on fALS mutations and studies with human sALS tissues have provided evidence for DNA damage in both forms of ALS. These findings have detected an elevated level of DSB sensor proteins, DNA damage markers and a significant increase in DNA damage factors, which are implicated in contributing to neuronal death in ALS patients (Kim et al., 2020; Wang et al., 2018; Konopka et al., 2020; Mitra et al., 2019; C. Walker et al., 2017; Farg et al., 2017). Hence the accumulation of DNA damage may contribute to neurodegeneration in ALS.

A growing body of evidence, from our group and others, has shown that PDI is protective against multiple ALS phenotypes associated with proteostasis, using both *in vitro* and *in vivo* models (Walker et al., 2010, Honjo et al., 2011, Parakh et al., 2018, Parakh et al., 2018, Parakh et al., 2020, Farg et al., 2012, Parakh et al., 2021, Jeon et al., 2014). PDI was found to inhibit the mislocalization of TDP-43 from the nucleus to cytoplasm, apoptosis, ER stress, and protein misfolding, and it restored ER-Golgi transport, and improved motor impairment in zebrafish and NMJ connectivity in $SOD1^{G93A}$ mice (Walker et al., 2010, Honjo et al., 2011, Parakh et al., 2018, Parakh et al., 2018, Parakh et al., 2020, Farg et al., 2012, Parakh et al., 2021, Jeon et al., 2014; Rozas et al., 2021). Previous results from our laboratory had suggested a possible protective capacity of PDI against DNA damage. However, these results were only preliminary and involved overexpression of PDI which is non-physiological. Thus, the current study has extended these findings by confirming the role of PDI against DNA damage using an alternative paradigm (knockdown of endogenous PDI). Moreover, they have shown for the first time that PDI protects against DNA damage-induced apoptosis and that the ALS mutants display impairment in this protective function.

PDI is a chaperone that distinguishes between misfolded and properly folded protein substrates (Klappa et al., 1997). As PDI is a highly effective chaperone, it binds to misfolded proteins via hydrophobic interactions (Klappa et al., 1997), and facilitates degradation of these misfolded proteins during ER stress (Molinari et al., 2002). This study shows that a mutant possessing only the chaperone activity of PDI (Quad) lacks the protective activity of WT PDI. This is in contrast to previous studies that have identified roles of other chaperones, cytoplasmic heat shock proteins (Hsp) in DNA damage repair (DDR). Hsp70 and Hsp90 were involved in DNA repair of DSBs (Knighton & Truman, 2019) and inhibition of Hsp90 by 17-(allylamino)-17-demethoxygeldanamycin (17-AAG) led to the loss of ATM, which is activated during DSB. Although ATM is part of the homologous recombination DNA repair pathway, which is

thought to be absent in neurons, it indicates that other chaperone functions in the DDR (Knighton & Truman, 2019). Similarly, Hsp70 and Hsp27 were shown to function in another DNA repair pathway, base excision repair (BER). These chaperones removed oxidized nucleobases formed by ROS with human AP endonuclease (HAP1) and DNA glycosylase (UDG) in HeLa cells (Mendez et al., 2000). Another study demonstrated that Hsp70 and Hsp90 relocated from their original cytoplasmic location to the nucleus following DNA damage induced by H_2O_2 or 8-hydroxyguanosine (8-OH-dG), also indicating that chaperones can also relocate during DNA damage, similar to the results of this study (Sottile & Nadin, 2018).

Along with its chaperone function, PDI also possesses redox activity, which was found to be essential for its protective activity in this study. This activity mediates the formation of disulphide bridges or isomerization of protein complexes with distinct oxidative folding pathways (Irvine et al., 2014; Schwaller et al., 2003). Interestingly, PDI's chaperone activity is modulated by its redox activity (C. Wang et al., 2013). The present study aimed to address the direct involvement of PDI against DNA damage given its success in mitigating other ALS phenotypes (Walker et al., 2010, Honjo et al., 2011, Parakh et al., 2018, Parakh et al., 2020, Farg et al., 2012, Parakh et al., 2021).

4.1. Knockdown of endogenous PDI

RNA interference (RNAi) is responsible for regulating genetic expression in many organisms (Sharp, 2001; Tuschl, 2001). Small interfering RNAs (siRNAs) have been used to knockdown specific endogenous gene expression by destroying the complementary mRNA in mammalian cells (Makimura et al., 2002; Whitehead et al., 2009). Neuroblastoma cell lines are commonly used to examine pathogenesis in ALS (Pasinelli et al., 1998) and in this study, we used the mouse Neuro2a cell line. It was first important to find the optimum PDI siRNA concentration to downregulate PDI in Neuro2a cells. Previously 100 nM PDI siRNA was needed to silence endogenous PDI in a mouse motor neuron like NSC-34 cell line (A. K. Walker et al., 2010). Similarly, for silencing endogenous PDI expression in Neuro2A cells, the current study showed that 100 nM concentration of siRNA led to the lowest expression levels of PDI. Knockdown in neuronal cell lines to investigate different ALS phenotypes is a widely used method, including by our group (Konopka et al., 2020; A. K. Walker et al., 2010; H. Wang et al., 2018). We previously showed that knockdown of TDP-43 increased DNA damage, identifying TDP-43 as a DNA repair protein (Konopka et al., 2020). Similarly, another study showed that FUS

knockdown also leads to more DNA damage (H. Wang et al., 2018). Hence, siRNA knockdown can be used to identify the normal physiological roles of proteins involved in the DDR and repair of DNA damage.

It was observed that with increasing concentrations of PDI siRNA in this study, there was a decreasing trend of PDI expression levels, except for 120 nM, when there was an increase. Whilst it is not possible to draw firm conclusions from this without additional experiments, one possible reason for this observation could be that higher concentration of siRNA could cause off-target activity in cells (Caffrey et al., 2011). Off-target effects of siRNA were first observed in studies with microarray profiling where specific gene expressions, *CYLD* and *SOAT* were used to evaluate the effects (Scacheri et al., 2004; Semizarov et al., 2003; Tschuch et al., 2008). These off-target effects were described as RNAi machinery saturation (Khan et al., 2009), stimulation of immunity such as interferon activation (Sledz et al., 2003), and cross-reaction of siRNAs with non-targeted genes with a limited sequence match (A. L. Jackson et al., 2003). These off-target effects could cause non-specific targeting, which could explain the higher expression level of PDI in cells with 120 nM PDI siRNA (Ki et al., 2010). Hence, it is important to evaluate the off-target effects of the siRNA to further improve the siRNA technique in future studies of DNA damage.

4.2. DNA damage is significantly increased with etoposide or H_2O_2 treatment in Neuro2a cells following endogenous PDI knockdown

As neurons cannot be resynthesized like other cellular molecules, DNA damage can significantly affect neuronal functions. Also, neurons do not go through the cell cycle, hence, neurons lack the time advantage of the cell cycle to repair DNA breaks (Branzei & Foiani, 2008). Hence they become more susceptible to DNA damage compared to other cells (Pan et al., 2014). Given that DNA damage is involved in neurodegenerative diseases, including ALS (Kim et al., 2020), understanding the mechanisms by which neurons are susceptible to DNA damage, or by which DNA repair could be enhanced, could potentially aid in designing more effective therapeutics that target DNA damage. This study used two common pharmacological agents, etoposide and H_2O_2, to induce DNA damage (Olson, 1988; Tamamori-Adachi et al., 2018; Valverde et al., 2018). Etoposide is a strong DNA damage inducer which interacts with nuclear enzyme topoisomerase II (Walles et al., 1996). H_2O_2 induces oxidative stress and ionizing radiation, which damage DNA (Dahm-Daphi, 2000). The results obtained in this study

imply that PDI is protective against both types of DNA damage.

To detect DNA damage, using immunocytochemistry the formation of ɣ-H2AX foci as a specific marker was examined (Mah et al., 2010). Histone H2AX is phosphorylated in the presence of DNA damage and the resulting phosphorylated protein functions in DNA repair processes by binding to sites of DNA damage (Siddiqui et al., 2015). Previous studies have investigated ɣ-H2AX as a DNA damage marker using both *in vitro* and *ex vivo* experiments (Celeste et al., 2003; Madigan, 2002; Olive & Banáth, 2004; Rogakou et al., 1998; Sedelnikova et al., 2004; Siddiqui et al., 2015).

When ɣ-H2AX locates to DSB sites, it initiates the recruitment of DNA repair enzymes to the damage sites (Olive & Banáth, 2004). Previous studies from our group and others have also used ɣ-H2AX as a DNA damage marker in ALS, both with *C9ORF72* (Farg et al., 2017) and *TARDBP* mutations (Konopka et al., 2020). In an ALS wobbler mice model (Junghans et al., 2022), in an *in vivo* thyroid cancer study (Lassmann et al., 2010), and in a study including human patients (Sánchez-Flores et al., 2015), ɣ-H2AX was used as a marker for DNA damage. Hence, ɣ-H2AX is widely used and a reliable marker of damage, including in ALS. The formation of ɣ-H2AX from H2A is one of the earliest responses to DSB formation, the most lethal form of DNA damage (Madigan, 2002). In this study, more ɣ-H2AX foci were present in cells transfected with PDI siRNA following treatment with either etoposide or H_2O_2. This implies that PDI is protective against the formation of DSB, although further experiments are required to validate this, using other markers of DSBs such as 53BP1. Furthermore, SSBs can also readily convert to DSBs, so it cannot be determined that PDI is protective only against DSBs (Cannan & Pederson, 2016).

4.3. PDI is protective against apoptosis following etoposide or H_2O_2 DNA damage treatment

When DNA damage is present, cells either engage DNA repair mechanisms or they die to protect the organism from deleterious genomes (Chatterjee & Walker, 2017). According to the Nomenclature Committee on Cell Death (NCDD), apoptosis is a regulated cell death pathway, which is involved in cell death induced by DNA damage in neurons (Galluzzi et al., 2018). Motor neurons are thought to die at least partially by apoptosis in ALS (Coppedè, 2011; Martin et al., 2007; Murakami et al., 2007). Apoptosis in neurons needs to be highly regulated as once

apoptosis begins, death is inevitable (Jiang & Wang, 2004; Martin et al., 2007; Susin et al., 1999). Regulating apoptosis mechanisms in neurons is therefore centrally important. The findings of the current study suggested a role for both endogenous and overexpressed PDI in apoptotic cell death in Neuro2a cell lines following DNA damage treatment with etoposide or H_2O_2. In this study it was observed that the percentage of cells with apoptotic nuclei significantly increased following PDI siRNA transfection, indicating the importance of PDI in preventing apoptosis in Neuro2a cells after DNA damage treatment. Similarly, significantly fewer cells with overexpressed PDI displayed apoptotic nuclei, again implying that PDI is involved in protecting cells from apoptosis after DNA damage.

The apoptotic pathway is mediated via mitochondria where its initiation triggers mitochondrial outer membrane permeabilization (MOMP), leading the release of proteins from the mitochondrial intermembrane, which are responsible for activating caspases (Jiang & Wang, 2004). B-cell lymphoma-2 or Bcl-2 proteins are major regulators of apoptosis in mitochondria, and Bax and Bak are two proapoptotic Bcl-2 members, which are released in the cytosol following ER stress (X. Wang et al., 2011; Youle & Strasser, 2008). Several other *in vitro* and *in vivo* studies have shown that PDI and its family members prevent apoptosis in cells associated with ER stress and protein misfolding (Corazzari et al., 2007; Hetz, 2005; Lovat et al., 2008; Muller et al., 2013; Tanaka et al., 2000; Uehara et al., 2006; S.-B. Wang et al., 2012). PDI is also protective against apoptosis induced by hypoxia or brain ischemia in astrocytes (Tanaka et al., 2000), and inhibiting PDI resulted in apoptosis due to nitrosative stress following increases in ROS (Uehara et al., 2006), oxidized low-density lipoprotein (Muller et al., 2013), and chemotherapeutics (Lovat et al., 2008). Interestingly, inhibition of PDI activities in rat brains suppresses apoptosis induced by misfolded proteins (Hoffstrom et al., 2010). Hence, these authors proposed that PDI plays a protective role in repairing misfolded proteins and balancing cellular homeostasis at an early stage of ER stress. Hence whilst previous studies focused on the role of PDI in apoptosis following ER stress, the current study implies that PDI also has a protective role against apoptosis induced by etoposide or H_2O_2 DNA damage. This implies the necessity of PDI for maintaining cellular viability, although the mechanism involved remains unclear. However, PDI can also initiate apoptosis when it accumulates in the ER at threshold levels following misfolded proteins (Hoffstrom et al., 2010). Hence together these results imply that PDI finely controls induction of apoptosis.

4.4. Translocation of PDI from ER to the nucleus

PDI is predominantly present in the ER (Freedman et al., 1994), although in some circumstances, it can also locate to other cellular locations, particularly the cellular surface and cytoplasm (Terada et al., 1995). This reflects its wide variety of normal cellular functions (Terada et al., 1995). It has been previously proposed that saturation of the ER-retention machinery or removal of the PDI KDEL sequence may result in PDI escape from the ER (Turano et al., 2002). In a previous study, it was shown that following ER stress, PDI levels were increased in the cytosol, implying that PDI is a protein reflux substrate (Igbaria et al., 2019). Protein reflux is a process whereby proteins are directed from the ER to the cytosol following ER stress (Igbaria et al., 2019), hence PDI alters its cellular localization in response to specific types of stress. Although the mechanisms by which PDI enters the nucleus are not still clear, this study reveals that PDI displays more localization in the nucleus following etoposide treatment. This finding suggests that PDI enters the nucleus following DNA damage, implying it has a direct role in the DDR. However further studies are required to confirm this possibility. Similarly, in previous *in vitro* studies, two proteins of the PDI family, PDI and ERp57, were detected in the nucleus in the nuclear matrix (Altieri et al., 1993; Clive & Greene, 1996; Coppari et al., 2002; Johnson et al., 1992; Ohtani et al., 1993). ERp57 was also found in the nuclear matrix isolated from chicken liver cells (Altieri et al., 1993) and both ERp57 and PDI were detected in the nuclear matrix of nuclei from human lymphocyte and monocytes (Gerner et al., 1999). The nuclear matrix is basically a meshwork of nuclear proteins, which provides dynamic structural and functional supports to DNA (Nickerson et al., 1997). Using immunohistochemistry, ERp57 was detected in the nuclei of rat gametes (Ohtani et al., 1993), fibroblasts of chicken embryos (Altieri et al., 1993), and HeLa cells (Coppari et al., 2002). It has been previously suggested that the presence of ERp57 and PDI in the nucleus indicates that these two proteins are involved in transcriptional mechanisms via their redox activity (Stein et al., 1996). Also, due to their redox activity, ERp57 and PDI might also play a role in forming disulphide bridges in the nuclear matrix, although this is unlikely given the redox conditions of the nucleus. PDI also the facilitates the binding of two important transcription factors, nuclear factor-kappaB (NF-κB) and AP-1 to DNA (Clive & Greene, 1996). NF-κB is a regulatory factor which modulates transactivations of multiple DDR genes (W. Wang et al., 2017). Hence this might may explain the involvement of PDI in the DDR, although further studies are required to identify this mechanism. Previously in our lab we have shown with confocal microscopy that PDI translocates to nucleus following DNA damage by taking Z-stack images (Shadfar et al., bioRxiv). Other than immunocytochemistry, we have also shown

with western blotting of nuclear and cytoplasmic fractions that PDI translocates to nucleus following DNA damage treatment (Shadfar et al., bioRxiv). Hence, together these studies suggest that PDI translocates from the ER to the nucleus under multiple circumstances, including DNA damage.

4.5. Interaction between PDI and ɣ-H2AX: Still an open question

To further examine whether PDI has a direct role in the DDR, an immunoprecipitation between PDI and ɣ-H2AX was performed. As suggested by the immunocytochemistry results, PDI may translocate to nucleus following DNA damage, thus an association between PDI and ɣ-H2AX would suggest it has a specific role at sites of DNA repair. Immunoprecipitation is a powerful method to detect protein-protein associations (Lin & Lai, 2017), although it cannot directly determine whether two proteins physically interact. It uses the specificity of antibodies to identify target proteins from complex combinations (Kaboord & Perr, 2008). However, the results obtained for the PDI and ɣ-H2AX immunoprecipitation was not conclusive because positive bands for PDI were observed in the mouse IgG isotype control IP sample. This demonstrates that further optimization is needed for these experiments because the IgG control antibody is a negative control. Hence, no band should be visible for samples precipitated with this antibody. Hence, whilst it is possible that PDI and ɣ-H2AX may indeed interact, this would be masked by the non-specific binding of the isotype control antibody. Further studies are therefore needed, such as by using another IgG isotype control antibody to determine whether there is an interaction between PDI and ɣ-H2AX. However, this was not possible due to time constraints in this study. It is important in the future to identify antibodies with less cross-reactivity and higher specificity. Only after further antibody optimization has been performed can it be investigated whether there is a direct association between PDI and ɣ-H2AX. It is also possible that PDI and ɣ-H2AX may interact with another protein following DNA damage, and thus they may interact indirectly. Hence, whether there is a direct interaction between PDI and ɣ-H2AX remains an open question.

4.6. ALS-associated PDI mutants PDI-D292N and PDI-R300H display impaired protective activity against DNA damage

Previously described PDI mutants, PDI-D292N and PDI-R300H, which are implicated as risk

factors for ALS, were used in this study (Gonzalez-Perez et al., 2015; Woehlbier et al., 2016). We previously showed that the PDI-D292N and PDI-R300H mutants lack the physiological oxidoreductase activity of PDI (Parakh et al., 2020) and the protective activity against *SOD1* and *TDP-43* ALS phenotypes *in vitro* and *in vivo* using cellular and zebrafish models (Parakh et al., 2020). Similarly, another group showed that PDI-D292N and PDI-R300H mutants inhibit neuronal functions by disrupting motor neuron connectivity in an ALS zebrafish model (Woehlbier et al., 2016). In addition, another PDI mutant, PDI-Quad was also examined in this study, which lacks the redox activity of PDI, and thus possesses only the chaperone activity (Parakh et al., 2020). Similarly, previously the Quad mutant lacked most of the protective activity of PDI-WT against proteostasis mechanisms, showing that the redox activity of PDI mediates its protective function against multiple ALS phenotypes (Parakh et al., 2020). The role of any of these mutants was not investigated previously against DNA damage in ALS.

In this study, the formation of ɣ-H2AX foci was examined as a marker of DNA damage. Interestingly, all three mutants displayed significantly more DNA damage compared to PDI-WT following etoposide treatment. Hence, this result shows that the ALS-associated PDI mutants are not protective against DNA damage and that the redox activity of PDI mediates this protective activity. Interestingly, both PDI-D292N and PDI-R300H showed significant difference in DNA damage compared to PDI-Quad, indicating that PDI-D292N and PDI-R300H have minimal protectivity against DNA damage. As there is no significant difference between PDI-Quad and EV populations following etoposide treatment, it can be determined that the PDI-Quad mutant has no protective activity against DNA damage. Furthermore, whilst PDI-WT cells displayed significantly less DNA damage than EV, only PDI-R300H cells treated with etoposide showed a significant difference to etoposide treated EV cells. This implies that this PDI-R300H mutant has more of the protective activity of PDI WT than PDI-D292N because PDI-D292N is not significantly different from etoposide treated EV group.

Previously our laboratory investigated the intracellular redox environment of Neuro2a cells transfected with PDI-Quad, PDI-D292N and PDI-R300H plasmids (Parakh et al., 2020), in both untreated cells and those treated with BMC ((±)-trans-1,2-Bis (2-mercaptoacetamido) cyclohexane), a synthetic dithiol that mimics the redox activity of PDI (Woycechowsky et al., 1999). Although PDI-D292N and PDI-Quad significantly modulated the redox environment induced by BMC compared to PDI-WT, PDI-R300H showed similar intracellular oxidation in

Neuro2a cells to PDI-WT (Parakh et al., 2020). Hence, whilst all these PDI-mutants lacked redox activity, however, only PDI-R300H showed a significant difference in redox activity in the BMC experiment (Parakh et al., 2020). This might indicate that PDI-R300H might retain some redox activity. Interestingly, given the current study also identified that PDI-R300H gave different results to the other two mutants compared to EV, together this implies that this mutant might still retain some residual redox activity, thus protecting the cells from DNA damage. However, this part of the study did not use any other DNA damage inducing agent except etoposide. Future studies should use other pharmacological agents, including H_2O_2 to induce oxidative DNA damage, which is particularly relevant to ALS. Future studies should also examine whether these ALS-associated PDI-mutants protect against DNA damage induced by ALS mutant *FUS*, *TDP-43* or *SOD-1*.

In summary, this study identifies novel aspects of the protective role of PDI against DNA damage in ALS. Figure 8 summarizes the overall findings of this thesis.

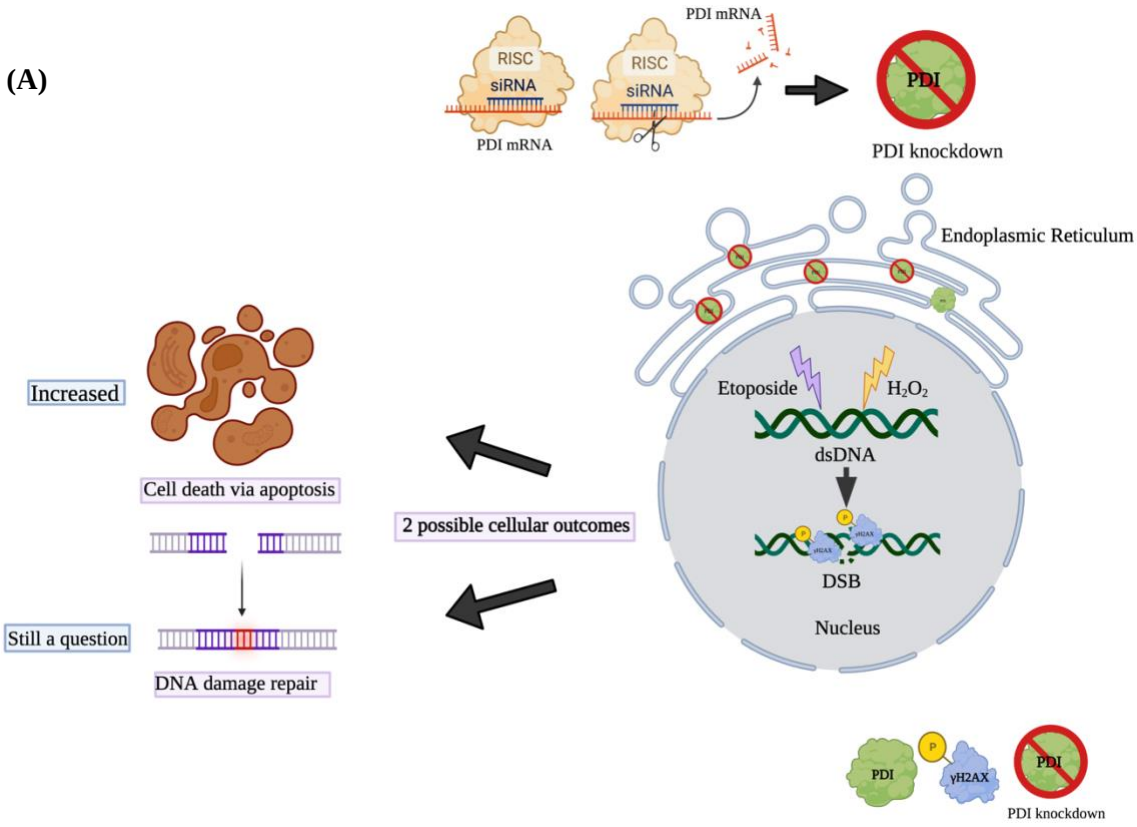

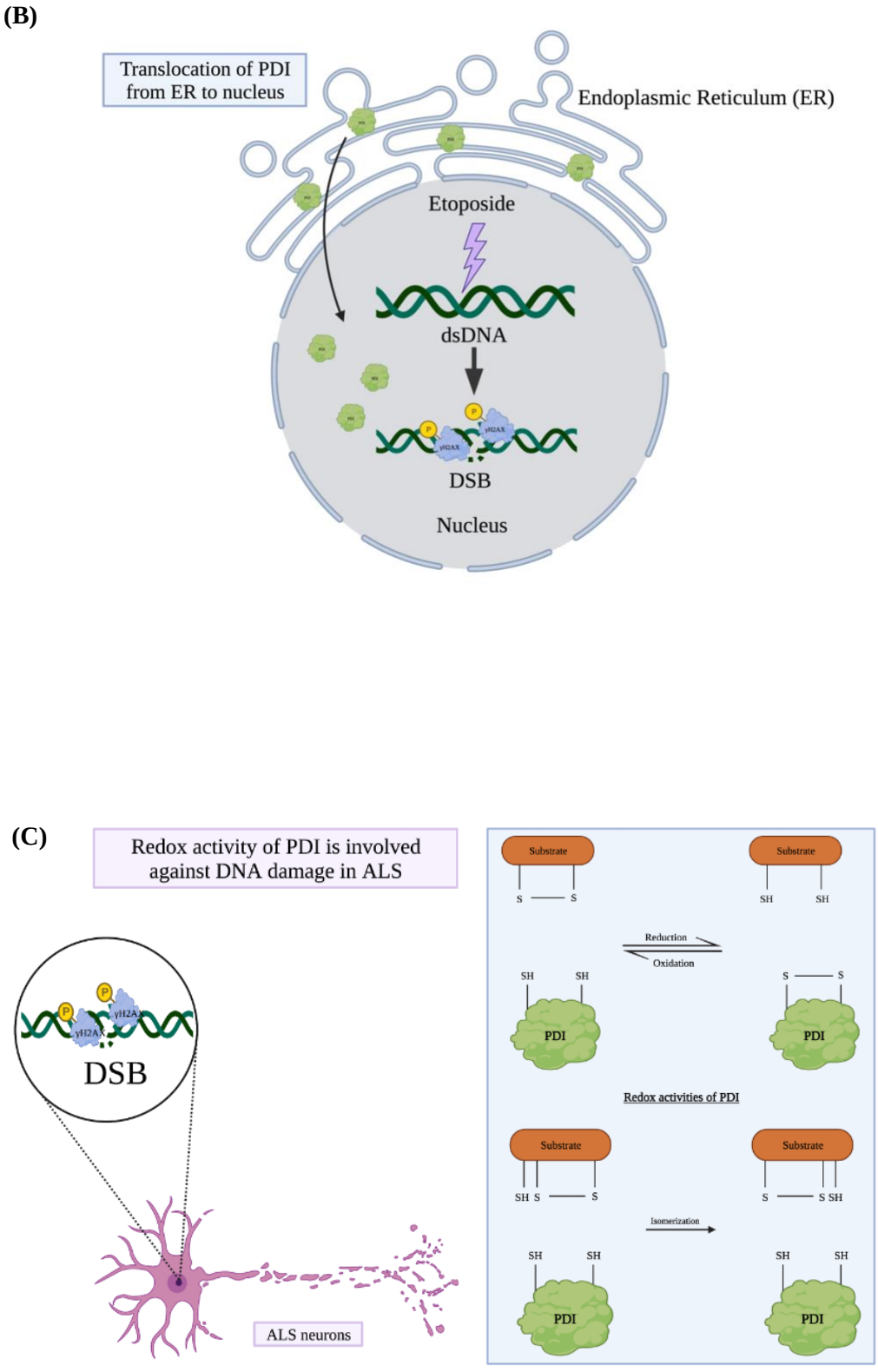

Figure 4: Schematic diagram presenting the findings of this thesis. (A) Knockdown of endogenous PDI induces both DNA damage and apoptosis in neuronal cell lines in response to

both etoposide and H_2O_2; (B) Endogenous PDI translocates into the nucleus following DNA damage induced by etoposide; (C) The redox activity of PDI mediates its protective role against DNA damage (D) The ALS-associated mutants lack the protective activity of PDI.

4.7. Future studies/Limitations of the current study

Although the present study implies that PDI plays a role against DNA damage, the results obtained should be further validated by future studies. Hence, some future directions arise from these findings. In this study, to confirm the findings of the siRNA experiments, we aimed to completely knockout the endogenous PDI gene by generating a PDI-knockout cell line using CRISPR/Cas9 methods. CRISPR/Cas9 is a popular technique to edit targeted genes to understand different biological mechanisms (Ran et al., 2013). CRISPR/Cas is a naturally occurring microbial immune system that uses RNA-guided nucleases to slice genetic elements which are foreign to the system (Deveau et al., 2010; Horvath & Barrangou, 2010). The main element of CRISPR/Cas9 is the guide RNA with 20-nt sequences to direct the Cas9 nuclease to cleave the desired gene (Ran et al., 2013). We did not identify a PDI CRISPR/Cas9 knockout line in this study and due to time limitations, it was not possible to repeat this experiment. Future studies should therefore aim to further screen for additional PDI-CRISPR clones and identify a clonal PDI knockout line, and then investigate whether more DNA damage is present in this line. This would have the advantage of examining DNA damage in a clonal population which would not be dependent on transfection efficiency, unlike the siRNA experiments.

Another future direction is to examine additional cellular models rather than using cell lines. The findings obtained here with etoposide and H_2O_2 could be further validated using iPSC-derived motor neurons or primary neurons. The advantages of iPSC models are that they can be directly prepared from human patients, including the most common sporadic form of ALS, and they do not display artificial protein overexpression (Singh et al., 2015). They also display key features of motor neurons (Singh et al., 2015). Similarly, primary neurons retain more *in vivo* functions and markers of neurons than neuronal cell lines (Sahu et al., 2019).

The location of PDI following DNA damage also requires further investigation. Subcellular fractionation should be performed to validate the result obtained using immunocytochemistry. Also, future studies can also examine the cellular localisation of PDI following DNA damage induced with other reagent such as H_2O_2, or more importantly, induction by ALS-associated

mutant forms of TDP-43, C9ORF72 or FUS. Future studies should also investigate the molecular mechanisms by which PDI specifically functions in the DDR.

Cells with fragmented nuclei or condensed nuclei, visualised by Hoechst or DAPI, were identified as undergoing apoptosis in this study (A. K. Walker et al., 2010). In future studies, additional markers of apoptosis could be examined, such as activated capase-3 by ICC or the Terminal deoxynucleotidyl transferase dUTP nick end labeling (TUNEL) assay (Duan et al., 2003). This assay detects the fragmentation of DNA to quantify DNA damage induced apoptotic cell death (Mirzayans & Murray, 2020). Future studies should also investigate the molecular mechanism by which PDI alleviates apoptosis in neuronal cell lines.

Future studies should further investigate the roles of PDI-D292N, PDI-R300H and PDI-Quad against DNA damage using another marker such as 53-bp1 and another DNA damage inducer such as H_2O_2. Also, it would also be interesting in future studies to examine if these mutants also relocate to the nucleus or if they are also protective against apoptosis upon DNA damage induction.

DNA damage is implicated in other neurodegenerative disease (Coppedè & Migliore, 2015), and PDI is also implicated in these diseases (Parakh & Atkin, 2015). Hence it is possible that PDI may also be protective against DNA damage in other NDs. Future studies should further look at the role of PDI in other NDs.

5. Conclusions

ALS is a multifactorial disease where DNA damage is now implicated as an important mechanism contributing to pathogenesis. Preliminary results from our laboratory previously showed that overexpressed PDI was protective against DNA damage. However, this thesis provided first evidence that endogenous PDI also prevents DNA damage, induced by either etoposide or H_2O_2 treatment using *in vitro* cellular models. This represents a more physiological paradigm that artificial protein overexpression. This thesis also provided evidence for the first time that PDI is protective against apoptosis induced by DNA damage, and that PDI translocates to the nucleus followed by DNA damage treatment with etoposide. Furthermore, the findings described here show the important redox-based protective of PDI against DNA damage in ALS. Lastly, ALS-associated PDI-mutants displayed less protective

activity against DNA damage compared to PDI-WT indicating in ALS, this may contribute to DNA damage. Therefore, together these results broaden our understanding of DNA damage, both the basic mechanisms and in ALS. Hence, in future it will be interesting to further investigate the molecular mechanisms by which PDI is involved against DNA damage, both in normal physiology and in ALS. A proper understating of these mechanisms may eventually aid in the design and development of novel therapeutics for ALS based on preventing DNA damage.

6. References

Abe, K., Aoki, M., Tsuji, S., Itoyama, Y., Sobue, G., Togo, M., Hamada, C., Tanaka, M., Akimoto, M., Nakamura, K., Takahashi, F., Kondo, K., Yoshino, H., Abe, K., Aoki, M., Tsuji, S., Itoyama, Y., Sobue, G., Togo, M., … Yoshino, H. (2017). Safety and efficacy of edaravone in well defined patients with amyotrophic lateral sclerosis: a randomised, double-blind, placebo-controlled trial. *The Lancet Neurology*, *16*(7), 505–512. https://doi.org/10.1016/S1474-4422(17)30115-1

Abel, E. L. (2007). Football Increases the Risk for Lou Gehrig's Disease, Amyotrophic Lateral Sclerosis. *Perceptual and Motor Skills*, *104*(3_suppl), 1251–1254. https://doi.org/10.2466/pms.104.4.1251-1254

Ali Khan, H., & Mutus, B. (2014). Protein disulfide isomerase a multifunctional protein with multiple physiological roles. *Frontiers in Chemistry*, *2*. https://doi.org/10.3389/fchem.2014.00070

Altieri, F., Maras, B., Eufemi, M., Ferraro, A., & Turano, C. (1993). Purification of a 57-kDa Nuclear Matrix Protein Associated with Thiol:Protein-Disulfide Oxidoreductase and Phospholipase C Activities. *Biochemical and Biophysical Research Communications*, *194*(3), 992–1000. https://doi.org/10.1006/bbrc.1993.1919

Andreu, C. I., Woehlbier, U., Torres, M., & Hetz, C. (2012). Protein disulfide isomerases in neurodegeneration: From disease mechanisms to biomedical applications. *FEBS Letters*, *586*(18), 2826–2834. https://doi.org/10.1016/j.febslet.2012.07.023

Appenzeller-Herzog, C., & Ellgaard, L. (2008). The human PDI family: Versatility packed into a single fold. *Biochimica et Biophysica Acta (BBA) - Molecular Cell Research*, *1783*(4), 535–548. https://doi.org/10.1016/j.bbamcr.2007.11.010

Armon, C. (2009). Smoking may be considered an established risk factor for sporadic ALS. *Neurology*, *73*(20), 1693–1698. https://doi.org/10.1212/WNL.0b013e3181c1df48

Ayala, A., Muñoz, M. F., & Argüelles, S. (2014). Lipid Peroxidation: Production, Metabolism, and Signaling Mechanisms of Malondialdehyde and 4-Hydroxy-2-Nonenal. *Oxidative Medicine and Cellular Longevity*, *2014*, 1–31. https://doi.org/10.1155/2014/360438

Balendra, R., & Isaacs, A. M. (2018). C9orf72-mediated ALS and FTD: multiple pathways to disease. *Nature Reviews Neurology*, *14*(9), 544–558. https://doi.org/10.1038/s41582-018-0047-2

Benham, A. M. (2012). The Protein Disulfide Isomerase Family: Key Players in Health and Disease. *Antioxidants & Redox Signaling*, *16*(8), 781–789.

https://doi.org/10.1089/ars.2011.4439

Benkler, C., O'Neil, A. L., Slepian, S., Qian, F., Weinreb, P. H., & Rubin, L. L. (2018). Aggregated SOD1 causes selective death of cultured human motor neurons. *Scientific Reports*, *8*(1), 16393. https://doi.org/10.1038/s41598-018-34759-z

Bensimon, G., Lacomblez, L., & Meininger, V. (1994). A Controlled Trial of Riluzole in Amyotrophic Lateral Sclerosis. *New England Journal of Medicine*, *330*(9), 585–591. https://doi.org/10.1056/NEJM199403033300901

Boesch, P., Weber-Lotfi, F., Ibrahim, N., Tarasenko, V., Cosset, A., Paulus, F., Lightowlers, R. N., & Dietrich, A. (2011). DNA repair in organelles: Pathways, organization, regulation, relevance in disease and aging. *Biochimica et Biophysica Acta (BBA) - Molecular Cell Research*, *1813*(1), 186–200. https://doi.org/10.1016/j.bbamcr.2010.10.002

Bonafede, R., & Mariotti, R. (2017). ALS Pathogenesis and Therapeutic Approaches: The Role of Mesenchymal Stem Cells and Extracellular Vesicles. *Frontiers in Cellular Neuroscience, 11*. https://doi.org/10.3389/fncel.2017.00080

Bordoni, M., Pansarasa, O., Dell'Orco, M., Crippa, V., Gagliardi, S., Sproviero, D., Bernuzzi, S., Diamanti, L., Ceroni, M., Tedeschi, G., Poletti, A., & Cereda, C. (2019). Nuclear Phospho-SOD1 Protects DNA from Oxidative Stress Damage in Amyotrophic Lateral Sclerosis. *Journal of Clinical Medicine*, *8*(5), 729. https://doi.org/10.3390/jcm8050729

Branzei, D., & Foiani, M. (2008). Regulation of DNA repair throughout the cell cycle. *Nature Reviews Molecular Cell Biology*, *9*(4), 297–308. https://doi.org/10.1038/nrm2351

Brem, R. (2005). XRCC1 is required for DNA single-strand break repair in human cells. *Nucleic Acids Research*, *33*(8), 2512–2520. https://doi.org/10.1093/nar/gki543

Buehler, E., Chen, Y.-C., & Martin, S. (2012). C911: A Bench-Level Control for Sequence Specific siRNA Off-Target Effects. *PLoS ONE*, *7*(12), e51942. https://doi.org/10.1371/journal.pone.0051942

Bunton-Stasyshyn, R. K. A., Saccon, R. A., Fratta, P., & Fisher, E. M. C. (2015). SOD1 Function and Its Implications for Amyotrophic Lateral Sclerosis Pathology. *The Neuroscientist*, *21*(5), 519–529. https://doi.org/10.1177/1073858414561795

Burma, S., Chen, B. P., Murphy, M., Kurimasa, A., & Chen, D. J. (2001). ATM Phosphorylates Histone H2AX in Response to DNA Double-strand Breaks. *Journal of Biological Chemistry*, *276*(45), 42462–42467. https://doi.org/10.1074/jbc.C100466200

Burton E. Tropp. (2011). *Molecular Biology: Genes to Proteins* (4th ed.). Jones & Bartlett Learning.

Caffrey, D. R., Zhao, J., Song, Z., Schaffer, M. E., Haney, S. A., Subramanian, R. R., Seymour, A. B., & Hughes, J. D. (2011). siRNA Off-Target Effects Can Be Reduced at Concentrations That Match Their Individual Potency. *PLoS ONE*, *6*(7), e21503. https://doi.org/10.1371/journal.pone.0021503

Calingasan, N. Y., Chen, J., Kiaei, M., & Beal, M. F. (2005). β-amyloid 42 accumulation in the lumbar spinal cord motor neurons of amyotrophic lateral sclerosis patients. *Neurobiology of Disease*, *19*(1–2), 340–347. https://doi.org/10.1016/j.nbd.2005.01.012

Cannan, W. J., & Pederson, D. S. (2016). Mechanisms and Consequences of Double-Strand DNA Break Formation in Chromatin. *Journal of Cellular Physiology*, *231*(1), 3–14. https://doi.org/10.1002/jcp.25048

Celeste, A., Fernandez-Capetillo, O., Kruhlak, M. J., Pilch, D. R., Staudt, D. W., Lee, A., Bonner, R. F., Bonner, W. M., & Nussenzweig, A. (2003). Histone H2AX phosphorylation is dispensable for the initial recognition of DNA breaks. *Nature Cell Biology*, *5*(7), 675–679. https://doi.org/10.1038/ncb1004

Chan, K., Resnick, M. A., & Gordenin, D. A. (2013). The choice of nucleotide inserted opposite abasic sites formed within chromosomal DNA reveals the polymerase activities participating in translesion DNA synthesis. *DNA Repair*, *12*(11), 878–889. https://doi.org/10.1016/j.dnarep.2013.07.008

Chang, H. H. Y., Pannunzio, N. R., Adachi, N., & Lieber, M. R. (2017). Non-homologous DNA end joining and alternative pathways to double-strand break repair. *Nature Reviews Molecular Cell Biology*, *18*(8), 495–506. https://doi.org/10.1038/nrm.2017.48

Chatterjee, N., & Walker, G. C. (2017). Mechanisms of DNA damage, repair, and mutagenesis. *Environmental and Molecular Mutagenesis*, *58*(5), 235–263. https://doi.org/10.1002/em.22087

Chen, W., Guo, L., Li, M., Wei, C., Li, S., & Xu, R. (2022). The pathogenesis of amyotrophic lateral sclerosis: Mitochondrial dysfunction, protein misfolding and epigenetics. *Brain Research*, *1786*, 147904. https://doi.org/10.1016/j.brainres.2022.147904

Chichiarelli, S., Ferraro, A., Altieri, F., Eufemi, M., Coppari, S., Grillo, C., Arcangeli, V., & Turano, C. (2007). The stress protein ERp57/GRP58 binds specific DNA sequences in HeLa cells. *Journal of Cellular Physiology*, *210*(2), 343–351. https://doi.org/10.1002/jcp.20824

Chiò, A., Calvo, A., Dossena, M., Ghiglione, P., Mutani, R., & Mora, G. (2009). ALS in Italian professional soccer players: The risk is still present and could be soccer-specific. *Amyotrophic Lateral Sclerosis*, *10*(4), 205–209.

https://doi.org/10.1080/17482960902721634

Chio, A., Calvo, A., Mazzini, L., Cantello, R., Mora, G., Moglia, C., Corrado, L., D'Alfonso, S., Majounie, E., Renton, A., Pisano, F., Ossola, I., Brunetti, M., Traynor, B. J., & Restagno, G. (2012). Extensive genetics of ALS: A population-based study in Italy. *Neurology*, *79*(19), 1983–1989. https://doi.org/10.1212/WNL.0b013e3182735d36

Chiò, A., Logroscino, G., Hardiman, O., Swingler, R., Mitchell, D., Beghi, E., Traynor, B. G., & On Behalf of the Eurals Consortium. (2009). Prognostic factors in ALS: A critical review. *Amyotrophic Lateral Sclerosis*, *10*(5–6), 310–323. https://doi.org/10.3109/17482960802566824

Chio, A., Mora, G., Leone, M., Mazzini, L., Cocito, D., Giordana, M. T., Bottacchi, E., & Mutani, R. (2002). Early symptom progression rate is related to ALS outcome: A prospective population-based study. *Neurology*, *59*(1), 99–103. https://doi.org/10.1212/WNL.59.1.99

Clive, D. R., & Greene, J. J. (1996). Cooperation of protein disulfide isomerase and redox environment in the regulation of NF-κB and AP1 binding to DNA. *Cell Biochemistry and Function*, *14*(1), 49–55. https://doi.org/10.1002/cbf.638

Cooke, M. S., Evans, M. D., Dizdaroglu, M., & Lunec, J. (2003). Oxidative DNA damage: mechanisms, mutation, and disease. *The FASEB Journal*, *17*(10), 1195–1214. https://doi.org/10.1096/fj.02-0752rev

Coppari, S., Altieri, F., Ferraro, A., Chichiarelli, S., Eufemi, M., & Turano, C. (2002). Nuclear localization and DNA interaction of protein disulfide isomerase ERp57 in mammalian cells. *Journal of Cellular Biochemistry*, *85*(2), 325–333. https://doi.org/10.1002/jcb.10137

Coppedè, F. (2011). An Overview of DNA Repair in Amyotrophic Lateral Sclerosis. *The Scientific World JOURNAL*, *11*, 1679–1691. https://doi.org/10.1100/2011/853474

Coppedè, F., & Migliore, L. (2015). DNA damage in neurodegenerative diseases. *Mutation Research/Fundamental and Molecular Mechanisms of Mutagenesis*, *776*, 84–97. https://doi.org/10.1016/j.mrfmmm.2014.11.010

Corazzari, M., Lovat, P. E., Armstrong, J. L., Fimia, G. M., Hill, D. S., Birch-Machin, M., Redfern, C. P. F., & Piacentini, M. (2007). Targeting homeostatic mechanisms of endoplasmic reticulum stress to increase susceptibility of cancer cells to fenretinide-induced apoptosis: the role of stress proteins ERdj5 and ERp57. *British Journal of Cancer*, *96*(7), 1062–1071. https://doi.org/10.1038/sj.bjc.6603672

Corcia, P., Couratier, P., Blasco, H., Andres, C. R., Beltran, S., Meininger, V., & Vourc'h, P.

(2017). Genetics of amyotrophic lateral sclerosis. *Revue Neurologique*, *173*(5), 254–262. https://doi.org/10.1016/j.neurol.2017.03.030

Dahl, E. S., & Aird, K. M. (2017). Ataxia-Telangiectasia Mutated Modulation of Carbon Metabolism in Cancer. *Frontiers in Oncology*, *7*. https://doi.org/10.3389/fonc.2017.00291

Dahm-Daphi, C. S. W. A. J. (2000). Comparison of biological effects of DNA damage induced by ionizing radiation and hydrogen peroxide in CHO cells. *International Journal of Radiation Biology*, *76*(1), 67–75. https://doi.org/10.1080/095530000139023

Davies RJ. (1995). *Royal Irish Academy Medal Lecture. Ultraviolet radiation damage in DNA.* (Vol. 23). Biochem Soc Trans .

De Bont, R. (2004). Endogenous DNA damage in humans: a review of quantitative data. *Mutagenesis*, *19*(3), 169–185. https://doi.org/10.1093/mutage/geh025

Deveau, H., Garneau, J. E., & Moineau, S. (2010). CRISPR/Cas System and Its Role in Phage-Bacteria Interactions. *Annual Review of Microbiology*, *64*(1), 475–493. https://doi.org/10.1146/annurev.micro.112408.134123

Dip, R., Camenisch, U., & Naegeli, H. (2004). Mechanisms of DNA damage recognition and strand discrimination in human nucleotide excision repair. *DNA Repair*, *3*(11), 1409–1423. https://doi.org/10.1016/j.dnarep.2004.05.005

Dormann, D., & Haass, C. (2013). Fused in sarcoma (FUS): An oncogene goes awry in neurodegeneration. *Molecular and Cellular Neuroscience*, *56*, 475–486. https://doi.org/10.1016/j.mcn.2013.03.006

Duan, W. R., Garner, D. S., Williams, S. D., Funckes-Shippy, C. L., Spath, I. S., & Blomme, E. A. (2003). Comparison of immunohistochemistry for activated caspase-3 and cleaved cytokeratin 18 with the TUNEL method for quantification of apoptosis in histological sections of PC-3 subcutaneous xenografts. *The Journal of Pathology*, *199*(2), 221–228. https://doi.org/10.1002/path.1289

Duffy, J. R., Peach, R. K., & Strand, E. A. (2007). Progressive Apraxia of Speech as a Sign of Motor Neuron Disease. *American Journal of Speech-Language Pathology*, *16*(3), 198–208. https://doi.org/10.1044/1058-0360(2007/025)

Elmore, S. (2007). Apoptosis: A Review of Programmed Cell Death. *Toxicologic Pathology*, *35*(4), 495–516. https://doi.org/10.1080/01926230701320337

Eustermann, S., Wu, W.-F., Langelier, M.-F., Yang, J.-C., Easton, L. E., Riccio, A. A., Pascal, J. M., & Neuhaus, D. (2015). Structural Basis of Detection and Signaling of DNA Single-Strand Breaks by Human PARP-1. *Molecular Cell*, *60*(5), 742–754.

https://doi.org/10.1016/j.molcel.2015.10.032

Fang, F., Ye, W., Weisskopf, M. G., Gallo, V., O'Reilly, E. J., Vineis, P., Ascherio, A., & Armon, C. (2010). Smoking may be considered an established risk factor for sporadic ALS. *Neurology*, *74*(23), 1927–1929. https://doi.org/10.1212/WNL.0b013e3181e038e9

Farg, M. A., Konopka, A., Soo, K. Y., Ito, D., & Atkin, J. D. (2017). The DNA damage response (DDR) is induced by the C9orf72 repeat expansion in amyotrophic lateral sclerosis. *Human Molecular Genetics*, *26*(15), 2882–2896. https://doi.org/10.1093/hmg/ddx170

Farg, M. A., Soo, K. Y., Walker, A. K., Pham, H., Orian, J., Horne, M. K., Warraich, S. T., Williams, K. L., Blair, I. P., & Atkin, J. D. (2012). Mutant FUS induces endoplasmic reticulum stress in amyotrophic lateral sclerosis and interacts with protein disulfide-isomerase. *Neurobiology of Aging*, *33*(12), 2855–2868. https://doi.org/10.1016/j.neurobiolaging.2012.02.009

Fell, V. L., & Schild-Poulter, C. (2012). Ku Regulates Signaling to DNA Damage Response Pathways through the Ku70 von Willebrand A Domain. *Molecular and Cellular Biology*, *32*(1), 76–87. https://doi.org/10.1128/MCB.05661-11

Ferguson, T. A., & Elman, L. B. (2007). Clinical presentation and diagnosis of Amyotrophic Lateral Sclerosis. *NeuroRehabilitation*, *22*(6), 409–416. https://doi.org/10.3233/NRE-2007-22602

Ferrari, I., Verpelli, C., Crespi, A., Sala, C., Fornasari, D., & Pietrini, G. (2018). SOD1 stimulates lamellipodial protrusions in Neuro 2A cell lines. *Communicative & Integrative Biology*, *11*(3), 1–7. https://doi.org/10.1080/19420889.2018.1486652

Freedman, R. B., Hirst, T. R., & Tuite, M. F. (1994). Protein disulphide isomerase: building bridges in protein folding. *Trends in Biochemical Sciences*, *19*(8), 331–336. https://doi.org/10.1016/0968-0004(94)90072-8

Friedberg, E. C. (2005). Suffering in silence: the tolerance of DNA damage. *Nature Reviews Molecular Cell Biology*, *6*(12), 943–953. https://doi.org/10.1038/nrm1781

Galluzzi, L., Vitale, I., Aaronson, S. A., Abrams, J. M., Adam, D., Agostinis, P., Alnemri, E. S., Altucci, L., Amelio, I., Andrews, D. W., Annicchiarico-Petruzzelli, M., Antonov, A. V., Arama, E., Baehrecke, E. H., Barlev, N. A., Bazan, N. G., Bernassola, F., Bertrand, M. J. M., Bianchi, K., … Kroemer, G. (2018). Molecular mechanisms of cell death: recommendations of the Nomenclature Committee on Cell Death 2018. *Cell Death & Differentiation*, *25*(3), 486–541. https://doi.org/10.1038/s41418-017-0012-4

Gerner, C., Holzmann, K., Meissner, M., Gotzmann, J., Grimm, R., & Sauermann, G. (1999).

Reassembling proteins and chaperones in human nuclear matrix protein fractions. *Journal of Cellular Biochemistry*, *74*(2), 145–151.

Goldberger, R. F., Epstein, C. J., & Anfinsen, C. B. (1963). Acceleration of Reactivation of Reduced Bovine Pancreatic Ribonuclease by a Microsomal System from Rat Liver. *Journal of Biological Chemistry*, *238*(2), 628–635. https://doi.org/10.1016/S0021-9258(18)81309-6

Gonzalez-Perez, P., Woehlbier, U., Chian, R.-J., Sapp, P., Rouleau, G. A., Leblond, C. S., Daoud, H., Dion, P. A., Landers, J. E., Hetz, C., & Brown, R. H. (2015). Identification of rare protein disulfide isomerase gene variants in amyotrophic lateral sclerosis patients. *Gene*, *566*(2), 158–165. https://doi.org/10.1016/j.gene.2015.04.035

Gordon, P. H., Cheng, B., Katz, I. B., Pinto, M., Hays, A. P., Mitsumoto, H., & Rowland, L. P. (2006). The natural history of primary lateral sclerosis. *Neurology*, *66*(5), 647–653. https://doi.org/10.1212/01.wnl.0000200962.94777.71

Gottlieb, T. M., & Jackson, S. P. (1993). The DNA-dependent protein kinase: Requirement for DNA ends and association with Ku antigen. *Cell*, *72*(1), 131–142. https://doi.org/10.1016/0092-8674(93)90057-W

Goutman, S. A., Hardiman, O., Al-Chalabi, A., Chió, A., Savelieff, M. G., Kiernan, M. C., & Feldman, E. L. (2022). Emerging insights into the complex genetics and pathophysiology of amyotrophic lateral sclerosis. *The Lancet Neurology*. https://doi.org/10.1016/S1474-4422(21)00414-2

Grek, C., & Townsend, D. M. (2014). Protein Disulfide Isomerase Superfamily in Disease and the Regulation of Apoptosis. *Endoplasmic Reticulum Stress in Diseases*, *1*(1). https://doi.org/10.2478/ersc-2013-0001

Grillo, C., D'Ambrosio, C., Scaloni, A., Maceroni, M., Merluzzi, S., Turano, C., & Altieri, F. (2006). Cooperative activity of Ref-1/APE and ERp57 in reductive activation of transcription factors. *Free Radical Biology and Medicine*, *41*(7), 1113–1123. https://doi.org/10.1016/j.freeradbiomed.2006.06.016

Guerrero, E. N., Mitra, J., Wang, H., Rangaswamy, S., Hegde, P. M., Basu, P., Rao, K. S., & Hegde, M. L. (2019). Amyotrophic lateral sclerosis-associated TDP-43 mutation Q331K prevents nuclear translocation of XRCC4-DNA ligase 4 complex and is linked to genome damage-mediated neuronal apoptosis. *Human Molecular Genetics*, *28*(18), 3161–3162. https://doi.org/10.1093/hmg/ddz141

Gupta, A., Hunt, C. R., Chakraborty, S., Pandita, R. K., Yordy, J., Ramnarain, D. B., Horikoshi, N., & Pandita, T. K. (2014). Role of 53BP1 in the Regulation of DNA Double-Strand

Break Repair Pathway Choice. *Radiation Research*, *181*(1), 1–8. https://doi.org/10.1667/RR13572.1

Hashimoto, S., Okada, K., & Imaoka, S. (2008). Interaction between Bisphenol Derivatives and Protein Disulphide Isomerase (PDI) and Inhibition of PDI Functions: Requirement of Chemical Structure for Binding to PDI. *Journal of Biochemistry*, *144*(3), 335–342. https://doi.org/10.1093/jb/mvn075

Hess, D. T., Matsumoto, A., Kim, S.-O., Marshall, H. E., & Stamler, J. S. (2005). Protein S-nitrosylation: purview and parameters. *Nature Reviews Molecular Cell Biology*, *6*(2), 150–166. https://doi.org/10.1038/nrm1569

Hetz, C. (2005). The Disulfide Isomerase Grp58 Is a Protective Factor against Prion Neurotoxicity. *Journal of Neuroscience*, *25*(11), 2793–2802. https://doi.org/10.1523/JNEUROSCI.4090-04.2005

Hoffstrom, B. G., Kaplan, A., Letso, R., Schmid, R. S., Turmel, G. J., Lo, D. C., & Stockwell, B. R. (2010). Inhibitors of protein disulfide isomerase suppress apoptosis induced by misfolded proteins. *Nature Chemical Biology*, *6*(12), 900–906. https://doi.org/10.1038/nchembio.467

Holliday, R., & Ho, T. (1998). Gene silencing and endogenous DNA methylation in mammalian cells. *Mutation Research/Fundamental and Molecular Mechanisms of Mutagenesis*, *400*(1–2), 361–368. https://doi.org/10.1016/S0027-5107(98)00034-7

Honjo, Y., Kaneko, S., Ito, H., Horibe, T., Nagashima, M., Nakamura, M., Fujita, K., Takahashi, R., Kusaka, H., & Kawakami, K. (2011). Protein disulfide isomerase-immunopositive inclusions in patients with amyotrophic lateral sclerosis. *Amyotrophic Lateral Sclerosis*, *12*(6), 444–450. https://doi.org/10.3109/17482968.2011.594055

Horvath, P., & Barrangou, R. (2010). CRISPR/Cas, the Immune System of Bacteria and Archaea. *Science*, *327*(5962), 167–170. https://doi.org/10.1126/science.1179555

Huang, R.-X., & Zhou, P.-K. (2020). DNA damage response signaling pathways and targets for radiotherapy sensitization in cancer. *Signal Transduction and Targeted Therapy*, *5*(1), 60. https://doi.org/10.1038/s41392-020-0150-x

Iacoangeli, A., Al Khleifat, A., Jones, A. R., Sproviero, W., Shatunov, A., Opie-Martin, S., Morrison, K. E., Shaw, P. J., Shaw, C. E., Fogh, I., Dobson, R. J., Newhouse, S. J., & Al-Chalabi, A. (2019). C9orf72 intermediate expansions of 24–30 repeats are associated with ALS. *Acta Neuropathologica Communications*, *7*(1), 115. https://doi.org/10.1186/s40478-019-0724-4

Igbaria, A., Merksamer, P. I., Trusina, A., Tilahun, F., Johnson, J. R., Brandman, O., Krogan,

N. J., Weissman, J. S., & Papa, F. R. (2019). Chaperone-mediated reflux of secretory proteins to the cytosol during endoplasmic reticulum stress. *Proceedings of the National Academy of Sciences*, *116*(23), 11291–11298. https://doi.org/10.1073/pnas.1904516116

Ikenaka, K., Ishigaki, S., Iguchi, Y., Kawai, K., Fujioka, Y., Yokoi, S., Abdelhamid, R. F., Nagano, S., Mochizuki, H., Katsuno, M., & Sobue, G. (2020). Characteristic Features of FUS Inclusions in Spinal Motor Neurons of Sporadic Amyotrophic Lateral Sclerosis. *Journal of Neuropathology & Experimental Neurology*, *79*(4), 370–377. https://doi.org/10.1093/jnen/nlaa003

Irvine, A. G., Wallis, A. K., Sanghera, N., Rowe, M. L., Ruddock, L. W., Howard, M. J., Williamson, R. A., Blindauer, C. A., & Freedman, R. B. (2014). Protein Disulfide-Isomerase Interacts with a Substrate Protein at All Stages along Its Folding Pathway. *PLoS ONE*, *9*(1), e82511. https://doi.org/10.1371/journal.pone.0082511

Jackson, A. L., Bartz, S. R., Schelter, J., Kobayashi, S. V, Burchard, J., Mao, M., Li, B., Cavet, G., & Linsley, P. S. (2003). Expression profiling reveals off-target gene regulation by RNAi. *Nature Biotechnology*, *21*(6), 635–637. https://doi.org/10.1038/nbt831

Jackson, S. P., & Bartek, J. (2009). The DNA-damage response in human biology and disease. *Nature*, *461*(7267), 1071–1078. https://doi.org/10.1038/nature08467

Jaul, E., & Barron, J. (2017). Age-Related Diseases and Clinical and Public Health Implications for the 85 Years Old and Over Population. *Frontiers in Public Health*, *5*. https://doi.org/10.3389/fpubh.2017.00335

Jeon, G. S., Nakamura, T., Lee, J.-S., Choi, W.-J., Ahn, S.-W., Lee, K.-W., Sung, J.-J., & Lipton, S. A. (2014). Potential Effect of S-Nitrosylated Protein Disulfide Isomerase on Mutant SOD1 Aggregation and Neuronal Cell Death in Amyotrophic Lateral Sclerosis. *Molecular Neurobiology*, *49*(2), 796–807. https://doi.org/10.1007/s12035-013-8562-z

Jiang, X., & Wang, X. (2004). Cytochrome C-mediated apoptosis. *Annual Review of Biochemistry*, *73*, 87–106. https://doi.org/10.1146/annurev.biochem.73.011303.073706

Johnson, E., Henzel, W., & Deisseroth, A. (1992). An isoform of protein disulfide isomerase isolated from chronic myelogenous leukemia cells alters complex formation between nuclear proteins and regulatory regions of interferon-inducible genes. *The Journal of Biological Chemistry*, *267*(20), 14412–14417.

Junghans, M., John, F., Cihankaya, H., Schliebs, D., Winklhofer, K. F., Bader, V., Matschke, J., Theiss, C., & Matschke, V. (2022). ROS scavengers decrease γH2ax spots in motor neuronal nuclei of ALS model mice in vitro. *Frontiers in Cellular Neuroscience*, *16*. https://doi.org/10.3389/fncel.2022.963169

Kaboord, B., & Perr, M. (2008). Isolation of proteins and protein complexes by immunoprecipitation. *Methods in Molecular Biology (Clifton, N.J.)*, *424*, 349–364. https://doi.org/10.1007/978-1-60327-064-9_27

Kato, S., Sumi-Akamaru, H., Fujimura, H., Sakoda, S., Kato, M., Hirano, A., Takikawa, M., & Ohama, E. (2001). Copper chaperone for superoxide dismutase co-aggregates with superoxide dismutase 1 (SOD1) in neuronal Lewy body-like hyaline inclusions: an immunohistochemical study on familial amyotrophic lateral sclerosis with SOD1 gene mutation. *Acta Neuropathologica*, *102*(3), 233–238. https://doi.org/10.1007/s004010000355

Kemmink, J., Darby, N. J., Dijkstra, K., Nilges, M., & Creighton, T. E. (1997). The folding catalyst protein disulfide isomerase is constructed of active and inactive thioredoxin modules. *Current Biology*, *7*(4), 239–245. https://doi.org/10.1016/S0960-9822(06)00119-9

Khan, A. A., Betel, D., Miller, M. L., Sander, C., Leslie, C. S., & Marks, D. S. (2009). Transfection of small RNAs globally perturbs gene regulation by endogenous microRNAs. *Nature Biotechnology*, *27*(6), 549–555. https://doi.org/10.1038/nbt.1543

Ki, K. H., Park, D. Y., Lee, S. H., Kim, N. Y., Choi, B. M., & Noh, G. J. (2010). The optimal concentration of siRNA for gene silencing in primary cultured astrocytes and microglial cells of rats. *Korean Journal of Anesthesiology*, *59*(6), 403. https://doi.org/10.4097/kjae.2010.59.6.403

Kiefer, J. (n.d.). Effects of Ultraviolet Radiation on DNA. In *Chromosomal Alterations* (pp. 39–53). Springer Berlin Heidelberg. https://doi.org/10.1007/978-3-540-71414-9_3

Kiernan, M. C., Vucic, S., Cheah, B. C., Turner, M. R., Eisen, A., Hardiman, O., Burrell, J. R., & Zoing, M. C. (2011). Amyotrophic lateral sclerosis. *The Lancet*, *377*(9769), 942–955. https://doi.org/10.1016/S0140-6736(10)61156-7

Kim, B. W., Jeong, Y. E., Wong, M., & Martin, L. J. (2020). DNA damage accumulates and responses are engaged in human ALS brain and spinal motor neurons and DNA repair is activatable in iPSC-derived motor neurons with SOD1 mutations. *Acta Neuropathologica Communications*, *8*(1), 7. https://doi.org/10.1186/s40478-019-0874-4

Klappa, P., Hawkins, H. C., & Freedman, R. B. (1997). Interactions Between Protein Disulphide Isomerase and Peptides. *European Journal of Biochemistry*, *248*(1), 37–42. https://doi.org/10.1111/j.1432-1033.1997.t01-1-00037.x

Knighton, L. E., & Truman, A. W. (2019). *Role of the Molecular Chaperones Hsp70 and Hsp90 in the DNA Damage Response* (pp. 345–358). https://doi.org/10.1007/978-3-030-

03952-3_18

Kok, J. R., Palminha, N. M., Dos Santos Souza, C., El-Khamisy, S. F., & Ferraiuolo, L. (2021). DNA damage as a mechanism of neurodegeneration in ALS and a contributor to astrocyte toxicity. *Cellular and Molecular Life Sciences*, *78*(15), 5707–5729. https://doi.org/10.1007/s00018-021-03872-0

Konopka, A., & Atkin, J. (2018). The Emerging Role of DNA Damage in the Pathogenesis of the C9orf72 Repeat Expansion in Amyotrophic Lateral Sclerosis. *International Journal of Molecular Sciences*, *19*(10), 3137. https://doi.org/10.3390/ijms19103137

Konopka, A., Whelan, D. R., Jamali, M. S., Perri, E., Shahheydari, H., Toth, R. P., Parakh, S., Robinson, T., Cheong, A., Mehta, P., Vidal, M., Ragagnin, A. M. G., Khizhnyak, I., Jagaraj, C. J., Galper, J., Grima, N., Deva, A., Shadfar, S., Nicholson, G. A., … Atkin, J. D. (2020). Impaired NHEJ repair in amyotrophic lateral sclerosis is associated with TDP-43 mutations. *Molecular Neurodegeneration*, *15*(1), 51. https://doi.org/10.1186/s13024-020-00386-4

Krokan, H. E., & Bjoras, M. (2013). Base Excision Repair. *Cold Spring Harbor Perspectives in Biology*, *5*(4), a012583–a012583. https://doi.org/10.1101/cshperspect.a012583

Kuna, M., Mahdi, F., Chade, A. R., & Bidwell, G. L. (2018). Molecular Size Modulates Pharmacokinetics, Biodistribution, and Renal Deposition of the Drug Delivery Biopolymer Elastin-like Polypeptide. *Scientific Reports*, *8*(1), 7923. https://doi.org/10.1038/s41598-018-24897-9

Kwiatkowski, T. J., Bosco, D. A., LeClerc, A. L., Tamrazian, E., Vanderburg, C. R., Russ, C., Davis, A., Gilchrist, J., Kasarskis, E. J., Munsat, T., Valdmanis, P., Rouleau, G. A., Hosler, B. A., Cortelli, P., de Jong, P. J., Yoshinaga, Y., Haines, J. L., Pericak-Vance, M. A., Yan, J., … Brown, R. H. (2009). Mutations in the *FUS/TLS* Gene on Chromosome 16 Cause Familial Amyotrophic Lateral Sclerosis. *Science*, *323*(5918), 1205–1208. https://doi.org/10.1126/science.1166066

Laboissière, M. C. A., Sturley, S. L., & Raines, R. T. (1995). The Essential Function of Protein-disulfide Isomerase Is to Unscramble Non-native Disulfide Bonds. *Journal of Biological Chemistry*, *270*(47), 28006–28009. https://doi.org/10.1074/jbc.270.47.28006

Lacomblez, L., Bensimon, G., Meininger, V., Leigh, P. ., & Guillet, P. (1996). Dose-ranging study of riluzole in amyotrophic lateral sclerosis. *The Lancet*, *347*(9013), 1425–1431. https://doi.org/10.1016/S0140-6736(96)91680-3

LaMantia, M., & Lennarz, W. J. (1993). The essential function of yeast protein disulfide isomerase does not reside in its isomerase activity. *Cell*, *74*(5), 899–908.

https://doi.org/10.1016/0092-8674(93)90469-7

Lambert, N., & Freedman, R. B. (1985). The latency of rat liver microsomal protein disulphide-isomerase. *Biochemical Journal*, *228*(3), 635–645. https://doi.org/10.1042/bj2280635

Lassmann, M., Hänscheid, H., Gassen, D., Biko, J., Meineke, V., Reiners, C., & Scherthan, H. (2010). In Vivo Formation of γ-H2AX and 53BP1 DNA Repair Foci in Blood Cells After Radioiodine Therapy of Differentiated Thyroid Cancer. *Journal of Nuclear Medicine*, *51*(8), 1318–1325. https://doi.org/10.2967/jnumed.109.071357

Li, X., & Heyer, W.-D. (2008). Homologous recombination in DNA repair and DNA damage tolerance. *Cell Research*, *18*(1), 99–113. https://doi.org/10.1038/cr.2008.1

Lin, J.-S., & Lai, E.-M. (2017). Protein-Protein Interactions: Co-Immunoprecipitation. *Methods in Molecular Biology (Clifton, N.J.)*, *1615*, 211–219. https://doi.org/10.1007/978-1-4939-7033-9_17

Lindahl, T. (1979). *DNA Glycosylases, Endonucleases for Apurinic/Apyrimidinic Sites, and Base Excision-Repair* (pp. 135–192). https://doi.org/10.1016/S0079-6603(08)60800-4

Lindahl, T. (1993). Instability and decay of the primary structure of DNA. *Nature*, *362*(6422), 709–715. https://doi.org/10.1038/362709a0

LINDAHL, T., & BARNES, D. E. (2000). Repair of Endogenous DNA Damage. *Cold Spring Harbor Symposia on Quantitative Biology*, *65*(0), 127–134. https://doi.org/10.1101/sqb.2000.65.127

Liu, Y., Ji, W., Shergalis, A., Xu, J., Delaney, A. M., Calcaterra, A., Pal, A., Ljungman, M., Neamati, N., & Rehemtulla, A. (2019). Activation of the Unfolded Protein Response via Inhibition of Protein Disulfide Isomerase Decreases the Capacity for DNA Repair to Sensitize Glioblastoma to Radiotherapy. *Cancer Research*, *79*(11), 2923–2932. https://doi.org/10.1158/0008-5472.CAN-18-2540

Löbrich, M., Shibata, A., Beucher, A., Fisher, A., Ensminger, M., Goodarzi, A. A., Barton, O., & Jeggo, P. A. (2010). γH2AX foci analysis for monitoring DNA double-strand break repair: Strengths, limitations and optimization. *Cell Cycle*, *9*(4), 662–669. https://doi.org/10.4161/cc.9.4.10764

Loechler, E. L. (1994). A Violation of the Swain-Scott Principle, and Not SN1 versus SN2Reaction Mechanisms, Explains Why Carcinogenic Alkylating Agents Can Form Different Proportions of Adducts at Oxygen versus Nitrogen in DNA. *Chemical Research in Toxicology*, *7*(3), 277–280. https://doi.org/10.1021/tx00039a001

Lopez-Gonzalez, R., Lu, Y., Gendron, T. F., Karydas, A., Tran, H., Yang, D., Petrucelli, L., Miller, B. L., Almeida, S., & Gao, F.-B. (2016). Poly(GR) in C9ORF72 -Related

ALS/FTD Compromises Mitochondrial Function and Increases Oxidative Stress and DNA Damage in iPSC-Derived Motor Neurons. *Neuron*, *92*(2), 383–391. https://doi.org/10.1016/j.neuron.2016.09.015

Lovat, P. E., Corazzari, M., Armstrong, J. L., Martin, S., Pagliarini, V., Hill, D., Brown, A. M., Piacentini, M., Birch-Machin, M. A., & Redfern, C. P. F. (2008). Increasing Melanoma Cell Death Using Inhibitors of Protein Disulfide Isomerases to Abrogate Survival Responses to Endoplasmic Reticulum Stress. *Cancer Research*, *68*(13), 5363–5369. https://doi.org/10.1158/0008-5472.CAN-08-0035

Luch, A. (2009). *On the impact of the molecule structure in chemical carcinogenesis* (pp. 151–179). https://doi.org/10.1007/978-3-7643-8336-7_6

Madigan, J. P. (2002). DNA double-strand break-induced phosphorylation of Drosophila histone variant H2Av helps prevent radiation-induced apoptosis. *Nucleic Acids Research*, *30*(17), 3698–3705. https://doi.org/10.1093/nar/gkf496

Mah, L.-J., El-Osta, A., & Karagiannis, T. C. (2010). γH2AX: a sensitive molecular marker of DNA damage and repair. *Leukemia*, *24*(4), 679–686. https://doi.org/10.1038/leu.2010.6

Makimura, H., Mizuno, T. M., Mastaitis, J. W., Agami, R., & Mobbs, C. V. (2002). Reducing hypothalamic AGRP by RNA interference increases metabolic rate and decreases body weight without influencing food intake. *BMC Neuroscience*, *3*, 18. https://doi.org/10.1186/1471-2202-3-18

Manjaly, Z. R., Scott, K. M., Abhinav, K., Wijesekera, L., Ganesalingam, J., Goldstein, L. H., Janssen, A., Dougherty, A., Willey, E., Stanton, B. R., Turner, M. R., Ampong, M.-A., Sakel, M., Orrell, R. W., Howard, R., Shaw, C. E., Leigh, P. N., & Al-Chalabi, A. (2010). The sex ratio in amyotrophic lateral sclerosis: A population based study. *Amyotrophic Lateral Sclerosis*, *11*(5), 439–442. https://doi.org/10.3109/17482961003610853

Martin, L. J., Liu, Z., Chen, K., Price, A. C., Pan, Y., Swaby, J. A., & Golden, W. C. (2007). Motor neuron degeneration in amyotrophic lateral sclerosis mutant superoxide dismutase-1 transgenic mice: Mechanisms of mitochondriopathy and cell death. *The Journal of Comparative Neurology*, *500*(1), 20–46. https://doi.org/10.1002/cne.21160

Mason, P. A., & Lightowlers, R. N. (2003). Why do mammalian mitochondria possess a mismatch repair activity? *FEBS Letters*, *554*(1–2), 6–9. https://doi.org/10.1016/S0014-5793(03)01169-4

Mavragani, I. V., Nikitaki, Z., Kalospyros, S. A., & Georgakilas, A. G. (2019). Ionizing Radiation and Complex DNA Damage: From Prediction to Detection Challenges and Biological Significance. *Cancers*, *11*(11), 1789. https://doi.org/10.3390/cancers11111789

Meisler, M. H., Russ, C., Montgomery, K. T., Greenway, M., Ennis, S., Hardiman, O., Figlewicz, D. A., Quenneville, N. R., Conibear, E., & Brown, R. H. (2008). Evaluation of the Golgi trafficking protein VPS54 (*wobbler*) as a candidate for ALS. *Amyotrophic Lateral Sclerosis*, *9*(3), 141–148. https://doi.org/10.1080/17482960801934403

Mejzini, R., Flynn, L. L., Pitout, I. L., Fletcher, S., Wilton, S. D., & Akkari, P. A. (2019). ALS Genetics, Mechanisms, and Therapeutics: Where Are We Now? *Frontiers in Neuroscience*, *13*. https://doi.org/10.3389/fnins.2019.01310

Mendez, F., Sandigursky, M., Franklin, W. A., Kenny, M. K., Kureekattil, R., & Bases, R. (2000). Heat-shock proteins associated with base excision repair enzymes in HeLa cells. *Radiation Research*, *153*(2), 186–195. https://doi.org/10.1667/0033-7587(2000)153[0186:hspawb]2.0.co;2

Mertz, T., Harcy, V., & Roberts, S. (2017). Risks at the DNA Replication Fork: Effects upon Carcinogenesis and Tumor Heterogeneity. *Genes*, *8*(1), 46. https://doi.org/10.3390/genes8010046

Michaelson, N., Facciponte, D., Bradley, W., & Stommel, E. (2017). Cytokine expression levels in ALS: A potential link between inflammation and BMAA-triggered protein misfolding. *Cytokine & Growth Factor Reviews*, *37*, 81–88. https://doi.org/10.1016/j.cytogfr.2017.05.001

Miller, R. G., Mitchell, J. D., & Moore, D. H. (2012). Riluzole for amyotrophic lateral sclerosis (ALS)/motor neuron disease (MND). *Cochrane Database of Systematic Reviews*. https://doi.org/10.1002/14651858.CD001447.pub3

Mirkin, S. M. (2008). Discovery of alternative DNA structures: a heroic decade (1979-1989). *Frontiers in Bioscience*, *13*(13), 1064. https://doi.org/10.2741/2744

Mirzayans, R., & Murray, D. (2020). Do TUNEL and Other Apoptosis Assays Detect Cell Death in Preclinical Studies? *International Journal of Molecular Sciences*, *21*(23), 9090. https://doi.org/10.3390/ijms21239090

Mitra, J., Guerrero, E. N., Hegde, P. M., Liachko, N. F., Wang, H., Vasquez, V., Gao, J., Pandey, A., Taylor, J. P., Kraemer, B. C., Wu, P., Boldogh, I., Garruto, R. M., Mitra, S., Rao, K. S., & Hegde, M. L. (2019). Motor neuron disease-associated loss of nuclear TDP-43 is linked to DNA double-strand break repair defects. *Proceedings of the National Academy of Sciences*, *116*(10), 4696–4705. https://doi.org/10.1073/pnas.1818415116

Molinari, M., Galli, C., Piccaluga, V., Pieren, M., & Paganetti, P. (2002). Sequential assistance of molecular chaperones and transient formation of covalent complexes during protein degradation from the ER. *Journal of Cell Biology*, *158*(2), 247–257.

https://doi.org/10.1083/jcb.200204122

Mora, J. S. (2017). Edaravone for treatment of early-stage ALS. *The Lancet Neurology*, *16*(10), 772. https://doi.org/10.1016/S1474-4422(17)30289-2

Moreno-Herrero, F., de Jager, M., Dekker, N. H., Kanaar, R., Wyman, C., & Dekker, C. (2005). Mesoscale conformational changes in the DNA-repair complex Rad50/Mre11/Nbs1 upon binding DNA. *Nature*, *437*(7057), 440–443. https://doi.org/10.1038/nature03927

Moser, J. M., Bigini, P., & Schmitt-John, T. (2013). The wobbler mouse, an ALS animal model. *Molecular Genetics and Genomics*, *288*(5–6), 207–229. https://doi.org/10.1007/s00438-013-0741-0

Muller, C., Bandemer, J., Vindis, C., Camaré, C., Mucher, E., Guéraud, F., Larroque-Cardoso, P., Bernis, C., Auge, N., Salvayre, R., & Negre-Salvayre, A. (2013). Protein Disulfide Isomerase Modification and Inhibition Contribute to ER Stress and Apoptosis Induced by Oxidized Low Density Lipoproteins. *Antioxidants & Redox Signaling*, *18*(7), 731–742. https://doi.org/10.1089/ars.2012.4577

Murakami, T., Nagai, M., Miyazaki, K., Morimoto, N., Ohta, Y., Kurata, T., Takehisa, Y., Kamiya, T., & Abe, K. (2007). Early decrease of mitochondrial DNA repair enzymes in spinal motor neurons of presymptomatic transgenic mice carrying a mutant SOD1 gene. *Brain Research*, *1150*, 182–189. https://doi.org/10.1016/j.brainres.2007.02.057

Neumann, M., Sampathu, D. M., Kwong, L. K., Truax, A. C., Micsenyi, M. C., Chou, T. T., Bruce, J., Schuck, T., Grossman, M., Clark, C. M., McCluskey, L. F., Miller, B. L., Masliah, E., Mackenzie, I. R., Feldman, H., Feiden, W., Kretzschmar, H. A., Trojanowski, J. Q., & Lee, V. M.-Y. (2006). Ubiquitinated TDP-43 in Frontotemporal Lobar Degeneration and Amyotrophic Lateral Sclerosis. *Science*, *314*(5796), 130–133. https://doi.org/10.1126/science.1134108

Niccoli, T., Partridge, L., & Isaacs, A. M. (2017). Ageing as a risk factor for ALS/FTD. *Human Molecular Genetics*, *26*(R2), R105–R113. https://doi.org/10.1093/hmg/ddx247

Nickerson, J. A., Krockmalnic, G., Wan, K. M., & Penman, S. (1997). The nuclear matrix revealed by eluting chromatin from a cross-linked nucleus. *Proceedings of the National Academy of Sciences*, *94*(9), 4446–4450. https://doi.org/10.1073/pnas.94.9.4446

O'Driscoll, M., Macpherson, P., Xu, Y.-Z., & Karran, P. (1999). The cytotoxicity of DNA carboxymethylation and methylation by the model carboxymethylating agent azaserine in human cells. *Carcinogenesis*, *20*(9), 1855–1862. https://doi.org/10.1093/carcin/20.9.1855

Ohtani, H., Wakui, H., Ishino, T., Komatsuda, A., & Miura, A. B. (1993). An isoform of protein disulfide isomerase is expressed in the developing acrosome of spermatids during rat

spermiogenesis and is transported into the nucleus of mature spermatids and epididymal spermatozoa. *Histochemistry*, *100*(6), 423–429. https://doi.org/10.1007/BF00267822

Olive, P. L., & Banáth, J. P. (2004). Phosphorylation of histone H2AX as a measure of radiosensitivity. *International Journal of Radiation Oncology*Biology*Physics*, *58*(2), 331–335. https://doi.org/10.1016/j.ijrobp.2003.09.028

Olson, M. J. (1988). DNA strand breaks induced by hydrogen peroxide in isolated rat hepatocytes. *Journal of Toxicology and Environmental Health*, *23*(3), 407–423. https://doi.org/10.1080/15287398809531123

Oskarsson, B., Horton, D. K., & Mitsumoto, H. (2015). Potential Environmental Factors in Amyotrophic Lateral Sclerosis. *Neurologic Clinics*, *33*(4), 877–888. https://doi.org/10.1016/j.ncl.2015.07.009

Paganoni, S., Macklin, E. A., Hendrix, S., Berry, J. D., Elliott, M. A., Maiser, S., Karam, C., Caress, J. B., Owegi, M. A., Quick, A., Wymer, J., Goutman, S. A., Heitzman, D., Heiman-Patterson, T., Jackson, C. E., Quinn, C., Rothstein, J. D., Kasarskis, E. J., Katz, J., … Cudkowicz, M. E. (2020). Trial of Sodium Phenylbutyrate–Taurursodiol for Amyotrophic Lateral Sclerosis. *New England Journal of Medicine*, *383*(10), 919–930. https://doi.org/10.1056/NEJMoa1916945

Pan, L., Penney, J., & Tsai, L.-H. (2014). Chromatin Regulation of DNA Damage Repair and Genome Integrity in the Central Nervous System. *Journal of Molecular Biology*, *426*(20), 3376–3388. https://doi.org/10.1016/j.jmb.2014.08.001

Parakh, S., & Atkin, J. D. (2015). Novel roles for protein disulphide isomerase in disease states: a double edged sword? *Frontiers in Cell and Developmental Biology*, *3*. https://doi.org/10.3389/fcell.2015.00030

Parakh, S., Jagaraj, C. J., Vidal, M., Ragagnin, A. M. G., Perri, E. R., Konopka, A., Toth, R. P., Galper, J., Blair, I. P., Thomas, C. J., Walker, A. K., Yang, S., Spencer, D. M., & Atkin, J. D. (2018). ERp57 is protective against mutant SOD1-induced cellular pathology in amyotrophic lateral sclerosis. *Human Molecular Genetics*, *27*(8), 1311–1331. https://doi.org/10.1093/hmg/ddy041

Parakh, S., Perri, E. R., Vidal, M., Sultana, J., Shadfar, S., Mehta, P., Konopka, A., Thomas, C. J., Spencer, D. M., & Atkin, J. D. (2021). Protein disulphide isomerase (PDI) is protective against amyotrophic lateral sclerosis (ALS)-related mutant Fused in Sarcoma (FUS) in in vitro models. *Scientific Reports*, *11*(1), 17557. https://doi.org/10.1038/s41598-021-96181-2

Parakh, S., Shadfar, S., Perri, E. R., Ragagnin, A. M. G., Piattoni, C. V., Fogolín, M. B., Yuan,

K. C., Shahheydari, H., Don, E. K., Thomas, C. J., Hong, Y., Comini, M. A., Laird, A. S., Spencer, D. M., & Atkin, J. D. (2020). The Redox Activity of Protein Disulfide Isomerase Inhibits ALS Phenotypes in Cellular and Zebrafish Models. *IScience*, *23*(5), 101097. https://doi.org/10.1016/j.isci.2020.101097

Parakh, S., Spencer, D. M., Halloran, M. A., Soo, K. Y., & Atkin, J. D. (2013). Redox Regulation in Amyotrophic Lateral Sclerosis. *Oxidative Medicine and Cellular Longevity*, *2013*, 1–12. https://doi.org/10.1155/2013/408681

Pasinelli, P., Borchelt, D. R., Houseweart, M. K., Cleveland, D. W., & Brown, R. H. (1998). Caspase-1 is activated in neural cells and tissue with amyotrophic lateral sclerosis-associated mutations in copper-zinc superoxide dismutase. *Proceedings of the National Academy of Sciences*, *95*(26), 15763–15768. https://doi.org/10.1073/pnas.95.26.15763

Paull, T. T., Rogakou, E. P., Yamazaki, V., Kirchgessner, C. U., Gellert, M., & Bonner, W. M. (2000). A critical role for histone H2AX in recruitment of repair factors to nuclear foci after DNA damage. *Current Biology*, *10*(15), 886–895. https://doi.org/10.1016/S0960-9822(00)00610-2

Pellegata, N. S., Antoniono, R. J., Redpath, J. L., & Stanbridge, E. J. (1996). DNA damage and p53-mediated cell cycle arrest: A reevaluation. *Proceedings of the National Academy of Sciences*, *93*(26), 15209–15214. https://doi.org/10.1073/pnas.93.26.15209

Perkins, E. M., Burr, K., Banerjee, P., Mehta, A. R., Dando, O., Selvaraj, B. T., Suminaite, D., Nanda, J., Henstridge, C. M., Gillingwater, T. H., Hardingham, G. E., Wyllie, D. J. A., Chandran, S., & Livesey, M. R. (2021). Altered network properties in C9ORF72 repeat expansion cortical neurons are due to synaptic dysfunction. *Molecular Neurodegeneration*, *16*(1), 13. https://doi.org/10.1186/s13024-021-00433-8

Podhorecka, M., Skladanowski, A., & Bozko, P. (2010). H2AX Phosphorylation: Its Role in DNA Damage Response and Cancer Therapy. *Journal of Nucleic Acids*, *2010*, 1–9. https://doi.org/10.4061/2010/920161

Polo, L. M., Xu, Y., Hornyak, P., Garces, F., Zeng, Z., Hailstone, R., Matthews, S. J., Caldecott, K. W., Oliver, A. W., & Pearl, L. H. (2019). Efficient Single-Strand Break Repair Requires Binding to Both Poly(ADP-Ribose) and DNA by the Central BRCT Domain of XRCC1. *Cell Reports*, *26*(3), 573-581.e5. https://doi.org/10.1016/j.celrep.2018.12.082

Polo, S. E., & Jackson, S. P. (2011). Dynamics of DNA damage response proteins at DNA breaks: a focus on protein modifications. *Genes & Development*, *25*(5), 409–433. https://doi.org/10.1101/gad.2021311

Prasad, A., Bharathi, V., Sivalingam, V., Girdhar, A., & Patel, B. K. (2019). Molecular

mechanisms of TDP-43 misfolding and pathology in amyotrophic lateral sclerosis. In *Frontiers in Molecular Neuroscience* (Vol. 12). Frontiers Media S.A. https://doi.org/10.3389/fnmol.2019.00025

Pupillo, E., Messina, P., Logroscino, G., Zoccolella, S., Chiò, A., Calvo, A., Corbo, M., Lunetta, C., Micheli, A., Millul, A., Vitelli, E., & Beghi, E. (2012). Trauma and amyotrophic lateral sclerosis: a case-control study from a population-based registry. *European Journal of Neurology*, *19*(12), 1509–1517. https://doi.org/10.1111/j.1468-1331.2012.03723.x

Ran, F. A., Hsu, P. D., Wright, J., Agarwala, V., Scott, D. A., & Zhang, F. (2013). Genome engineering using the CRISPR-Cas9 system. *Nature Protocols*, *8*(11), 2281–2308. https://doi.org/10.1038/nprot.2013.143

Rastogi, R. P., Richa, Kumar, A., Tyagi, M. B., & Sinha, R. P. (2010). Molecular Mechanisms of Ultraviolet Radiation-Induced DNA Damage and Repair. *Journal of Nucleic Acids*, *2010*, 1–32. https://doi.org/10.4061/2010/592980

Ratti, A., & Buratti, E. (2016). Physiological functions and pathobiology of TDP-43 and FUS/TLS proteins. *Journal of Neurochemistry*, *138*, 95–111. https://doi.org/10.1111/jnc.13625

Renton, A. E., Chiò, A., & Traynor, B. J. (2014). State of play in amyotrophic lateral sclerosis genetics. *Nature Neuroscience*, *17*(1), 17–23. https://doi.org/10.1038/nn.3584

Renton, A. E., Majounie, E., Waite, A., Simón-Sánchez, J., Rollinson, S., Gibbs, J. R., Schymick, J. C., Laaksovirta, H., van Swieten, J. C., Myllykangas, L., Kalimo, H., Paetau, A., Abramzon, Y., Remes, A. M., Kaganovich, A., Scholz, S. W., Duckworth, J., Ding, J., Harmer, D. W., … Traynor, B. J. (2011). A Hexanucleotide Repeat Expansion in C9ORF72 Is the Cause of Chromosome 9p21-Linked ALS-FTD. *Neuron*, *72*(2), 257–268. https://doi.org/10.1016/j.neuron.2011.09.010

Rogakou, E. P., Pilch, D. R., Orr, A. H., Ivanova, V. S., & Bonner, W. M. (1998). DNA Double-stranded Breaks Induce Histone H2AX Phosphorylation on Serine 139. *Journal of Biological Chemistry*, *273*(10), 5858–5868. https://doi.org/10.1074/jbc.273.10.5858

Rosen, D. R., Siddique, T., Patterson, D., Figlewicz, D. A., Sapp, P., Hentati, A., Donaldson, D., Goto, J., O'Regan, J. P., Deng, H.-X., Rahmani, Z., Krizus, A., McKenna-Yasek, D., Cayabyab, A., Gaston, S. M., Berger, R., Tanzi, R. E., Halperin, J. J., Herzfeldt, B., … Brown, R. H. (1993). Mutations in Cu/Zn superoxide dismutase gene are associated with familial amyotrophic lateral sclerosis. *Nature*, *362*(6415), 59–62. https://doi.org/10.1038/362059a0

Rozas, P., Pinto, C., Martínez Traub, F., Díaz, R., Pérez, V., Becerra, D., Ojeda, P., Ojeda, J., Wright, M. T., Mella, J., Plate, L., Henríquez, J. P., Hetz, C., & Medinas, D. B. (2021). Protein disulfide isomerase ERp57 protects early muscle denervation in experimental ALS. *Acta Neuropathologica Communications*, *9*(1), 21. https://doi.org/10.1186/s40478-020-01116-z

Rutherford, N. J., Heckman, M. G., DeJesus-Hernandez, M., Baker, M. C., Soto-Ortolaza, A. I., Rayaprolu, S., Stewart, H., Finger, E., Volkening, K., Seeley, W. W., Hatanpaa, K. J., Lomen-Hoerth, C., Kertesz, A., Bigio, E. H., Lippa, C., Knopman, D. S., Kretzschmar, H. A., Neumann, M., Caselli, R. J., … Rademakers, R. (2012). Length of normal alleles of C9ORF72 GGGGCC repeat do not influence disease phenotype. *Neurobiology of Aging*, *33*(12), 2950.e5-2950.e7. https://doi.org/10.1016/j.neurobiolaging.2012.07.005

Rydberg, B., & Lindahl, T. (1982). Nonenzymatic methylation of DNA by the intracellular methyl group donor S-adenosyl-L-methionine is a potentially mutagenic reaction. *The EMBO Journal*, *1*(2), 211–216. https://doi.org/10.1002/j.1460-2075.1982.tb01149.x

Sahu, M. P., Nikkilä, O., Lågas, S., Kolehmainen, S., & Castrén, E. (2019). Culturing primary neurons from rat hippocampus and cortex. *Neuronal Signaling*, *3*(2). https://doi.org/10.1042/NS20180207

Sánchez-Flores, M., Pásaro, E., Bonassi, S., Laffon, B., & Valdiglesias, V. (2015). γH2AX Assay as DNA Damage Biomarker for Human Population Studies: Defining Experimental Conditions. *Toxicological Sciences*, *144*(2), 406–413. https://doi.org/10.1093/toxsci/kfv011

Scacheri, P. C., Rozenblatt-Rosen, O., Caplen, N. J., Wolfsberg, T. G., Umayam, L., Lee, J. C., Hughes, C. M., Shanmugam, K. S., Bhattacharjee, A., Meyerson, M., & Collins, F. S. (2004). Short interfering RNAs can induce unexpected and divergent changes in the levels of untargeted proteins in mammalian cells. *Proceedings of the National Academy of Sciences*, *101*(7), 1892–1897. https://doi.org/10.1073/pnas.0308698100

Schreiber, V., Amé, J.-C., Dollé, P., Schultz, I., Rinaldi, B., Fraulob, V., Ménissier-de Murcia, J., & de Murcia, G. (2002). Poly(ADP-ribose) Polymerase-2 (PARP-2) Is Required for Efficient Base Excision DNA Repair in Association with PARP-1 and XRCC1. *Journal of Biological Chemistry*, *277*(25), 23028–23036. https://doi.org/10.1074/jbc.M202390200

Schultz, L. B., Chehab, N. H., Malikzay, A., & Halazonetis, T. D. (2000). P53 Binding Protein 1 (53bp1) Is an Early Participant in the Cellular Response to DNA Double-Strand Breaks. *Journal of Cell Biology*, *151*(7), 1381–1390. https://doi.org/10.1083/jcb.151.7.1381

Schwaller, M., Wilkinson, B., & Gilbert, H. F. (2003). Reduction-Reoxidation Cycles Contribute to Catalysis of disulfide Isomerization by Protein-disulfide Isomerase. *Journal of Biological Chemistry*, *278*(9), 7154–7159. https://doi.org/10.1074/jbc.M211036200

Sedelnikova, O. A., Horikawa, I., Zimonjic, D. B., Popescu, N. C., Bonner, W. M., & Barrett, J. C. (2004). Senescing human cells and ageing mice accumulate DNA lesions with unrepairable double-strand breaks. *Nature Cell Biology*, *6*(2), 168–170. https://doi.org/10.1038/ncb1095

Segal, A. W. (2005). HOW NEUTROPHILS KILL MICROBES. *Annual Review of Immunology*, *23*(1), 197–223. https://doi.org/10.1146/annurev.immunol.23.021704.115653

Sellier, C., Campanari, M., Julie Corbier, C., Gaucherot, A., Kolb-Cheynel, I., Oulad-Abdelghani, M., Ruffenach, F., Page, A., Ciura, S., Kabashi, E., & Charlet-Berguerand, N. (2016). Loss of C9 <scp>ORF</scp> 72 impairs autophagy and synergizes with polyQ Ataxin-2 to induce motor neuron dysfunction and cell death. *The EMBO Journal*, *35*(12), 1276–1297. https://doi.org/10.15252/embj.201593350

Semizarov, D., Frost, L., Sarthy, A., Kroeger, P., Halbert, D. N., & Fesik, S. W. (2003). Specificity of short interfering RNA determined through gene expression signatures. *Proceedings of the National Academy of Sciences*, *100*(11), 6347–6352. https://doi.org/10.1073/pnas.1131959100

Sharp, P. A. (2001). RNA interference—2001. *Genes & Development*, *15*(5), 485–490. https://doi.org/10.1101/gad.880001

Shaw, P. J., Ince, P. G., Falkous, G., & Mantle, D. (1995). Oxidative damage to protein in sporadic motor neuron disease spinal cord. *Annals of Neurology*, *38*(4), 691–695. https://doi.org/10.1002/ana.410380424

Siddiqui, M. S., François, M., Fenech, M. F., & Leifert, W. R. (2015). Persistent γH2AX: A promising molecular marker of DNA damage and aging. *Mutation Research/Reviews in Mutation Research*, *766*, 1–19. https://doi.org/10.1016/j.mrrev.2015.07.001

Simpson, E. P., Henry, Y. K., Henkel, J. S., Smith, R. G., & Appel, S. H. (2004). Increased lipid peroxidation in sera of ALS patients: A potential biomarker of disease burden. *Neurology*, *62*(10), 1758–1765. https://doi.org/10.1212/WNL.62.10.1758

Singh, V. K., Kalsan, M., Kumar, N., Saini, A., & Chandra, R. (2015). Induced pluripotent stem cells: applications in regenerative medicine, disease modeling, and drug discovery. *Frontiers in Cell and Developmental Biology*, *3*. https://doi.org/10.3389/fcell.2015.00002

Sledz, C. A., Holko, M., de Veer, M. J., Silverman, R. H., & Williams, B. R. G. (2003).

Activation of the interferon system by short-interfering RNAs. *Nature Cell Biology*, *5*(9), 834–839. https://doi.org/10.1038/ncb1038

Smeyers, J., Banchi, E.-G., & Latouche, M. (2021). C9ORF72: What It Is, What It Does, and Why It Matters. *Frontiers in Cellular Neuroscience*, *15*. https://doi.org/10.3389/fncel.2021.661447

Sottile, M. L., & Nadin, S. B. (2018). Heat shock proteins and DNA repair mechanisms: an updated overview. *Cell Stress and Chaperones*, *23*(3), 303–315. https://doi.org/10.1007/s12192-017-0843-4

Spencer, P. S., Lagrange, E., & Camu, W. (2019). ALS and environment: Clues from spatial clustering? *Revue Neurologique*, *175*(10), 652–663. https://doi.org/10.1016/j.neurol.2019.04.007

Sreedharan, J., Blair, I. P., Tripathi, V. B., Hu, X., Vance, C., Rogelj, B., Ackerley, S., Durnall, J. C., Williams, K. L., Buratti, E., Baralle, F., de Belleroche, J., Mitchell, J. D., Leigh, P. N., Al-Chalabi, A., Miller, C. C., Nicholson, G., & Shaw, C. E. (2008). TDP-43 Mutations in Familial and Sporadic Amyotrophic Lateral Sclerosis. *Science*, *319*(5870), 1668–1672. https://doi.org/10.1126/science.1154584

Stein, G. S., van Wijnen, A. J., Stein, J., Lian, J. B., & Montecino, M. (1996). *Contributions of Nuclear Architecture to Transcriptional Control* (pp. 251–278). https://doi.org/10.1016/S0074-7696(08)61233-4

Suk, T. R., & Rousseaux, M. W. C. (2020). The role of TDP-43 mislocalization in amyotrophic lateral sclerosis. *Molecular Neurodegeneration*, *15*(1), 45. https://doi.org/10.1186/s13024-020-00397-1

Sun, Y., Curle, A. J., Haider, A. M., & Balmus, G. (2020). The role of DNA damage response in amyotrophic lateral sclerosis. *Essays in Biochemistry*, *64*(5), 847–861. https://doi.org/10.1042/EBC20200002

Susin, S. A., Lorenzo, H. K., Zamzami, N., Marzo, I., Snow, B. E., Brothers, G. M., Mangion, J., Jacotot, E., Costantini, P., Loeffler, M., Larochette, N., Goodlett, D. R., Aebersold, R., Siderovski, D. P., Penninger, J. M., & Kroemer, G. (1999). Molecular characterization of mitochondrial apoptosis-inducing factor. *Nature*, *397*(6718), 441–446. https://doi.org/10.1038/17135

Sutedja, N. A., Veldink, J. H., Fischer, K., Kromhout, H., Heederik, D., Huisman, M. H. B., Wokke, J. H. J., & van den Berg, L. H. (2009). Exposure to chemicals and metals and risk of amyotrophic lateral sclerosis: A systematic review. *Amyotrophic Lateral Sclerosis*, *10*(5–6), 302–309. https://doi.org/10.3109/17482960802455416

Swinnen, B., & Robberecht, W. (2014). The phenotypic variability of amyotrophic lateral sclerosis. *Nature Reviews Neurology*, *10*(11), 661–670. https://doi.org/10.1038/nrneurol.2014.184

Tak, Y. J., Park, J.-H., Rhim, H., & Kang, S. (2020). ALS-Related Mutant SOD1 Aggregates Interfere with Mitophagy by Sequestering the Autophagy Receptor Optineurin. *International Journal of Molecular Sciences*, *21*(20), 7525. https://doi.org/10.3390/ijms21207525

Tamamori-Adachi, M., Koga, A., Susa, T., Fujii, H., Tsuchiya, M., Okinaga, H., Hisaki, H., Iizuka, M., Kitajima, S., & Okazaki, T. (2018). DNA damage response induced by Etoposide promotes steroidogenesis via GADD45A in cultured adrenal cells. *Scientific Reports*, *8*(1), 9636. https://doi.org/10.1038/s41598-018-27938-5

Tanaka, S., Uehara, T., & Nomura, Y. (2000). Up-regulation of Protein-disulfide Isomerase in Response to Hypoxia/Brain Ischemia and Its Protective Effect against Apoptotic Cell Death. *Journal of Biological Chemistry*, *275*(14), 10388–10393. https://doi.org/10.1074/jbc.275.14.10388

Terada, K., Manchikalapudi, P., Noiva, R., Jauregui, H. O., Stockert, R. J., & Schilsky, M. L. (1995). Secretion, Surface Localization, Turnover, and Steady State Expression of Protein Disulfide Isomerase in Rat Hepatocytes. *Journal of Biological Chemistry*, *270*(35), 20410–20416. https://doi.org/10.1074/jbc.270.35.20410

Tian, G., Xiang, S., Noiva, R., Lennarz, W. J., & Schindelin, H. (2006). The Crystal Structure of Yeast Protein Disulfide Isomerase Suggests Cooperativity between Its Active Sites. *Cell*, *124*(1), 61–73. https://doi.org/10.1016/j.cell.2005.10.044

Tohgi, H., Abe, T., Yamazaki, K., Murata, T., Ishizaki, E., & Isobe, C. (1999). Remarkable increase in cerebrospinal fluid 3-nitrotyrosine in patients with sporadic amyotrophic lateral sclerosis. *Annals of Neurology*, *46*(1), 129–131. https://doi.org/10.1002/1531-8249(199907)46:1<129::AID-ANA21>3.0.CO;2-Y

Tschuch, C., Schulz, A., Pscherer, A., Werft, W., Benner, A., Hotz-Wagenblatt, A., Barrionuevo, L., Lichter, P., & Mertens, D. (2008). Off-target effects of siRNA specific for GFP. *BMC Molecular Biology*, *9*(1), 60. https://doi.org/10.1186/1471-2199-9-60

Tubbs, A., & Nussenzweig, A. (2017). Endogenous DNA Damage as a Source of Genomic Instability in Cancer. *Cell*, *168*(4), 644–656. https://doi.org/10.1016/j.cell.2017.01.002

Turano, C., Coppari, S., Altieri, F., & Ferraro, A. (2002). Proteins of the PDI family: Unpredicted non-ER locations and functions. *Journal of Cellular Physiology*, *193*(2), 154–163. https://doi.org/10.1002/jcp.10172

Turner, M. R., & Swash, M. (2015). The expanding syndrome of amyotrophic lateral sclerosis: a clinical and molecular odyssey. *Journal of Neurology, Neurosurgery & Psychiatry*, *86*(6), 667–673. https://doi.org/10.1136/jnnp-2014-308946

Tuschl, T. (2001). RNA Interference and Small Interfering RNAs. *ChemBioChem*, *2*(4), 239–245. https://doi.org/10.1002/1439-7633(20010401)2:4<239::AID-CBIC239>3.0.CO;2-R

Tyzack, G. E., Luisier, R., Taha, D. M., Neeves, J., Modic, M., Mitchell, J. S., Meyer, I., Greensmith, L., Newcombe, J., Ule, J., Luscombe, N. M., & Patani, R. (2019). Widespread FUS mislocalization is a molecular hallmark of amyotrophic lateral sclerosis. *Brain*, *142*(9), 2572–2580. https://doi.org/10.1093/brain/awz217

Uehara, T., Nakamura, T., Yao, D., Shi, Z.-Q., Gu, Z., Ma, Y., Masliah, E., Nomura, Y., & Lipton, S. A. (2006). S-Nitrosylated protein-disulphide isomerase links protein misfolding to neurodegeneration. *Nature*, *441*(7092), 513–517. https://doi.org/10.1038/nature04782

Valentine, J. S., Doucette, P. A., & Zittin Potter, S. (2005). COPPER-ZINC SUPEROXIDE DISMUTASE AND AMYOTROPHIC LATERAL SCLEROSIS. *Annual Review of Biochemistry*, *74*(1), 563–593. https://doi.org/10.1146/annurev.biochem.72.121801.161647

Valverde, M., Lozano-Salgado, J., Fortini, P., Rodriguez-Sastre, M. A., Rojas, E., & Dogliotti, E. (2018). Hydrogen Peroxide-Induced DNA Damage and Repair through the Differentiation of Human Adipose-Derived Mesenchymal Stem Cells. *Stem Cells International*, *2018*, 1–10. https://doi.org/10.1155/2018/1615497

Vance, C., Rogelj, B., Hortobágyi, T., De Vos, K. J., Nishimura, A. L., Sreedharan, J., Hu, X., Smith, B., Ruddy, D., Wright, P., Ganesalingam, J., Williams, K. L., Tripathi, V., Al-Saraj, S., Al-Chalabi, A., Leigh, P. N., Blair, I. P., Nicholson, G., de Belleroche, J., … Shaw, C. E. (2009). Mutations in FUS, an RNA Processing Protein, Cause Familial Amyotrophic Lateral Sclerosis Type 6. *Science*, *323*(5918), 1208–1211. https://doi.org/10.1126/science.1165942

VanderWaal, R. P., Spitz, D. R., Griffith, C. L., Higashikubo, R., & Roti Roti, J. L. (2002). Evidence that protein disulfide isomerase (PDI) is involved in DNA-nuclear matrix anchoring. *Journal of Cellular Biochemistry*, *85*(4), 689–702. https://doi.org/10.1002/jcb.10169

Verma, A., & Berger, J. R. (2006). ALS syndrome in patients with HIV-1 infection. *Journal of the Neurological Sciences*, *240*(1–2), 59–64. https://doi.org/10.1016/j.jns.2005.09.005

Walker, A. K., Farg, M. A., Bye, C. R., McLean, C. A., Horne, M. K., & Atkin, J. D. (2010). Protein disulphide isomerase protects against protein aggregation and is S-nitrosylated in

amyotrophic lateral sclerosis. *Brain*, *133*(1), 105–116. https://doi.org/10.1093/brain/awp267

Walker, C., Herranz-Martin, S., Karyka, E., Liao, C., Lewis, K., Elsayed, W., Lukashchuk, V., Chiang, S.-C., Ray, S., Mulcahy, P. J., Jurga, M., Tsagakis, I., Iannitti, T., Chandran, J., Coldicott, I., De Vos, K. J., Hassan, M. K., Higginbottom, A., Shaw, P. J., … El-Khamisy, S. F. (2017). C9orf72 expansion disrupts ATM-mediated chromosomal break repair. *Nature Neuroscience*, *20*(9), 1225–1235. https://doi.org/10.1038/nn.4604

Walker, J. R., Corpina, R. A., & Goldberg, J. (2001). Structure of the Ku heterodimer bound to DNA and its implications for double-strand break repair. *Nature*, *412*(6847), 607–614. https://doi.org/10.1038/35088000

Walles, S. A. S., Zhou, R., & Liliemark, E. (1996). DNA damage induced by etoposide; a comparison of two different methods for determination of strand breaks in DNA. *Cancer Letters*, *105*(2), 153–159. https://doi.org/10.1016/0304-3835(96)04266-8

Wang, C., Li, W., Ren, J., Fang, J., Ke, H., Gong, W., Feng, W., & Wang, C. (2013). Structural Insights into the Redox-Regulated Dynamic Conformations of Human Protein Disulfide Isomerase. *Antioxidants & Redox Signaling*, *19*(1), 36–45. https://doi.org/10.1089/ars.2012.4630

Wang, H., Guo, W., Mitra, J., Hegde, P. M., Vandoorne, T., Eckelmann, B. J., Mitra, S., Tomkinson, A. E., Van Den Bosch, L., & Hegde, M. L. (2018). Mutant FUS causes DNA ligation defects to inhibit oxidative damage repair in Amyotrophic Lateral Sclerosis. *Nature Communications*, *9*(1), 3683. https://doi.org/10.1038/s41467-018-06111-6

Wang, H., Kodavati, M., Britz, G. W., & Hegde, M. L. (2021). DNA Damage and Repair Deficiency in ALS/FTD-Associated Neurodegeneration: From Molecular Mechanisms to Therapeutic Implication. *Frontiers in Molecular Neuroscience*, *14*. https://doi.org/10.3389/fnmol.2021.784361

Wang, S.-B., Shi, Q., Xu, Y., Xie, W.-L., Zhang, J., Tian, C., Guo, Y., Wang, K., Zhang, B.-Y., Chen, C., Gao, C., & Dong, X.-P. (2012). Protein Disulfide Isomerase Regulates Endoplasmic Reticulum Stress and the Apoptotic Process during Prion Infection and PrP Mutant-Induced Cytotoxicity. *PLoS ONE*, *7*(6), e38221. https://doi.org/10.1371/journal.pone.0038221

Wang, W., Mani, A. M., & Wu, Z.-H. (2017). DNA damage-induced nuclear factor-kappa B activation and its roles in cancer progression. *Journal of Cancer Metastasis and Treatment*, *3*(3), 45. https://doi.org/10.20517/2394-4722.2017.03

Wang, X., Olberding, K. E., White, C., & Li, C. (2011). Bcl-2 proteins regulate ER membrane

permeability to luminal proteins during ER stress-induced apoptosis. *Cell Death & Differentiation*, *18*(1), 38–47. https://doi.org/10.1038/cdd.2010.68

Watanabe, M., Dykes-Hoberg, M., Cizewski Culotta, V., Price, D. L., Wong, P. C., & Rothstein, J. D. (2001). Histological Evidence of Protein Aggregation in Mutant SOD1 Transgenic Mice and in Amyotrophic Lateral Sclerosis Neural Tissues. *Neurobiology of Disease*, *8*(6), 933–941. https://doi.org/10.1006/nbdi.2001.0443

Waters, T. R., & Swann, P. F. (1998). Kinetics of the Action of Thymine DNA Glycosylase. *Journal of Biological Chemistry*, *273*(32), 20007–20014. https://doi.org/10.1074/jbc.273.32.20007

Webster, C. P., Smith, E. F., Shaw, P. J., & De Vos, K. J. (2017). Protein Homeostasis in Amyotrophic Lateral Sclerosis: Therapeutic Opportunities? *Frontiers in Molecular Neuroscience*, *10*. https://doi.org/10.3389/fnmol.2017.00123

Whitehead, K. A., Langer, R., & Anderson, D. G. (2009). Knocking down barriers: advances in siRNA delivery. *Nature Reviews Drug Discovery*, *8*(2), 129–138. https://doi.org/10.1038/nrd2742

Whiteley, E. M., Hsu, T.-A., & Betenbaugh, M. J. (1997). Thioredoxin Domain Non-equivalence and Anti-chaperone Activity of Protein Disulfide Isomerase Mutants in Vivo. *Journal of Biological Chemistry*, *272*(36), 22556–22563. https://doi.org/10.1074/jbc.272.36.22556

Wiebauer, K., & Jiricny, J. (1990). Mismatch-specific thymine DNA glycosylase and DNA polymerase beta mediate the correction of G.T mispairs in nuclear extracts from human cells. *Proceedings of the National Academy of Sciences*, *87*(15), 5842–5845. https://doi.org/10.1073/pnas.87.15.5842

Wilkinson, B., & Gilbert, H. F. (2004). Protein disulfide isomerase. *Biochimica et Biophysica Acta (BBA) - Proteins and Proteomics*, *1699*(1–2), 35–44. https://doi.org/10.1016/j.bbapap.2004.02.017

Woehlbier, U., Colombo, A., Saaranen, M. J., Pérez, V., Ojeda, J., Bustos, F. J., Andreu, C. I., Torres, M., Valenzuela, V., Medinas, D. B., Rozas, P., Vidal, R. L., Lopez-Gonzalez, R., Salameh, J., Fernandez-Collemann, S., Muñoz, N., Matus, S., Armisen, R., Sagredo, A., … Hetz, C. (2016). <scp>ALS</scp> -linked protein disulfide isomerase variants cause motor dysfunction. *The EMBO Journal*, *35*(8), 845–865. https://doi.org/10.15252/embj.201592224

Woycechowsky, K. J., Wittrup, K. D., & Raines, R. T. (1999). A small-molecule catalyst of protein folding in vitro and in vivo. *Chemistry & Biology*, *6*(12), 871–879.

https://doi.org/10.1016/S1074-5521(00)80006-X

Wyatt, M. D., & Pittman, D. L. (2006). Methylating Agents and DNA Repair Responses: Methylated Bases and Sources of Strand Breaks. *Chemical Research in Toxicology*, *19*(12), 1580–1594. https://doi.org/10.1021/tx060164e

Xu, S., Liu, Y., Yang, K., Wang, H., Shergalis, A., Kyani, A., Bankhead, A., Tamura, S., Yang, S., Wang, X., Wang, C., Rehemtulla, A., Ljungman, M., & Neamati, N. (2019). Inhibition of protein disulfide isomerase in glioblastoma causes marked downregulation of DNA repair and DNA damage response genes. *Theranostics*, *9*(8), 2282–2298. https://doi.org/10.7150/thno.30621

Xu, S., Sankar, S., & Neamati, N. (2014). Protein disulfide isomerase: a promising target for cancer therapy. *Drug Discovery Today*, *19*(3), 222–240. https://doi.org/10.1016/j.drudis.2013.10.017

Xu, Y.-F., Zhang, Y.-J., Lin, W.-L., Cao, X., Stetler, C., Dickson, D. W., Lewis, J., & Petrucelli, L. (2011). Expression of mutant TDP-43 induces neuronal dysfunction in transgenic mice. *Molecular Neurodegeneration*, *6*(1), 73. https://doi.org/10.1186/1750-1326-6-73

Youle, R. J., & Strasser, A. (2008). The BCL-2 protein family: opposing activities that mediate cell death. *Nature Reviews Molecular Cell Biology*, *9*(1), 47–59. https://doi.org/10.1038/nrm2308

Zhang, F., Ström, A.-L., Fukada, K., Lee, S., Hayward, L. J., & Zhu, H. (2007). Interaction between Familial Amyotrophic Lateral Sclerosis (ALS)-linked SOD1 Mutants and the Dynein Complex. *Journal of Biological Chemistry*, *282*(22), 16691–16699. https://doi.org/10.1074/jbc.M609743200

Zhao, C., Devlin, A., Chouhan, A. K., Selvaraj, B. T., Stavrou, M., Burr, K., Brivio, V., He, X., Mehta, A. R., Story, D., Shaw, C. E., Dando, O., Hardingham, G. E., Miles, G. B., & Chandran, S. (2020). Mutant *C9orf72* human iPSC-derived astrocytes cause non-cell autonomous motor neuron pathophysiology. *Glia*, *68*(5), 1046–1064. https://doi.org/10.1002/glia.23761

Zhao, C., Tyndyk, M., Eide, I., & Hemminki, K. (1999). Endogenous and background DNA adducts by methylating and 2-hydroxyethylating agents. *Mutation Research/Fundamental and Molecular Mechanisms of Mutagenesis*, *424*(1–2), 117–125. https://doi.org/10.1016/S0027-5107(99)00013-5

7. Appendix

7.1.

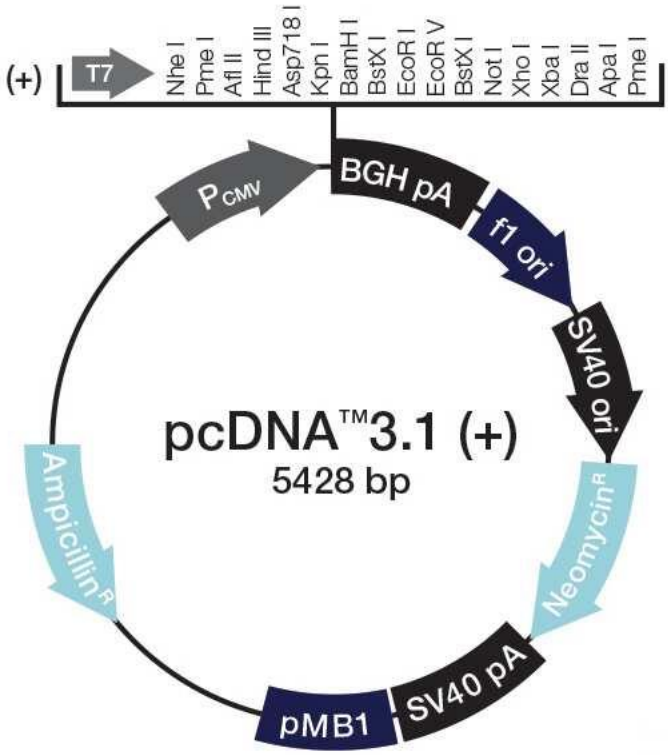

Figure 7.1: Schematic of pcDNA3.1(+) expression vector. This expression vector has Ampicillin resistance with Cytomegalovirus (CMV) promoter for high-level expression and no tag. For enhanced mRNA stability, it has got Bovine Growth Hormone (BGH) polyadenylation signal and transcription termination sequence. It also has SV40 origin for episomal replication.

7.2.

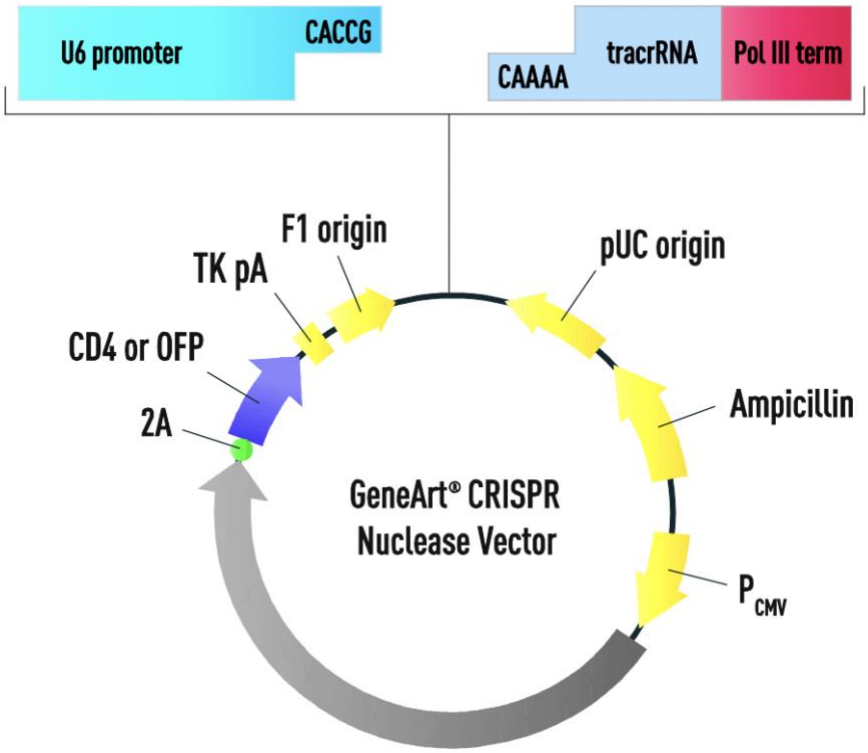

Figure 7.2: Schematic of CRISPR nuclease expression vector. This vector has Ampicillin resistance with U6 or Cytomegalovirus (CMV) promoter for high-level expression and OFP (red (orange) fluorescence) fusion protein tag.